สมบัติเชิงแม่เหล็กไฟฟ้ายังผลของคอมพอสิตเชิงเส้นและไม่เชิงเส้น

นายชนินทร์ โพธิสุข

วิทยานิพนธ์นี้เป็นส่วนหนึ่งของการศึกษาตามหลักสูตรปริญญาวิทยาศาสตรดุษฎีบัณฑิต
สาขาวิชาฟิสิกส์ ภาควิชาฟิสิกส์
คณะวิทยาศาสตร์ จุฬาลงกรณ์มหาวิทยาลัย
ปีการศึกษา 2555

ลิขสิทธิ์ของจุฬาลงกรณ์มหาวิทยาลัย
บทคัดย่อและแฟ้มข้อมูลฉบับเต็มของวิทยานิพนธ์ตั้งแต่ปีการศึกษา 2554 ที่ให้บริการในคลังปัญญาจุฬาฯ (CUIR)
เป็นแฟ้มข้อมูลของนิสิตเจ้าของวิทยานิพนธ์ที่ส่งผ่านทางบัณฑิตวิทยาลัย
The abstract and full text of theses from the academic year 2011 in Chulalongkorn University Intellectual Repository(CUIR)
are the thesis authors' files submitted through the Graduate School.

EFFECTIVE ELECTROMAGNETIC PROPERTIES OF LINEAR AND NONLINEAR COMPOSITES

Mr. Chanin Potisook

A Dissertation Submitted in Partial Fulfillment of the Requirements
for the Degree of Doctor of Philosophy Program in Physics
Department of Physics
Faculty of Science
Chulalongkorn University
Academic Year 2012
Copyright of Chulalongkorn University

Thesis Title	EFFECTIVE ELECTROMAGNETIC PROPERTIES OF LINEAR AND NONLINEAR COMPOSITES
By	Mr. Chanin Potisook
Field of Study	Physics
Thesis Advisor	Associate Professor Mayuree Natenapit, Ph.D.

Accepted by the Faculty of Science, Chulalongkorn University in Partial Fulfillment of the Requirements for the Doctoral Degree

..... Dean of the Faculty of Science
(Professor Supot Hannongbua, Dr.rer.nat)

THESIS COMMITTEE

..... Chairman
(Assistant Professor Kajornyod Yoodee, Ph.D.)

..... Thesis Advisor
(Associate Professor Mayuree Natenapit, Ph.D.)

..... Examiner
(Assistant Professor Patcha Chatraphorn, Ph.D.)

..... Examiner
(Assistant Professor Auttakit Chatrabhuti, Ph.D.)

..... External Examiner
(Assistant Professor Sutee Boonchui, Ph.D.)

ชนินทร์ โพธิสุข : สมบัติยังผลเชิงแม่เหล็กไฟฟ้าของวัสดุคอมพอสิตที่เป็นเชิงเส้นและไม่เชิง (EFFECTIVE ELECTROMAGNETIC PROPERTIES OF LINEAR AND NONLINEAR COMPOSITES) อ. ที่ปรึกษาวิทยานิพนธ์หลัก : รศ.ดร.มยุรี เนตรนภิส , 81 หน้า.

ได้ศึกษาคอมพอสิตที่ประกอบด้วยกลุ่มทรงกลมสองชนิดที่ไม่เป็นสารแม่เหล็กกระจายตัวอยู่รวมกันแบบสุ่ม โดยอาศัยทฤษฎีการกระเจิงของมี ทำให้สามารถคำนวณสภาพการมีขั้วเชิงแม่เหล็กและสภาพการมีขั้วเชิงไฟฟ้าของทรงกลมเหล่านี้ได้ ซึ่งปริมาณเหล่านี้ได้ถูกนำไปใช้ในการคำนวณสภาพยอมยังผลและสภาพให้ซึมผ่านได้ยังผลของคอมพอสิตดังกล่าว สมบัติยังผลเหล่านี้ได้ถูกนำมาใช้เพื่อออกแบบคอมพอสิตที่มีดัชนีหักเหเป็นลบในช่วงความถี่อินฟราเรด นอกจากนี้ยังได้ศึกษาลักษณะการแผ่ของคลื่นระนาบในตัวกลางแบบแอนไอโซทรอปิกแกนคู่โดยคำนึงถึงการสูญเสียพลังงานของคลื่น เงื่อนไขทั่วไปของการเกิดความเร็วเฟสเป็นลบได้ถูกแสดงในรูปแบบของตัวแปรวัสดุและทิศทางการแผ่ของคลื่นในตัวกลาง นอกจากนี้ยังได้มีการคำนวณเชิงตัวเลขของมุมระหว่างพอยติงเวกเตอร์เฉลี่ยและความเร็วเฟสเพื่อยืนยันผลเชิงทฤษฎี อีกทั้งได้ศึกษาปัญหาการหักเหของคลื่นที่เคลื่อนที่จากที่ว่างไปยังตัวกลางแอนไอโซทรอปิกแกนคู่ที่มีการสูญเสีย เพื่อที่จะหาเงื่อนไขของการเกิดมุมหักเหที่เป็นลบ สุดท้ายนี้ได้ศึกษาการตอบสนองยังผลเชิงไดอิเล็กทริกอันดับสูงของคอมพอสิตที่ประกอบด้วยสารฝังกระจายทรงกระบอกรีไม่เชิงเส้นซึ่งกระจายตัวแบบสุ่มอยู่ภายในตัวกลางเชิงเส้น ได้มีการหาสูตรทั่วไปสำหรับการหาสัมประสิทธิ์ยังผลดีซีถึงอันดับที่ 9 โดยใช้วิธีสนามเฉลี่ย และนำไปวิเคราะห์ผลของรูปทรงของสารฝังกระจายต่อค่าสัมประสิทธิ์ยังผล จากนั้นได้ศึกษาการตอบสนองแบบเอซียังผลแบบกึ่งสถิตของคอมพอสิตภายใต้สนามไฟฟ้าภายนอกรูปไซน์ และได้มีการหาความสัมพันธ์ทั่วไปของการตอบสนองยังแบบผลเอซีต่อการตอบสนองยังผลแบบดีซี ซึ่งความสัมพันธ์ที่ได้สามารถใช้ได้กับคอมพอสิตแบบไม่เชิงเส้นอย่างอ่อนแบบไอโซทรอปิกทุกชนิด

ภาควิชา.....ฟิสิกส์..... ลายมือชื่อนิสิต.....

สาขาวิชา.....ฟิสิกส์..... ลายมือชื่อ อ.ที่ปรึกษาวิทยานิพนธ์หลัก.....

ปีการศึกษา....2555.....

4872570023 : MAJOR PHYSICS
KEYWORDS : Negative Phase Velocity / Negative Refraction / Biaxial Anisotropic Lossy Media/ Nonlinear Dielectric Composite/ Effective Nonlinear Coefficient/ Effective AC Response

CHANIN POTISOOK : EFFECTIVE ELECTROMAGNETIC PROPERTIES OF LINEAR AND NONLINEAR COMPOSITES. ADVISOR : ASSOC. PROF. MAYUREE NATENAPIT, Ph.D., 81 pp.

A composite structure consisting of randomly distributed two groups of nonmagnetic spheres is investigated. The electric and magnetic polarizabilities of these spheres are determined using Mie scattering theory and then used to calculate the effective permittivity and the effective permeability of the composite. Based on these effective properties, the design procedures to obtain a negative refractive index at infrared frequencies are reported. Furthermore, the characteristics of the plane wave propagations in biaxial anisotropic lossy media are investigated. The general condition on the negative phase velocity for homogeneous plane waves is provided in terms of material parameters and the propagation direction. The numerical calculations for the angles between the average Poynting vector and the phase velocity are performed in order to justify the theoretical analysis. In addition, the refraction between free space and the biaxial anisotropic lossy media are also considered and the general condition on the negative angle of refraction is derived. Finally the higher-order dielectric responses of composites composed of weakly nonlinear elliptic cylindrical inclusions randomly embedded in linear media are investigated. The general formulae for effective DC coefficients are derived by the average field method up to the ninth order and then applied to analyze the effects of inclusion shapes on the effective response. The quasi-static AC response of the composites under sinusoidal electric fields are also investigated. The general relationships between the effective DC and AC coefficients are established, which are applicable to all weakly nonlinear isotropic composites.

Department : .....Physics..... Student's Signature .....
Field of Study : .....Physics... Advisor's Signature .....
Academic Year : .....2012.....

Acknowledgements

First of all, I would like to express my sincere gratitude to my advisor Assoc. Prof. Dr. Mayuree Natenapit for the continuous support of my Ph.D study and research, for her patience, motivation, enthusiasm, and immense knowledge. Her guidance has helped me through the research and writing up this thesis.

Besides my advisor, I would like to thank the rest of my thesis committee: Asst. Prof. Dr. Kajornyod Yoodee, Asst. Prof. Dr. Patcha Chatraphorn, Asst. Prof. Dr. Auttakit Chatrabhuti and Asst. Prof. Dr. Sutee Boonchui, for their encouragement, comments and questions.

Sincere thanks are extended to all friends of the Department of Physics for their suggestions, assistance and friendship.

Prince Maha Vajiralongkorn Fund and the 90^{th} Anniversary of Chulalongkorn University Fund (Ratchadaphiseksomphot Endowment Fund) are gratefully acknowledged.

Finally, the greatest gratitude is expressed to my family for their love and understanding.

Contents

page

Chapter **Page**

Page

List of Figures

Figure **Page**

Figure **Page**

Figure **Page**

Figure **Page**

List of Abbreviations

E	electric field
D	electric displacement
B	magnetic induction
H	magnetic field intensity
ε	permittivity
μ	permeability
ε_r	relative permittivity
ε_r'	real part of relative permittivity
ε_r''	imaginary part of relative permittivity
μ_r	relative permeability
μ_r'	real part of relative permeability
μ_r''	imaginary part of relative permeability
DC	direct current
AC	alternating current
λ	wavelength
ω	angular frequency
k	wave number
f	frequency
c	the speed of light
θ_i	incident angle
θ_r	reflection angle
θ_t	refraction angle
P	polarization

$\mathbf{M}$	magnetization
$\mathbf{S}_{av}$	average Poynting vector
ε_0	permittivity of free space
$\tilde{\chi}_{\mathrm{E}}$	complex electric susceptibility
$\tilde{\chi}_{\mathrm{M}}$	complex magnetic susceptibility
χ_{E}	electric susceptibility
$\chi_{\mathrm{E}}^{(n)}$	the nth nonlinear electric susceptibility
Φ	electric potential
x, y, z	Cartesian coordinates
$\hat{\mathbf{x}}, \hat{\mathbf{y}}, \hat{\mathbf{z}}$	unit vectors of Cartesian coordinates
u, v	elliptic cylindrical coordinates
ε_{r1}	relative permittivity of group 1 spheres
ε_{r2}	relative permittivity of group 2 spheres
$\varepsilon(\infty)$	high-frequency limit of the permittivity
ω_L	longitudinal optical phonon frequency
ω_T	transverse optical phonon frequency
γ	damping coefficient
$\mathbf{r}$	position vector
t	time
e	electron charge
m_e	electron mass
N	number of electrons per unit volume
ω_p	plasma frequency

r, θ, ϕ	spherical coordinates
$\hat{\mathbf{r}}, \hat{\boldsymbol{\theta}}, \hat{\boldsymbol{\phi}}$	unit vectors of spherical coordinates
N_1	number of group 1 spheres per unit volume
N_2	number of group 2 spheres per unit volume
f_1	volume fraction of group 1 spheres
f_2	volume fraction of group 2 spheres
$\varepsilon_r^{\text{eff}}$	effective relative permittivity
μ_r^{eff}	effective relative permeability
α_e, α_m	electric and magnetic polarisabilities
α_{e1}, α_{m1}	electric and magnetic polarisabilities of spheres of group 1
α_{e2}, α_{m2}	electric and magnetic polarisabilities of spheres of group 2
a_n, b_n	2n-pole electric and magnetic scattering coefficients
$a_1^{(1)}, b_1^{(2)}$	electric and magnetic dipole scattering coefficients of spheres of group 1
$a_1^{(2)}, b_1^{(2)}$	electric and magnetic dipole scattering coefficients of spheres of group 2
n^{eff}	effective refractive index
$\bar{\bar{\varepsilon}}_r$	relative permittivity tensor
$\bar{\bar{\mu}}_r$	relative permeability tensor
$\varepsilon_{rx}, \varepsilon_{ry}, \varepsilon_{rz}$	diagonal components of a relative permittivity tensor
$\mu_{rx}, \mu_{ry}, \mu_{rz}$	diagonal components of a relative permeability tensor
ϕ	propagation angle
TE	transverse electric
$\mathbf{k}_1$	wave vector of an incident plane wave
$\mathbf{k}_t$	wave vector of a transmitted plane wave

$\mathbf{S}_t$	average Poynting vector of a transmitted plane wave
k_x	complex wave number along the x-direction
k_y	complex wave number along the y-direction
$\mathbf{E}^i$	electric field inside inclusion
$\mathbf{E}^m$	electric field inside medium
$\mathbf{D}^i$	electric displacement inside inclusion
$\mathbf{D}^m$	electric displacement inside medium
p	volume packing fraction of inclusion
ε_i	permittivity or the first-order dielectric coefficient of inclusions
ε_m	permittivity or the first-order dielectric coefficient of medium
ε_e	the effective first-order dielectric coefficient
χ_i	the third-order dielectric coefficient of inclusions
χ_e	the effective third-order dielectric coefficient
η_i	the fifth-order dielectric coefficient of inclusions
η_e	the effective fifth-order dielectric coefficient
δ_e	the effective seventh-order dielectric coefficient
μ_e	the effective ninth-order dielectric coefficient
$\varepsilon^*_{n\omega}$	the effective first-order dielectric coefficient at n^{th} harmonics
$\chi^*_{n\omega}$	the effective third-order dielectric coefficient at n^{th} harmonics
$\eta^*_{n\omega}$	the effective fifth-order dielectric coefficient at n^{th} harmonics
$\delta^*_{n\omega}$	the effective seventh-order dielectric coefficient at n^{th} harmonics
$\mu^*_{n\omega}$	the effective ninth-order dielectric coefficient at n^{th} harmonics
$\varepsilon^*_{\omega^m(3\omega)^n;k\omega}$	the effective first-order coupled coefficient at k^{th} harmonics

$\chi^*_{\omega^m(3\omega)^n;k\omega}$	the effective third-order coupled coefficient at k^{th} harmonics
$\eta^*_{\omega^m(3\omega)^n;k\omega}$	the effective fifth-order coupled coefficient at k^{th} harmonics
$\delta^*_{\omega^m(3\omega)^n;k\omega}$	the effective seventh-order coupled coefficient at k^{th} harmonics
$\mu^*_{\omega^m(3\omega)^n;k\omega}$	the effective ninth-order coupled coefficient at k^{th} harmonics

CHAPTER I

Introduction

Composites, structures consisting of two or more constituents that differ in chemical compositions, are very useful in many fields of pure and applied sciences. This is because their structures and constituent materials can be adjusted to provide effective bulk properties that are more suitable for applications than those found in natural materials. In some cases, the effective properties can differ considerably to that of the constituents. For example, if we combine a metal (high conductivity) with insulator (low conductivity) in alternating layers [1], we obtain an anisotropic composite with low conductivity in a direction perpendicular to the layers but high conductivity in a parallel direction. By combining two materials with positive thermal expansion coefficients into a porous structure [2], a negative thermal expansion coefficient can be achieved, resulting in a composite with decreasing volume when its temperature increases.

Among the physical properties of composites, electromagnetic properties are also the subject that have widely been studied and are the main topic of our work. This thesis is divided into two parts, concerning with linear and nonlinear composites, respectively. The adjective "linear" or "nonlinear" indicate whether that the composite constituents behave (in $\mathbf{D}-\mathbf{E}$ or $\mathbf{B}-\mathbf{H}$ relations) linearly or nonlinearly, when the composites are subject to external electromagnetic fields. The introduction and scope for each part are provided in subsequence sections.

1.1 Linear Electromagnetic Composites

One of the mainstream in the study of linear electromagnetic composites is to obtain a negative index of refraction. The original idea of negative refractive index date back to 1968 when a Russian physicists, Victor Vesselago [3] proposed the theoretical analysis of lossless materials with simultaneously $\varepsilon < 0$ and $\mu < 0$, and showed that certain uncommon phenomena occur such as a negative phase velocity, a negative refraction and a left-handed relation of the vectors $\mathbf{E}, \mathbf{H}, \mathbf{k}$ of a plane wave (hence the term left-handed media). These phenomena are shown in Figs. 1.1 and 1.2.

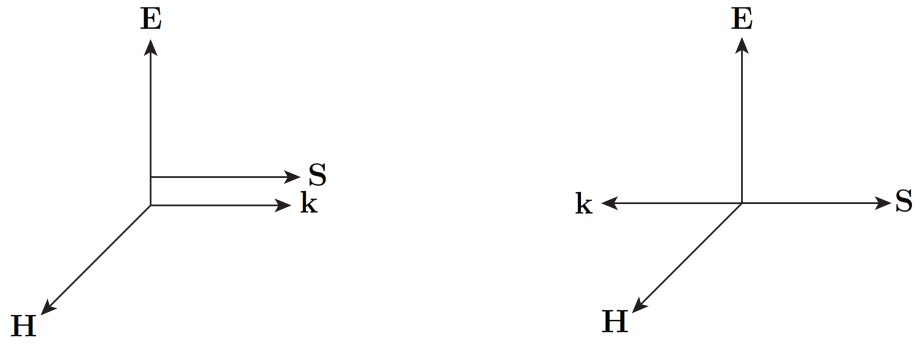

(a) $\varepsilon > 0$ and $\mu > 0$ (b) $\varepsilon < 0$ and $\mu < 0$

Figure 1.1: Relations of $\mathbf{E}, \mathbf{H}, \mathbf{k}$ of plane waves in (a) a medium with $\varepsilon > 0$ and $\mu > 0$, and (b) a medium with $\varepsilon < 0$ and $\mu < 0$. This figure also shows (a) a positive phase velocity where the phase velocity is parallel to the Poynting vector and (b) a negative phase velocity where the phase velocity is anti-parallel to the Poynting vector.

Vesselago also concluded that the refractive indexes of such media are negative, causing a negative angle of refraction between normal and left-handed media (Fig. 1.2). In 2000, Pendry [4] then showed that a planar lenses (Fig. 1.3) made by a medium with $\varepsilon = -1$ and $\mu = -1$ can focus electromagnetic waves on an area smaller than λ^2, which exceeds the resolution limit of ordinary lenses. Thus the image produced by this lenses is extremely sharp as if it is an object itself.

Because of this super lenses idea that negative index materials have received many attentions in the past few decades. However, naturally-occurring materials

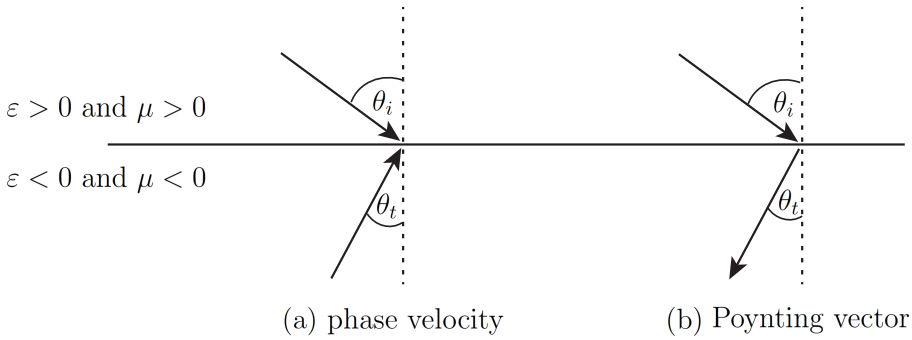

Figure 1.2: (a) phase velocity and (b) Poynting vector refractions when a plane wave travels from a normal medium with $\varepsilon > 0$ and $\mu > 0$ into a medium with $\varepsilon < 0$ and $\mu < 0$. This figure shows that the angle of refraction (θ_t) is negative.

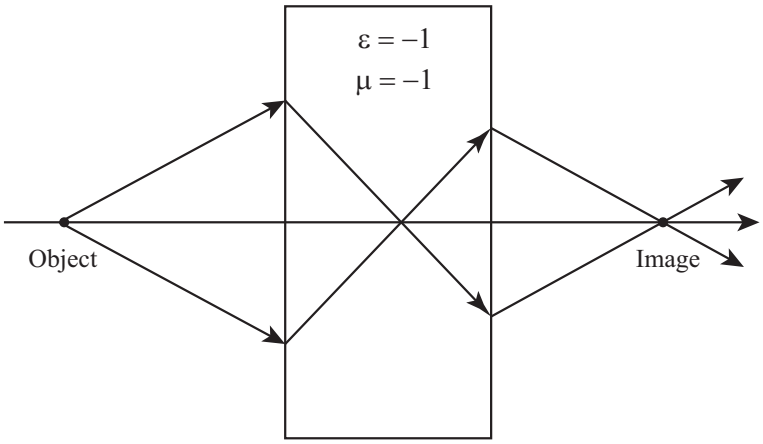

Figure 1.3: A planar slab made by a medium with $\varepsilon = -1$ and $\mu = -1$. This slab can be used as a lenses with extraordinary resolution power [4].

with simultaneously negative ε and μ have never been reported. So researchers have employed man-made structure materials or composites in order to obtain this property. For example, Pendry et al. [5, 6] designed composites composed of a periodic array of thin metallic wires and split ring resonators (SRRs), which provide a negative permittivity and a negative permeability, respectively. Smith et al. [7] used a certain combination of thin wires and SRRs to fabricate the first negative index composite which exhibited a negative refraction at microwave frequencies. For infrared regime, Wheeler et al. [8] designed a negative index composite consisting of periodic array of $LiTaO_3$ spheres coated by a drude model

semiconductor. Yannopapas [9] investigated two structures that can provide negative refractive indexes at infrared frequencies. The first one is a combination of alternating layers of $LiTaO_3$ and n-type Ge spheres and the second one is a fcc crystal whose lattice sites are randomly occupied by $LiTaO_3$ and n-type Ge spheres. For optical frequencies, Podolskiy et al. [10] reported a nanostructured composite consisting of a periodic array of pairs of parallel gold nanorods.

For isotropic lossless materials (materials that do not absorb electromagnetic energies, and can be characterized by real ε and real μ), a negative phase velocity implies a negative refraction and vice versa. Hence, the negative phase velocity has also been used as a criterion for isotropic lossy materials (materials that absorb electromagnetic energies, and can be characterized by complex ε and complex μ), to possess a negative refractive index. The general condition for the negative phase velocity of a uniform plane wave in isotropic lossy media is formally proposed by McCall et al. [11], including $\mathrm{Re}\{\varepsilon\} < 0$ and $\mathrm{Re}\{\mu\} < 0$ as a special case. A simpler equivalent condition has been presented by Depine and Lakhtakia [12] and its applicability to active media have been discussed in Refs. [13, 14]. However, in the problems of refraction concerning with lossy media, the transmitted waves are nonuniform [15] and their negative phase velocities do not always yield the negative refraction [16]. So in order to obtain a general criterion for the negative refraction in a certain medium, we should consider a refraction of the nonuniform transmitted wave rather than the phase velocity of a uniform plane wave propagation.

Because most negative index composites fabricated so far are anisotropic [7, 10], there are also many theoretical works concerning with negative refractions in anisotropic media. For example, Mckay and Lakhtakia [16] studied the negative phase velocity, negative refraction and counter position in a bianisotropic medium and showed that the positive phase velocity and the negative refraction can coexist. Woodley and Mojahedi [17] studied backward wave phenomena in anisotropic materials, where the angle between the phase and group velocities varies between 90^0 and 270^0. Ding et al. [18] presented the conditions for the negative phase velocity and the anomalous refraction in a biaxial anisotropic lossless medium, whilst Lui and Gao [19] further generalized the work of Ding et al. by covering

oblique orientations of the principal axes.

In this part, the scope of this thesis is as follows. First, the detailed derivation of the Lakhtakia-Depine relation is presented (chapter 3), then its special case, namely, $\mathrm{Re}\{\varepsilon_r\} < 0$ and $\mathrm{Re}\{\mu_r\} < 0$, where ε_r and μ_r are the relative permittivity and the relative permeability, respectively, is used to design a negative index composite at infrared frequencies (chapter 4). The structure of the composite consists of a randomly distributed two groups of $LiTaO_3$ and Drude semiconductor spheres randomly distributed in an otherwise free space. This structure is different from that of Yannopapas [9] because the spheres are not constrained to lattice sites of a fcc crystal. We also use a different method, namely, the resonance methods presented by Wheeler et al. [8] and arrive at a condition for calculating the plasma frequency of drude semiconductor spheres. This condition depends on both the packing fractions of the two groups of spheres and reduces to that presented in [8] when the composite consists solely of Drude semiconductor spheres.

As mentioned earlier, the Lakhtakia-Depine condition is derived from the negative phase velocity condition of the uniform plane wave and does not guarantee the negative refraction. However if we manage to make the electric and magnetic losses ($\mathrm{Im}\{\varepsilon\}$ and $\mathrm{Im}\{\mu\}$) to be very small, it can approach the Vesselago case and can be used as an approximate condition for a negative refraction.

Finally, the negative phase velocity and the negative refraction in anisotropic biaxial lossy media are investigated (chapter 5) and the general conditions for the two phenomena are derived. We also show numerically that the negative refraction can occur even if the phase velocity of the transmitted wave is positive. This emphasizes the fact that a negative phase velocity should not be used as a criterion for a negative refraction when dealing with lossy or anisotropic media.

1.2 Nonlinear Dielectric Composites

The effective response of nonlinear composites has attracted considerable recent attention due to the recognition of many phenomena caused by nonlinearity,

such as the dielectric breakdown in metal-insulator composites [20], strong enhancement of effective susceptibilities by local field effects [21-23] and the second- and third-harmonic generations in nonlinear dielectric composites [24, 25]. Several methods have been developed to estimate the effective DC properties of composites, such as the average energy method [26, 27], generalized Landau method [28], variational method [29] and the decoupling approximation [30]. For AC properties, Gu et al. [31] have formulated a theory for estimating the effective response of composites with an applied AC field of the form $\mathrm{E}_0 \sin \omega t$, based on the generalized Landau method and quasi-static approximation. Wei et al. further generalized the theory to cover composites under both DC and AC applied fields [32, 33] and under both fundamental and third-harmonic AC fields [34]. Recently, the general connection between DC and AC effective coefficients for the simple applied field E_0 and $\mathrm{E}_0 \sin(\omega t)$ has been proposed [35], which can be applied to all isotropic and weakly nonlinear composites.

Because the geometry of composite constituents can greatly affects the effective properties of composites, many published work have been devoted to the cases of nonspherical or noncylindrical inclusions. For example, the effective response of composites with slightly nonspherical inclusions was evaluated at finite frequencies [36], the shape effect of strongly nonlinear dielectric composite with elliptic cylindrical inclusions was evaluated by the decoupling approximation [37] and the effect of the orientation of ellipsoidal inclusions on the effective response has been analyzed by Giordano [38]. Lakhtakia et al. [39] has developed the Maxwell Garnett formalism for weakly nonlinear bianisotropic composites in which both the ellipsoidal inclusions and medium are anisotropic. Lakhtakia and Lakhtakia [40] generalized the Bruggeman formalism to anisotropic nonlinear composites with randomly distributed and similarly oriented ellipsoidal inclusions. Mackay [41] has used the strong-permittivity-fluctuation theory, which incorporates higher-order statistics of phase distributions, to estimate numerically the effective properties of anisotropic composites with third-order nonlinearity ellipsoidal inclusions. Gao et al. [42] have investigated strongly nonlinear two-dimensional isotropic composites in which one component is elliptic cylindrical in shape while the other is

perfect cylinders. The third-order enhancement of two dimensional semiconductor-insulator composites with identical elliptic cylinders has been explored by Yang et al. [43], where the frequency dependence and the effect of geometric anisotropy were reported. The treatment of two dimensional and isotropic nonlinear elliptical composites, including a distribution of inclusion shapes was also reported recently by Thongsri and Natenapit [44]. The analytic expression of the third-order effective nonlinear coefficient was derived for weakly nonlinear and dilute elliptical inclusions and the effective properties of high-order nonlinearity enhancement could be predicted but in numerical forms.

For more accurate predictions of nonlinear responses, the higher-order effective coefficients can not be neglected in many cases. However, the scope of the theoretical works reported to date concerning the higher-order response is very limited. Therefore, in this part, we focus on the higher-order nonlinear responses of weakly nonlinear composites. The structure investigated consists of weakly nonlinear inclusions distributed in a linear dielectric host. The nonlinearity in the inclusions is kept up to the fifth order while most published works considered nonlinearity of the composite constituents up to only the third order. The general formulae for computing the effective DC coefficients up to the ninth-order are derived using the perturbation method and the Landau formula (Sections 6.1.2 and 6.1.3). Then we apply these formula to predict the inclusion shape effects on the effective DC response of a weakly nonlinear composite with elliptic cylindrical inclusions (Sections 6.1.4 and 6.1.5). Finally, the quasi-static AC responses of weakly nonlinear composites subject to an applied AC electric field of the forms $\mathrm{E}_0 \sin(\omega t)$ and $\mathrm{E}_1 \sin \omega t + \mathrm{E}_3 \sin 3\omega t$ are investigated, and the general relationships between effective DC and AC coefficients are derived (Sections 6.2.1 and 6.2.2). The methodologies and results shown in this nonlinear part are from our published work in Refs. [35] and [45].

CHAPTER II

Theoretical Background

In this chapter, some basic concepts of electromagnetic fields in continuous media are briefly introduced. The definitions of the (complex) permittivity and the (complex) permeability are given. Losses due to electromagnetic wave propagations are investigated, resulting in the condition for the imaginary parts of the permittivity and the permeability. Next, nonlinear dielectric media under a static field is considered and the definitions of the nonlinear dielectric coefficients are given. Because the inclusions of nonlinear dielectric composites investigated in this thesis have an elliptic cylindrical shape, the general solution of Laplace equation in elliptic cylindrical coordinates is also demonstrated.

2.1 Electromagnetic Fields in Linear Media

2.1.1 Complex Permittivity and Complex Permeability

The electromagnetic fields in a macroscopic medium without free charge and free current densities satisfy Maxwell Equations

$$\nabla \cdot \mathbf{D} = 0, \tag{2.1}$$

$$\nabla \times \mathbf{E} = -\frac{\partial \mathbf{B}}{\partial t}, \tag{2.2}$$

$$\nabla \cdot \mathbf{B} = 0, \tag{2.3}$$

$$\nabla \times \mathbf{H} = \frac{\partial \mathbf{D}}{\partial t}, \tag{2.4}$$

where the electric displacement ($\mathbf{D}$) and the magnetic induction ($\mathbf{B}$) relate to the electric field ($\mathbf{E}$) and the magnetic field intensity ($\mathbf{H}$) via the Polarization ($\mathbf{P}$) and

Magnetization ($\mathbf{M}$) of the medium, respectively, as

$$\mathbf{D} = \varepsilon_0 \mathbf{E} + \mathbf{P}, \tag{2.5}$$

$$\mathbf{B} = \mu_0(\mathbf{H} + \mathbf{M}). \tag{2.6}$$

In order to simplify this type of problem, it is customary to Fourier analyze the fields as

$$\mathbf{F}(\mathbf{r}, t) = \int_{-\infty}^{\infty} \tilde{\mathbf{F}}(\mathbf{r}, \omega) e^{-i\omega t} d\omega, \tag{2.7}$$

where $\tilde{\mathbf{F}}(\mathbf{r}, t)$ represents all the vector fields that appear in the the Maxwell equations together with the constitutive relation (2.5) and (2.6). When look closely, we may notice that Eq. (2.7) is similar to the linear combination of the complex field $\tilde{\mathbf{F}}(\mathbf{r}, \omega) e^{-i\omega t}$ with different frequencies (ω). Therefore it is useful to study the effects of these complex fields at a particular frequency then get the solution of real problems by the linear combination (2.7). When using the Fourier integrals, the Maxwell equations become

$$\nabla \cdot \tilde{\mathbf{D}}(\mathbf{r}) = 0, \tag{2.8}$$

$$\nabla \times \tilde{\mathbf{E}}(\mathbf{r}) = i\omega \tilde{\mathbf{B}}(\mathbf{r}), \tag{2.9}$$

$$\nabla \cdot \tilde{\mathbf{B}}(\mathbf{r}) = 0, \tag{2.10}$$

$$\nabla \times \tilde{\mathbf{H}}(\mathbf{r}) = -i\omega \tilde{\mathbf{D}}(\mathbf{r}), \tag{2.11}$$

with

$$\tilde{\mathbf{D}}(\mathbf{r}) = \varepsilon_0 \tilde{\mathbf{E}}(\mathbf{r}) + \tilde{\mathbf{P}}(\mathbf{r}), \tag{2.12}$$

$$\tilde{\mathbf{B}}(\mathbf{r}) = \mu_0(\tilde{\mathbf{H}}(\mathbf{r}) + \tilde{\mathbf{M}}(\mathbf{r})), \tag{2.13}$$

where the ω dependence has been omitted for compact notations. A number of theoretical models employed to analyze the response of macroscopic media under these complex fields indicate that the polarization and the magnetization should be written as

$$\tilde{\mathbf{P}} = \varepsilon_0 \tilde{\chi}_{\mathrm{E}}(\omega) \tilde{\mathbf{E}}, \tag{2.14}$$

$$\tilde{\mathbf{M}} = \tilde{\chi}_{\mathrm{M}}(\omega) \tilde{\mathbf{H}}, \tag{2.15}$$

where $\tilde{\chi}_{\rm E}(\omega)$ and $\tilde{\chi}_{\rm M}(\omega)$ are the complex electric and magnetic susceptibilities, respectively. These quantities are complex because they come out from the analyses of responses of media with complex applied fields, for example, the well-known Drude model. With these two relations, the $\tilde{\mathbf{D}}-\tilde{\mathbf{E}}$ and $\tilde{\mathbf{B}}-\tilde{\mathbf{H}}$ relations can be constructed as

$$\tilde{\mathbf{D}} = \varepsilon(\omega)\tilde{\mathbf{E}}, \tag{2.16}$$

$$\tilde{\mathbf{B}} = \mu(\omega)\tilde{\mathbf{H}}, \tag{2.17}$$

where $\varepsilon=\varepsilon_0(1+\tilde{\chi}_E)$ and $\mu=\mu_0(1+\tilde{\chi}_M)$ are the complex permittivity and the complex permeability, respectively.

2.1.2 Electromagnetic Losses in Linear Media

In electromagnetic theory, the magnitude and the direction of the power flow can be calculated by the average Poynting vector

$$\mathbf{S}_{av} = \frac{1}{2}\mathrm{Re}\{\tilde{\mathbf{E}}\times\tilde{\mathbf{H}}^*\}. \tag{2.18}$$

So the average energy per unit time flowing out of an arbitrary closed surface S is

$$\frac{1}{2}\mathrm{Re}\Big\{\oint_S \tilde{\mathbf{E}}\times\tilde{\mathbf{H}}^*\cdot\hat{\mathbf{n}}da\Big\} = \frac{1}{2}\mathrm{Re}\Big\{\int_V \nabla\cdot(\tilde{\mathbf{E}}\times\tilde{\mathbf{H}}^*)dV\Big\}. \tag{2.19}$$

Using $\nabla\cdot(\tilde{\mathbf{E}}\times\tilde{\mathbf{H}}^*)=\tilde{\mathbf{H}}^*\cdot\nabla\times\tilde{\mathbf{E}}-\tilde{\mathbf{E}}\cdot(\nabla\times\tilde{\mathbf{H}}^*)=i\omega(\mu|\tilde{\mathbf{H}}|^2+\mu|\tilde{\mathbf{E}}|^2)$, we get

$$\begin{aligned}
\frac{1}{2}\mathrm{Re}\Big\{\oint \tilde{\mathbf{E}}\times\tilde{\mathbf{H}}^*\cdot\hat{\mathbf{n}}da\Big\} &= \frac{1}{2}\mathrm{Re}\Big\{i\omega\int_V(\mu|\tilde{\mathbf{H}}|^2+\varepsilon|\tilde{\mathbf{E}}|^2)dV\Big\} \\
&= -\frac{\omega}{2}\mathrm{Im}\Big\{\int_V(\mu|\tilde{\mathbf{H}}|^2+\varepsilon|\tilde{\mathbf{E}}|^2)dV\Big\} \\
\frac{1}{2}\mathrm{Re}\Big\{\oint \tilde{\mathbf{E}}\times\tilde{\mathbf{H}}^*\cdot\hat{\mathbf{n}}da\Big\} &= -\frac{\omega}{2}\int_V(\mathrm{Im}\{\mu\}|\tilde{\mathbf{H}}|^2+\mathrm{Im}\{\varepsilon\}|\tilde{\mathbf{E}}|^2)dV.
\end{aligned} \tag{2.20}$$

Since there should be some part of the electromagnetic energy converted into heat, the right-hand side of Eq. (2.20) should be negative, which means that

$$\int_V(\mathrm{Im}\{\mu\}|\tilde{\mathbf{H}}|^2+\mathrm{Im}\{\varepsilon\}|\tilde{\mathbf{E}}|^2)dV>0. \tag{2.21}$$

The two terms on the left side of Eq. (2.21) are losses due to the electric and magnetic fields, respectively. Since the energy dissipations from the fields should

always be positive, we assume that

$$\mathrm{Im}\{\varepsilon\} > 0 \quad \text{and} \quad \mathrm{Im}\{\mu\} > 0, \tag{2.22}$$

which indicates that ε and μ must lie on the upper half of the complex plane. This is the so-called passivity condition, which expresses the fact that media can only absorb the energy but not emit. Moreover, this condition is satisfied by many models of the permittivity and permeability concerned in our analyses and is the basic assumption of the derivation of the negative index conditions in Chapters 3 and 5.

2.2 Nonlinear Dielectric Media

2.2.1 Linear and Nonlinear Polarizations

For dielectric media in a static field, the polarization relates linearly to the electric field as

$$\mathbf{P} = \varepsilon_0 \chi_{\mathrm{E}} \mathbf{E}, \tag{2.23}$$

where χ_{E} is the linear (first-order) susceptibility. So the electric displacement takes the form

$$\mathbf{D} = \varepsilon_0 \mathbf{E} + \mathbf{P} = \varepsilon_0 (1 + \chi_e) \mathbf{E} = \varepsilon \mathbf{E}, \tag{2.24}$$

where ε is the permittivity or the first-order dielectric coefficient. Notice that Eqs. (2.23) and (2.24) are similar to Eqs. (2.14) and (2.16), except that the electric field is now static and the parameters χ_{E} and ε are real.

If the electric field is high enough, the polarization will also depend on the higher powers of the electric field. For example, suppose that the electric field is along an x-axis, the polarization takes the form

$$\mathrm{P}_x = \varepsilon_0 \chi_{\mathrm{E}}^{(1)} \mathrm{E}_x + \varepsilon_0 \chi_{\mathrm{E}}^{(2)} \mathrm{E}_x^2 + \varepsilon_0 \chi_{\mathrm{E}}^{(3)} \mathrm{E}_x^3 + ... \tag{2.25}$$

where $\chi_{\mathrm{E}}^{(n)}$ is called the nth-order nonlinear susceptibility. The condition for isotropy implies that the reversal of the electric field ($\mathrm{E}_x \to -\mathrm{E}_x$) should yields

the reversal of the polarization ($\mathrm{P}_x \to -\mathrm{P}_x$). Thus the terms with even powers should vanish, so we get

$$\mathrm{P}_x = \varepsilon_0 \chi_{\mathrm{E}}^{(1)} \mathrm{E}_x + \varepsilon_0 \chi_{\mathrm{E}}^{(3)} \mathrm{E}_x^3 + \varepsilon_0 \chi_{\mathrm{E}}^{(5)} \mathrm{E}_x^5 + \dots . \tag{2.26}$$

This can be written in full vector notation as

$$\mathbf{P} = \varepsilon_0 \chi_{\mathrm{E}}^{(1)} \mathbf{E} + \varepsilon_0 \chi_{\mathrm{E}}^{(3)} |\mathrm{E}|^2 \mathbf{E} + \varepsilon_0 \chi_{\mathrm{E}}^{(5)} |\mathrm{E}|^4 \mathbf{E} + ..., \tag{2.27}$$

where $\chi_{\mathrm{E}}^{(n)}$ is the nth-order nonlinear susceptibility. Hence the electric displacement also takes the power series form

$$\mathbf{D} = \varepsilon_0 \mathbf{E} + \mathbf{P} = \varepsilon \mathbf{E} + \chi |\mathrm{E}|^2 \mathbf{E} + \eta |\mathrm{E}|^4 \mathbf{E} + ..., \tag{2.28}$$

where $\varepsilon = \varepsilon_0 (1 + \chi_{\mathrm{E}}^{(1)})$, $\chi = \varepsilon_0 \chi_{\mathrm{E}}^{(3)}$, $\eta = \varepsilon_0 \chi_{\mathrm{E}}^{(5)}$, ... are called the first-, third- and fifth-order dielectric coefficients, respectively.

2.3 Laplace Equation in Elliptic Cylindrical Coordinates

In electrostatics, the electric potentials in linear dielectric media satisfy Laplace equation:

$$\nabla^2 \Phi = 0. \tag{2.29}$$

If the shapes of dielectric media are elliptic cylinders, it is useful to employ elliptic cylindrical coordinates (u, v) which relates to the cartesian coordinates as

$$x = a \cosh u \cos v, \tag{2.30}$$

$$y = a \sinh u \sin v, \tag{2.31}$$

where a is the focal length of the coordinate system. Fig. 2.1 show the characteristics of the elliptic cylindrical coordinates.

In terms of the elliptic cylindrical coordinates, the Laplace equation becomes

$$\frac{1}{a^2 \sqrt{\sinh^2 u + \sin^2 v}} \left(\frac{\partial^2 \Phi}{\partial u^2} + \frac{\partial^2 \Phi}{\partial v^2} \right) = 0, \tag{2.32}$$

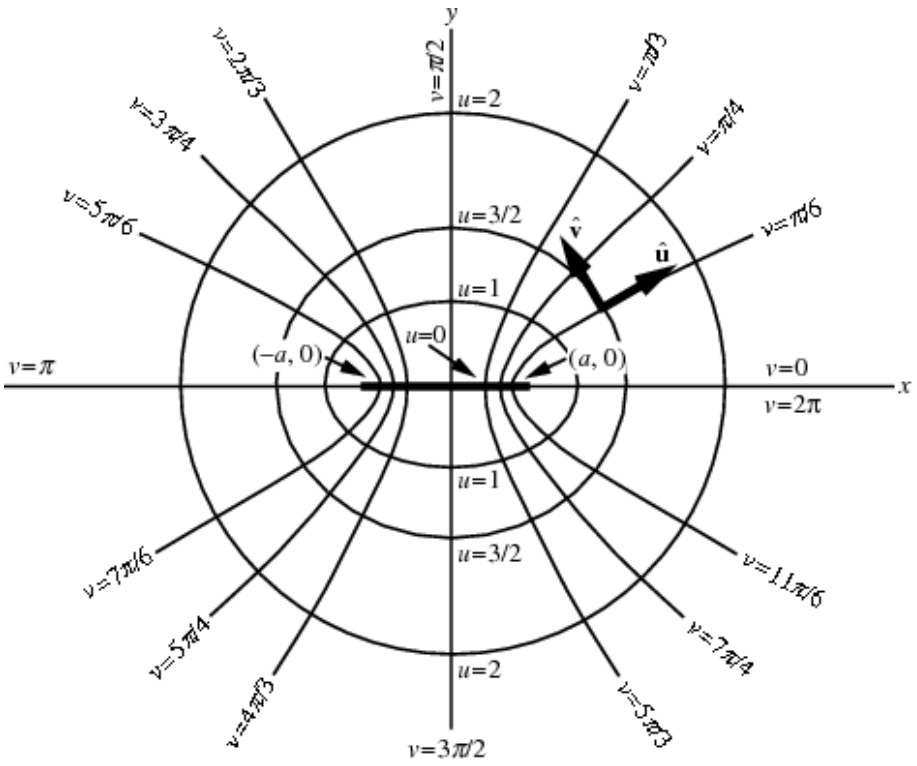

Figure 2.1: Elliptic cylindrical coordinates.

which has the general solution of the form [44]

$$\Phi(u,v) = \sum_{n=0}^{\infty} \left[(A_n \cosh(nu) + B_n e^{-nu}) \cos(nv) + (C_n \sinh(nu) + D_n e^{-nu}) \sin(nv) \right]. \tag{2.33}$$

This solution will be employed when solving the electric potentials of elliptic cylindrical inclusions in Chapter 6.

CHAPTER III

Lakhtakia-Depine Condition for a Negative Refractive Index

In this chapter, we show the derivation of a negative index condition using the negative phase velocity phenomena, in which the energy flow is antiparallel to the phase velocity of the wave. Although, in general, this condition does not imply a negative refraction, it can still be a good approximation for a negative refraction when the electric and magnetic losses ($\mathrm{Im}\{\varepsilon\}$ and $\mathrm{Im}\{\mu\}$) are small.

Consider a plane electromagnetic waves propagates along the z-axis in a linear isotropic medium whose relative permittivity and relative permeability are given by $\varepsilon_r(\omega) = \varepsilon(\omega)/\varepsilon_0$ and $\mu_r(\omega) = \mu(\omega)/\mu_0$, respectively, and subject to the passivity condition (Eq. (2.22))

$$\mathrm{Im}\{\varepsilon_r\} > 0 \quad \text{and} \quad \mathrm{Im}\{\mu_r\} > 0 \tag{3.1}$$

Let the electric field be along the x-axis so that

$$\tilde{\mathbf{E}}(\mathbf{r},t) \;=\; \mathrm{E}_0 e^{i(kz-\omega t)}\hat{\mathbf{x}}, \tag{3.2}$$

where E_0 is the amplitude and k is the wave number. It follows from Maxwell equations that

$$\boldsymbol{\nabla}\times\tilde{\mathbf{E}}(\mathbf{r},t) \;=\; i\omega\tilde{\mathbf{B}}(\mathbf{r},t) = i\omega\mu_0\mu_r(\omega)\tilde{\mathbf{H}}(\mathbf{r},t), \tag{3.3}$$

$$\boldsymbol{\nabla}\times\tilde{\mathbf{H}}(\mathbf{r},t) \;=\; -i\omega\tilde{\mathbf{D}}(\mathbf{r},t) = -i\omega\varepsilon_0\varepsilon_r(\omega)\tilde{\mathbf{E}}(\mathbf{r},t). \tag{3.4}$$

Hence we can obtain the magnetic field intensity as

$$\tilde{\mathbf{H}}(\mathbf{r},t) = \frac{1}{i\omega\mu_0\mu_r(\omega)}\boldsymbol{\nabla}\times\tilde{\mathbf{E}}(\mathbf{r},t) = \frac{k\mathrm{E}_0}{\omega\mu_0\mu_r(\omega)}e^{i(kz-\omega t)}\hat{\mathbf{y}}. \tag{3.5}$$

Applying the curl of Eq. (3.3) and using Eq. (3.4) yield

$$\begin{aligned}
\boldsymbol{\nabla}\times\boldsymbol{\nabla}\times\tilde{\mathbf{E}}(\mathbf{r},t) &= i\omega\mu_0\mu_r(\omega)\boldsymbol{\nabla}\times\tilde{\mathbf{H}}(\mathbf{r},t)\\
\boldsymbol{\nabla}(\boldsymbol{\nabla}\cdot\tilde{\mathbf{E}}(\mathbf{r},t))-\nabla^2\tilde{\mathbf{E}}(\mathbf{r},t) &= \omega^2\varepsilon_0\mu_0\varepsilon_r(\omega)\mu_r(\omega)\tilde{\mathbf{E}}(\mathbf{r},t)\\
k^2\tilde{\mathbf{E}}(\mathbf{r},t) &= \frac{\omega^2}{c^2}\varepsilon_r(\omega)\mu_r(\omega)\tilde{\mathbf{E}}(\mathbf{r},t). \qquad (3.6)
\end{aligned}$$

Therefore we obtain the dispersion relation as

$$k=\frac{\omega}{c}\sqrt{\varepsilon_r(\omega)\mu_r(\omega)}. \qquad (3.7)$$

The magnitude and direction of the power flow can be determined by the Poynting vector:

$$\begin{aligned}
\mathbf{S} &= \frac{1}{2}\mathrm{Re}\{\tilde{\mathbf{E}}(\mathbf{r},t)\times\tilde{\mathbf{H}}^*(\mathbf{r},t)\},\\
&= \frac{|\mathrm{E}_0|^2}{2\mu_0}\mathrm{Re}\left\{\frac{k}{\mu_r(\omega)}\right\}\exp(-2\mathrm{Im}\{k\}z)\hat{\mathbf{z}}. \qquad (3.8)
\end{aligned}$$

Since from Eq. (2.22), the relative permittivity and the relative permeability must lie on the upper-half of the complex plane. So we write

$$\varepsilon_r(\omega) = |\varepsilon_r(\omega)|e^{i\phi_\varepsilon}, \quad 0\le\phi_\varepsilon\le\pi, \qquad (3.9)$$

$$\mu_r(\omega) = |\mu_r(\omega)|e^{i\phi_\mu}, \quad 0\le\phi_\mu\le\pi. \qquad (3.10)$$

Consequently, the wave number takes the form

$$k_\pm=\pm\frac{\omega}{c}\sqrt{|\varepsilon_r(\omega)||\mu_r(\omega)|}e^{i(\phi_\varepsilon+\phi_\mu)/2}, \quad 0\le(\phi_\varepsilon+\phi_\mu)/2\le\pi, \qquad (3.11)$$

hence

$$\frac{k_\pm}{\mu_r(\omega)}=\pm\frac{\omega}{c}\sqrt{\frac{|\varepsilon_r(\omega)|}{|\mu_r(\omega)|}}e^{i(\phi_\varepsilon-\phi_\mu)/2}, \quad -\pi/2\le(\phi_\varepsilon-\phi_\mu)/2\le\pi/2. \qquad (3.12)$$

Using Eq. (3.12) in (3.8), we can conclude that the choice of k_+ always corresponds to the power flow in $+z$ direction and the choice of k_- always corresponds to the power flow in $-z$ direction. Rewriting Eq. (3.2) in terms of the real and imaginary parts of the wave number, we get

$$\tilde{\mathbf{E}}_\pm(\mathbf{r},t) = \mathrm{E}_0e^{-\mathrm{Im}\{k_\pm\}}e^{i(\mathrm{Re}\{k_\pm\}z-\omega t)}\hat{\mathbf{x}}. \qquad (3.13)$$

To derive the conditions for negative refractive index, we use the condition that the phase velocity and the power flow must be in the opposite directions. Since k_+ corresponds to the power flow in the $+z$ direction and k_- corresponds to the power flow in $-z$ direction, It can be seen from the exponential in the right hand side of Eq. (3.13) that the phase velocity is antiparallel to the power flow if

$$\mathrm{Re}\{k_+\} < 0 \quad \text{or} \quad \mathrm{Re}\{k_-\} > 0, \tag{3.14}$$

With the definition of complex refractive index $n = ck/\omega$, Eq. (3.14) can be written as

$$\mathrm{Re}\{n_+\} < 0 \quad \text{or} \quad \mathrm{Re}\{n_-\} > 0,, \tag{3.15}$$

where n_+ and n_- are the refractive index that lie on the upper half and the lower half complex plane, respectively. Using the result presented in Appendix A, Eqs. (3.14) can be written in terms of the relative permittivity and the relative permeability as

$$\varepsilon_r' \sqrt{\mu_r'^2 + \mu_r''^2} + \mu_r' \sqrt{\varepsilon_r'^2 + \varepsilon_r''^2} < 0, \tag{3.16}$$

where $\varepsilon_r' = \mathrm{Re}\{\varepsilon_r\}$, $\varepsilon_r'' = \mathrm{Im}\{\varepsilon_r\}$, $\mu_r' = \mathrm{Re}\{\mu_r\}$ and $\mu_r'' = \mathrm{Im}\{\mu_r\}$. It is obvious that if $\varepsilon_r' < 0$ and $\mu_r' < 0$, Eq. (2.39) is satisfied. This simple condition will be employed later in designing our composites.

CHAPTER IV

A Composite with Negative Refractive Index at Infrared Frequencies

In this chapter, we present a simple structure of composite which consists of two types of randomly distributed nonmagnetic spheres. Under the application of the external electromagnetic fields with the wavelength much larger than the diameters of the spheres (long-wavelength or quasi-static limit), Clausius-Mossotti relations [46] can be employed to evaluate the effective permittivity and the effective permeability of the composite. Then the design procedure for making their real parts to be both negative are presented.

Composites of Randomly Distributed Spheres

Effective Permittivity and Effective Permeability

Consider a composite of randomly distributed two groups of spheres (Figure 4.1). The first one have radius r_1 and the relative permittivity $\varepsilon_{r1} = \varepsilon_1/\varepsilon_0$ while the second one have radius r_2 and the relative permittivity $\varepsilon_{r2} = \varepsilon_2/\varepsilon_0$. Both groups are assumed to be nonmagnetic so their relative permeabilities are equal to unity.

If the wavelength of an electromagnetic wave that passes through the composite is much larger than the sizes of the spheres, the diffraction effects can be omitted so the structure of the composite can not be resolved then it can be treated as a homogeneous effective medium. This condition is called the long-wavelength

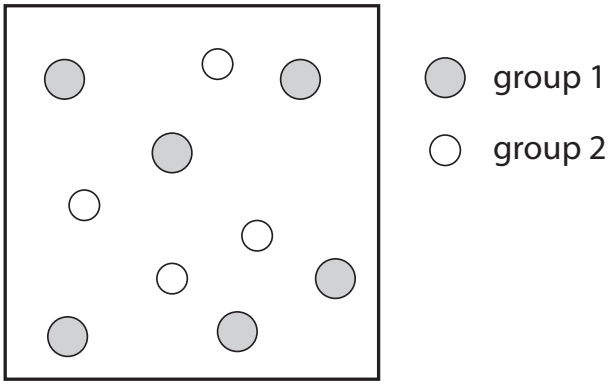

Figure 4.1: A composite consisting of two group of spheres randomly distributed in a free space

or quasi-static limit. The effective relative permittivity and the effective relative permeability of the composite can be estimated using the Clausius-Mossotti relations for mixtures of two types of molecules [46]

$$\frac{\mathrm{N}_1\alpha_{e1} + \mathrm{N}_2\alpha_{e2}}{3\varepsilon_0} = \left(\frac{\varepsilon_r^{\text{eff}} - 1}{\varepsilon_r^{\text{eff}} + 2}\right) \tag{4.1}$$

$$\frac{\mathrm{N}_1\alpha_{m1} + \mathrm{N}_2\alpha_{m2}}{3} = \left(\frac{\mu_r^{\text{eff}} - 1}{\mu_r^{\text{eff}} + 2}\right), \tag{4.2}$$

where α_{e1} and α_{m1} are electric and magnetic polarizabilites of type 1 molecules, α_{e2} and α_{m2} are electric and magnetic polarizabilites of the type 2 molecules. The numbers of molecules per unit volume of type 1 (N_1) and type 2 (N_2) are related to the volume fractions via $f_1 = \frac{4}{3}\pi r^3 N_1$ and $f_2 = \frac{4}{3}\pi r^3 N_2$, respectively.

To apply the Clausius-Mossotti relations, each sphere in the composite is treated as a molecule with both electric and magnetic polarizabilites. From Appendix B, the electric and magnetic polarizabilities of the first group of spheres are

$$\alpha_{e1} = 6\pi\varepsilon_0 i a_1^{(1)}/k_0^3, \tag{4.3}$$

$$\alpha_{m1} = 6\pi i b_1^{(1)}/k_0^3, \tag{4.4}$$

and for the second group are

$$\alpha_{e2} = 6\pi\varepsilon_0 i a_1^{(2)}/k_0^3, \tag{4.5}$$

$$\alpha_{m2} = 6\pi i b_1^{(2)}/k_0^3. \tag{4.6}$$

where $k_0 = \omega/c$ is the free space wave number, and the scattering coefficients $a_1^{(1)}, b_1^{(1)}, a_1^{(2)}$ and $b_1^{(2)}$ take the forms (Appendix B)

$$a_1^{(1)} = \frac{n_1\psi_1(n_1x_1)\psi_1'(x_1) - \psi_1(x_1)\psi_1'(n_1x_1)}{n_1\psi_1(n_1x_1)\xi_1'(x_1) - \xi_1(x_1)\psi_1'(n_1x_1)}, \tag{4.7}$$

$$b_1^{(1)} = \frac{\psi_1(n_1x_1)\psi_1'(x_1) - n_1\psi_1(x_1)\psi_1'(n_1x_1)}{\psi_1(n_1x_1)\xi_1'(x_1) - n_1\xi_1(x_1)\psi_1'(n_1x_1)}, \tag{4.8}$$

$$a_1^{(2)} = \frac{n_2\psi_1(n_2x_2)\psi_1'(x_2) - \psi_1(x_2)\psi_1'(n_2x_2)}{n_2\psi_1(n_2x_2)\xi_1'(x_2) - \xi_1(x_2)\psi_1'(n_2x_2)}, \tag{4.9}$$

$$b_1^{(2)} = \frac{\psi_1(n_2x_2)\psi_1'(x_2) - n_2\psi_1(x_2)\psi_1'(n_2x_2)}{\psi_1(n_2x_2)\xi_1'(x_2) - n_2\xi_1(x_2)\psi_1'(n_2x_2)}, \tag{4.10}$$

where $n_1 = \varepsilon_{r1}^2$, $n_2 = \varepsilon_{r1}^2$, $x_1 = k_0r_1$, $x_2 = k_0r_2$, and $\psi_1(z) = zj_1(z)$ and $\xi_1(z) = zh_1^{(1)}(z)$ are the Riccati-Bessel functions which relate to the spherical Bessel functions of the first and the third kinds, respectively. The prime denotes differentiation with respect to the argument.

Using Eqs (4.3)-(4.6) in Eqs (4.1) and (4.2), and solving for the effective relative permittivity and the effective relative permeability yield

$$\varepsilon_r^{\text{eff}} = \frac{k_0^3 + 4\pi i(N_1a_1^{(1)} + N_2a_1^{(2)})}{k_0^3 - 2\pi i(N_1a_1^{(1)} + N_2a_1^{(2)})}, \tag{4.11}$$

$$\mu_r^{\text{eff}} = \frac{k_0^3 + 4\pi i(N_1b_1^{(1)} + N_2b_1^{(2)})}{k_0^3 - 2\pi i(N_1b_1^{(1)} + N_2b_1^{(2)})}. \tag{4.12}$$

Expressions (4.11) and (4.12) show that the effective properties of the composite depend on the frequency of the wave (via $k_0 = \omega/c$) along with the densities, radii and permittivities of the two groups of spheres.

Negative Permeability

We will show how to obtain negative permeability $\text{Re}\{\mu_r^{\text{eff}}\} < 0$ by using the sphere of group 1. Notice that the effective permeability (Eq. (4.12)) depends on the properties of spheres of group 1 via the scattering coefficient $b_1^{(1)}$. If the denominator in Eq. (4.6) approaches zero, $b_1^{(1)}$ approaches ∞, resulting in $\lim_{b_1^{(1)}\to\infty} \mu_r^{\texttt{eff}} = -2$. Therefore we focus on the scattering coefficient resonance condition:

$$\psi_1(n_1x_1)\xi_1'(x_1) - n_1\xi_1(x_1)\psi_1'(n_1x_1) = 0. \tag{4.13}$$

By assuming that $\mathrm{Im}\{\varepsilon_{r1}\}$ is negligible, we arrive at

$$j_0(n_1 x_1) = \frac{\sin(n_1 x_1)}{n_1 x_1} = 0, \tag{4.14}$$

which imply that $n_1 x_1 = m\pi, m = 1, 2, 3, \ldots$. Hence the fundamental resonance frequency (m = 1) is

$$\omega_m^{res} = \frac{\pi c}{r_1 \sqrt{\varepsilon_{r1}}}. \tag{4.15}$$

The resonance frequencies of higher harmonics are not considered here because they provide smaller wavelengths, which may result in the inapplicability of the Clausius-Mossotti relations (because the derivation of Clausius-Mossotti relations is based on the long-wavelength or quasi-static approximation).

Using $\omega_m^{res} = 2\pi c/\lambda_0^{res}$ yields the ratio between the resonance wavelength and the diameter of the spheres of group 1

$$\frac{\lambda_0^{res}}{2r_1} = \sqrt{\varepsilon_{r1}}. \tag{4.16}$$

Since the wavelength should be much greater than the diameters of the spheres for the the Clausius-Mossotti relations to be applicable and for the composite to be treated as an effective homogeneous medium, we assume the minimum requirement for the long-wavelength limit condition to be $\lambda_0^{res}/2r_1 > 10$. This assumption was employed and tested with numerical calculations in [8]. Using this condition in Eq. (4.16), we obtain the condition for the permittivity of the group 1 sphere as $\varepsilon_{r1} > 100$, which is required to drive the magnetic scattering coefficient resonance.

The high values of the relative permittivity can be achieved at infrared frequencies by using polaritonic materials. The relative permittivity of polaritonic materials satisfy

$$\varepsilon_{r1}(\omega) = \varepsilon(\infty)\left(1 + \frac{\omega_L^2 - \omega_T^2}{\omega_T^2 - \omega^2 - i\omega\gamma}\right) \tag{4.17}$$

where $\varepsilon(\infty)$ is the high-frequency limit of the permittivity, ω_L is the longitudinal optical phonon frequency, ω_T is the transverse optical phonon frequency and γ is the damping coefficient.

Following the work of wheeler et al. [8], we choose $LiTaO_3$ as the polaritonic material for the spheres of group 1, which have the following parameters: $\varepsilon(\infty) = 13.4$, $\omega_L = 2\pi \times 7.46$ THz, $\omega_T = 2\pi \times 4.25$ THz and $\gamma = 2\pi \times 0.15$ THz.

Figure 4.2 shows that the condition $\mathrm{Re}\{\varepsilon_r\} > 100$ is satisfied with low electric loss ($\mathrm{Im}\{\varepsilon_r\}$) at the frequencies $3.5 - 3.8$ THz. At this frequency range, the value of $\mathrm{Re}\{\varepsilon_{r1}\}$ is between $100 - 150$, which corresponds (using eq. (4.15)) to the radii of $3.22 - 4.29$ μm. Therefore the radii of group 1 spheres must be chosen within this range.

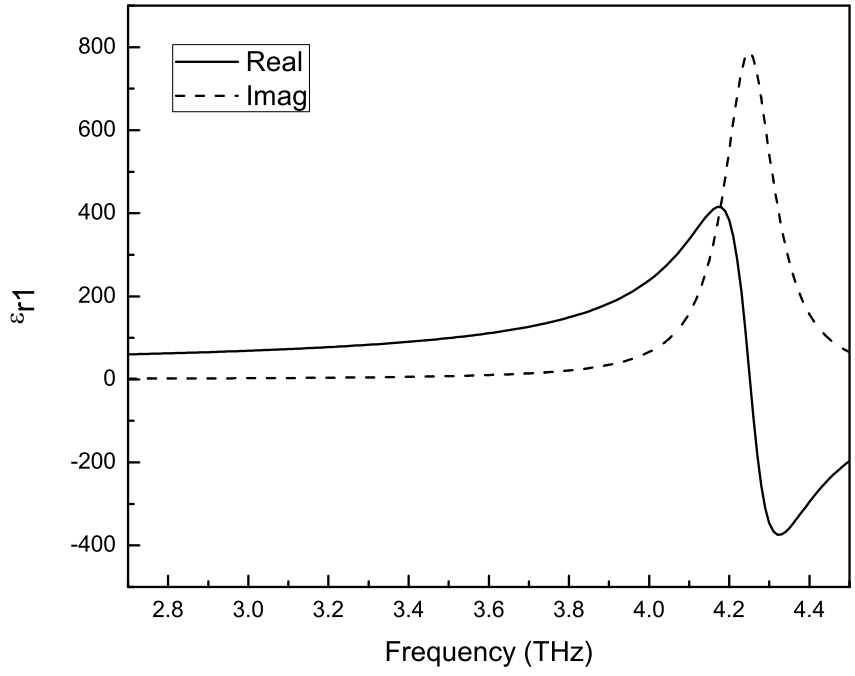

Figure 4.2: Characteristics of the relative permittivity of $LiTaO_3$ at frequencies between $2.7 - 4.5$ THz

As an example, we consider the effective relative permeability (μ_r^{eff}) of randomly distributed $LiTaO_3$ spheres with the following parameters: $f_1 = 0.27$, $f_2 = 0$ and $r_1 = 4$ μm. Figure 4.3 shows that the resonance frequency, where the $\mathrm{Re}\{\mu_r^{\mathrm{eff}}\}$ is most negative, is centered about 3.58 THz.

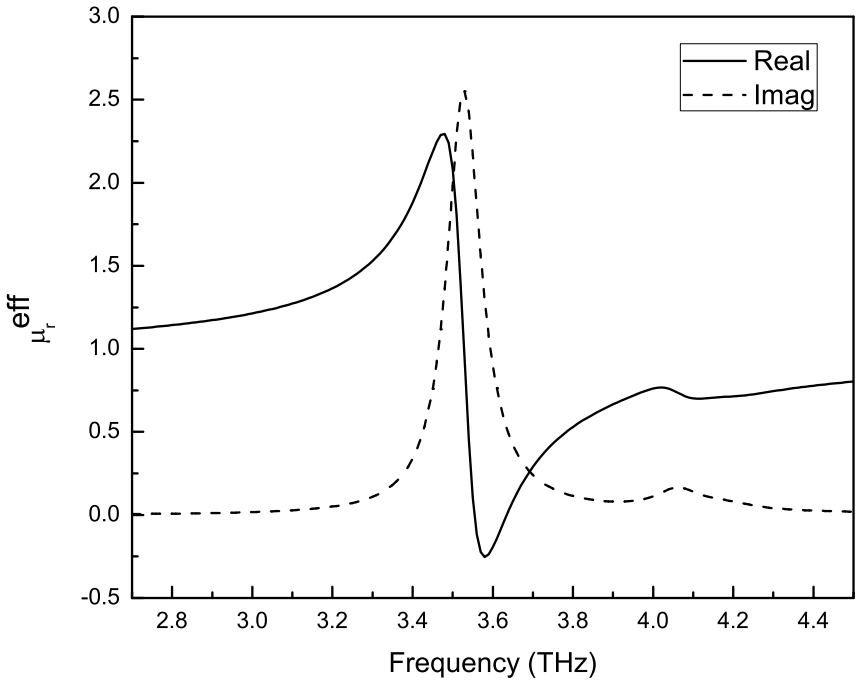

Figure 4.3: Characteristics of the relative effective permeabilities of the composites with $f_1 = 0.27$, $f_2 = 0$ and $r_1 = 4$ μm

Negative Permittivity

For spheres of group 2 to contribute a negative effective permittivity, the same method described in the previous section can be used to drive the resonance in $a_1^{(2)}$. However, it turns out that the resonance frequency in this case is higher than that of $b_1^{(1)}$, which requires even higher value of the relative permittivity. So instead of using the resonance of $a_1^{(2)}$, we use the resonance of $\varepsilon_r^{\text{eff}}$. The scattering coefficients $a_1^{(1)}$, $a_1^{(2)}$ can be expanded as

$$a_1^{(1)} = -i\frac{2}{3}\left(\frac{\varepsilon_{r1}-1}{\varepsilon_{r1}+2}\right)x_1^3 + O(x_1^5). \tag{4.18}$$

$$a_1^{(2)} = -i\frac{2}{3}\left(\frac{\varepsilon_{r2}-1}{\varepsilon_{r2}+2}\right)x_2^3 + O(x_2^5). \tag{4.19}$$

Using these series expansions in Eq. (4.11) and setting the denominator to zero, we get

$$f_1\left(\frac{\varepsilon_{r1}-1}{\varepsilon_{r1}+2}\right) + f_2\left(\frac{\varepsilon_{r1}-1}{\varepsilon_{r1}+2}\right) = 1. \tag{4.20}$$

Notice that, from the previous section $\varepsilon_{r1} \approx 100$ so $(\varepsilon_{r1}-1)/(\varepsilon_{r1}+2) \approx 1$. Therefore Eqs. (4.20) becomes

$$f_1 + f_2\left(\frac{\varepsilon_{r2}-1}{\varepsilon_{r2}+2}\right) = 1. \tag{4.21}$$

Solving for ε_{r2} yields

$$\varepsilon_{r2} = \frac{2f_1 - f_2 - 2}{1 - f_1 - f_2}, \tag{4.22}$$

Because $f_1 + f_2 < 1$, the relative permittivity (ε_{r2}) given in Eq. (4.22) is always negative.

It is well known in solid state physics that the permittivity model of free electron gas distributed uniformly over positively charged cores in the background can provide the required negative values. This so-called Drude model is depicted in Fig. 4.4, where the black dots indicate free electrons and the white spheres are positive background ions. Without applied electric field, electrons are free to roam around and the collisions can take place between other electrons and positive ions. If an applied electric field ($\mathbf{E}$) is present, the equation of motion for each electron

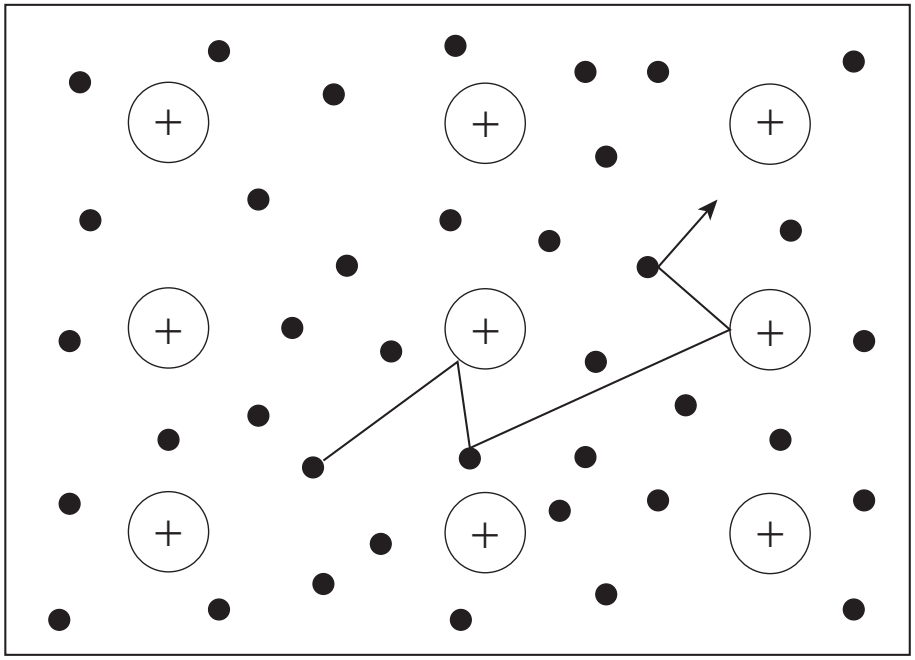

Figure 4.4: Drude model of free electron gas (black dots) on positive ion background (white spheres).

reads

$$m_e \frac{d^2\mathbf{r}}{dt^2} = -e\mathbf{E} - m_e\gamma\frac{d\mathbf{r}}{dt}, \tag{4.23}$$

where m_e is the electron mass, e is the charge of the electron and γ is the damping coefficient. On the right-hand side of Eq. (4.23), the first term is the electric force and the second term (the damping term) is due to the effects of collisions between other electrons and positive ions. Assuming that $\mathbf{E}$ and $\mathbf{r}$ have the time dependence $e^{-i\omega t}$, we get

$$\mathbf{r} = \frac{1}{\omega^2 + i\omega\gamma}\frac{e\mathbf{E}}{m_e}. \tag{4.24}$$

If the number of electrons per unit volume is N, the polarization is $\mathbf{P} = -e\mathrm{N}\mathbf{r}$. Thus

$$\mathbf{P} = -\frac{1}{\omega^2 + i\omega\gamma}\frac{e^2N}{m_e}\mathbf{E} = \epsilon_0\chi_E\mathbf{E}, \tag{4.25}$$

where $\chi_E = -\frac{1}{\omega^2+i\omega\gamma}\frac{e^2N}{m_e\varepsilon_0}$. With the definition of the relative permittivity $\varepsilon_{r2} = 1 + \chi_E$, we obtain

$$\varepsilon_{r2} = 1 - \frac{\omega_p^2}{\omega^2 + i\omega\gamma}, \tag{4.26}$$

where $\omega_p = e^2N/m_e\varepsilon_0$ is the plasma frequency. Notice that by neglecting the damping coefficient (γ), the relative permittivity is negative below the plasma frequency. This permittivity model is valid for metals (since they contains enormous numbers of free electrons) and also some doped semiconductors (Hence the name Drude model semiconductor). Because typical metals have plasma frequency in the ultraviolet region, they are not useful here. However, semiconductors can be made, via doping process, to have the plasma frequency in the required infrared region [8]. Thus the Drude model semiconductor will be used as a material for group 2 spheres.

Substituting Eqs. (4.26) into (4.22) and neglecting the damping coefficient, we get the condition for the plasma frequency as

$$\omega_p = \omega^{res}\sqrt{\frac{3(1-f_1)}{1-f_1-f_2}}, \tag{4.27}$$

where ω^{res} is the resonance frequency that make the denominator of $\varepsilon_r^{\text{eff}}$ in Eq. (4.11) to be zero. Therefore the value of $\varepsilon_r^{\text{eff}}$ should be very high around this frequency.

As an example, Let consider a structures of randomly distributed Drude semiconductor spheres. We choose $\omega^{res} = 2\pi \times 3.58$ THz, which corresponds to the magnetic resonance in the previous section. So, from Eq. (4.24), ω_p is about $2\pi \times 6.73$ THz. Other parameters are chosen as follows: $f_1 = 0$, $f_2 = 0.15$, $r_2 = 4\mu$m and $\gamma = \omega_p/100$. As shown in figures 4.5, The real part of $\varepsilon_r^{\text{eff}}$ have the peak negative value around 3.51 THz.

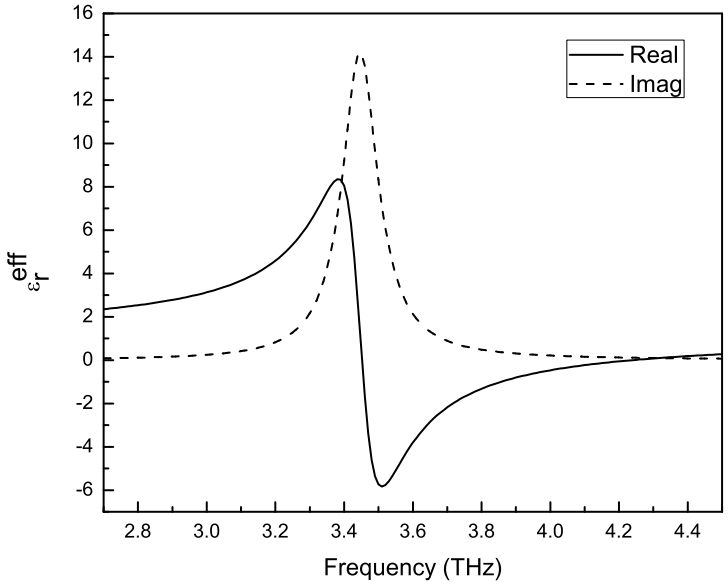

Figure 4.5: Characteristics of the relative effective permittivity of randomly distributed Drude semiconductor spheres. The parameters are $\omega_p = 2\pi \times 6.73$ THz, $f_1 = 0$, $f_2 = 0.15$ and $r_2 = 4$ μm.

Composites of $LiTaO_3$ and Drude semiconductor spheres

Now we combine the two group of spheres made of $LiTaO_3$ and Drude semiconductor. The permittivity resonance frequency (In section 4.1.3, it is ω^{res}) are chosen to be $2\pi \times 3.2$ THz in order to prevent the high losses in $\varepsilon_r^{\mathtt{eff}}$ and $\mu_r^{\mathtt{eff}}$ to coincide. The composite parameters are as follows: $f_1 = 0.27$, $f_2 = 0.15$, $r_1 = 4\mu$m and $r_2 = 4\mu$m. Fig. 4.6 and Fig. 4.7 show that the effective relative permittivity and the effective relative permeability are simultaneously negative. The refractive index is computed as $n^{\text{eff}} = \sqrt{\epsilon_r^{\text{eff}} \mu_r^{\text{eff}}}$ and ensuring that its imaginary part is positive so that the Lakhtakia-Depine relation (Eq. (3.16)) is satisfied with $\text{Re}\{n^{\text{eff}}\} < 0$. In Fig. 4.8, the graph of $\text{Re}\{n^{\text{eff}}\}$ shows negative values around 3.48 to 3.68 THz. Therefore this composite satisfy the Lakhtakia-Depine condition for negative refractive index around these infrared frequencies.

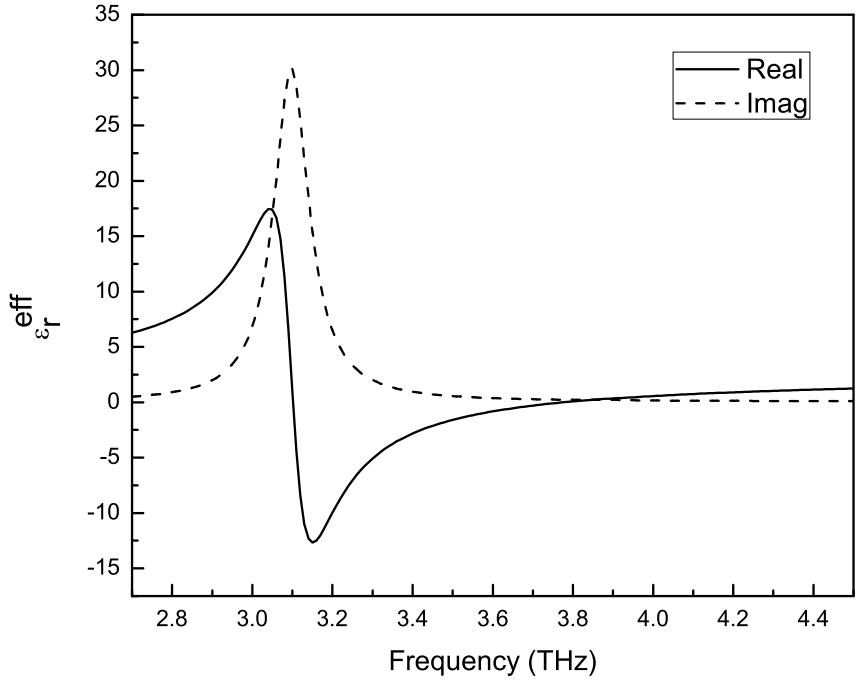

Figure 4.6: Characteristics of the relative effective permittivity of randomly distributed $LiTaO_3$ and Drude semiconductor spheres. The parameters are $\omega_p = 2\pi \times 3.2$ THz, $f_1 = 0.27$, $f_2 = 0.15$, $r_1 = 4$ μm and $r_2 = 4$ μm.

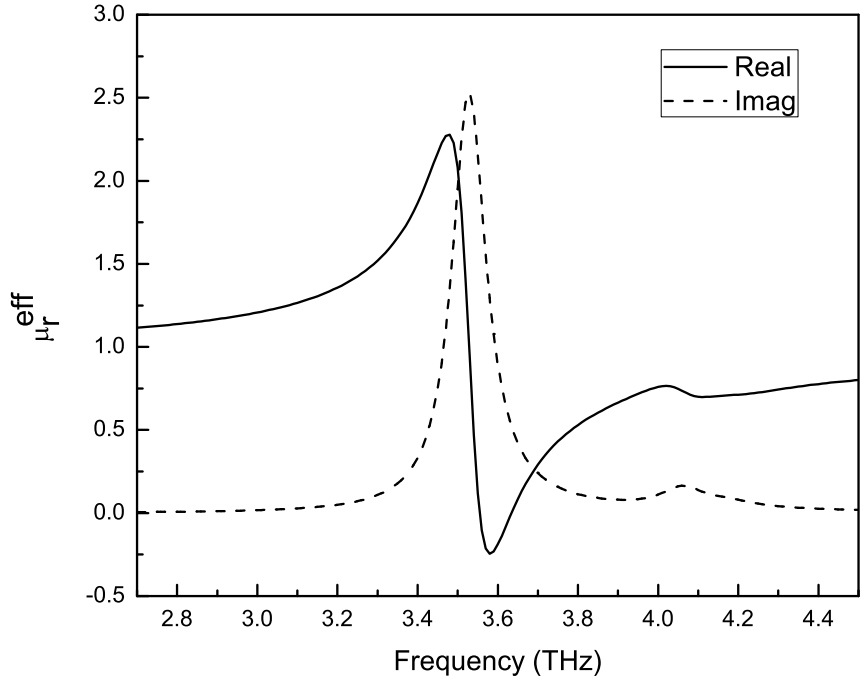

Figure 4.7: Characteristics of the relative effective permeability of randomly distributed $LiTaO_3$ and Drude semiconductor spheres. The parameters are $\omega_p = 2\pi \times 3.2$ THz, $f_1 = 0.27$, $f_2 = 0.15$, $r_1 = 4$ μm and $r_2 = 4$ μm.

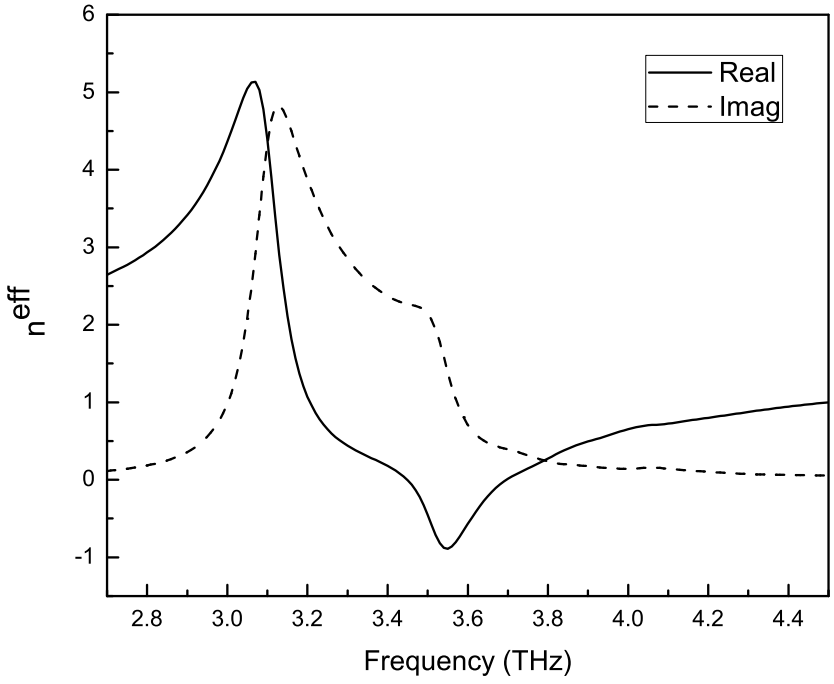

Figure 4.8: Characteristics of the complex refractive index of randomly distributed $LiTaO_3$ and Drude semiconductor spheres. The parameters are $\omega_p = 2\pi \times 3.2$ THz, $f_1 = 0.27$, $f_2 = 0.15$, $r_1 = 4$ μm and $r_2 = 4$ μm.

CHAPTER V

Negative Phase Velocity and Negative Refraction in Biaxial Anisotropic Lossy Media

Here, we focus on the characteristics of the plane wave propagations in biaxial anisotropic lossy media. In the medium principal axes (assumed here to be the x-, y- and z-axes), the relative permittivity and the relative permeability tensors take the forms:

$$\bar{\bar{\varepsilon}}_r = \begin{pmatrix} \varepsilon_{rx} & 0 & 0 \\ 0 & \varepsilon_{ry} & 0 \\ 0 & 0 & \varepsilon_{rz} \end{pmatrix} \quad \text{and} \quad \bar{\bar{\mu}}_r = \begin{pmatrix} \mu_{rx} & 0 & 0 \\ 0 & \mu_{ry} & 0 \\ 0 & 0 & \mu_{rz} \end{pmatrix}, \tag{5.1}$$

where the tensorial components are complex numbers, which subject to the passivity conditions:

$$\mathrm{Im}\{\varepsilon_{ri}\} > 0 \quad \text{and} \quad \mathrm{Im}\{\mu_{ri}\} > 0, \quad i = x, y, z. \tag{5.2}$$

Our investigation is divided into two parts. First we aim to obtain the general material condition for the negative phase velocity of uniform plane waves, in which the electric field is polarized along one of the medium principal axes. Secondly, we attempt to obtain the general condition for the negative refraction between the biaxial anisotropic lossy medium and free space. In both cases, the numerical calculations are also performed in order to show the consistency with the theoretical results.

5.1 Negative Phase Velocity for Uniform Plane Waves

Let us consider a uniform plane wave, with a z-polarized electric field, traveling parallel to the xy-plane in a biaxial anisotropic lossy medium as shown in Fig. 5.1. For this wave, we have

$$\mathbf{E} = \hat{\mathbf{z}} E_0 e^{i(k\hat{\boldsymbol{\rho}}\cdot\mathbf{r}-\omega t)}, \tag{5.3}$$

$$\mathbf{H} = \bar{\bar{\mu}}_r^{-1}\frac{k\hat{\boldsymbol{\rho}}\times\mathbf{E}}{\omega\mu_0} = \frac{kE_0}{\omega\mu_0}\left(\frac{\sin\phi}{\mu_{rx}}\hat{\mathbf{x}} - \frac{\cos\phi}{\mu_{ry}}\hat{\mathbf{y}}\right)e^{i(k\hat{\boldsymbol{\rho}}\cdot\mathbf{r}-\omega t)}, \tag{5.4}$$

where $\hat{\boldsymbol{\rho}}$ is the unit vector along the propagation direction and k is the wave number.

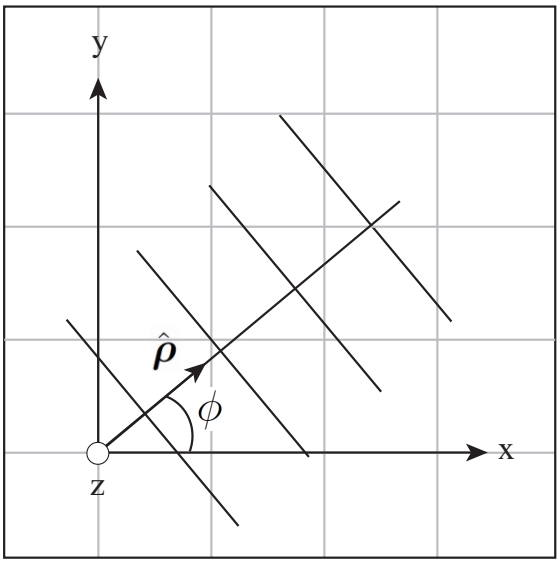

Figure 5.1: A uniform plane wave propagates in the biaxial anisotropic medium. The electric field polarization is along the z-axis and ϕ is the propagation angle.

From the Maxwell's equations, the dispersion relation is obtained as follows

$$k^2 = \frac{\omega^2}{c^2}\left(\frac{\varepsilon_{rz}\mu_{rx}\mu_{ry}}{\mu_{rx}\cos^2\phi + \mu_{ry}\sin^2\phi}\right). \tag{5.5}$$

For simplicity of our analysis, we write Eq. (5.5) in the simple form:

$$k^2 = \frac{\omega^2}{c^2}\varepsilon_{rz}\mu_{re}, \tag{5.6}$$

where

$$\mu_{re} = \frac{\mu_{rx}\mu_{ry}}{\mu_{rx}\cos^2\phi + \mu_{ry}\sin^2\phi}. \tag{5.7}$$

It can easily be shown that μ_{re} also lies on the upper half of the complex plane by considering its inverse:

$$\frac{1}{\mu_{re}} = \frac{\cos^2\phi}{\mu_{ry}} + \frac{\sin^2\phi}{\mu_{rx}}. \tag{5.8}$$

Since μ_{rx} and μ_{ry} are on the upper half plane, each term on the right and their sum must lie on the lower half plane. So the inverse of the sum must lie on the upper half plane.

The average Poynting vector for this wave is given by

$$\begin{aligned}\mathbf{S} = \frac{1}{2}\mathrm{Re}\{\mathbf{E}\times\mathbf{H}^*\} &= \frac{|E_0|^2}{2\omega\mu_0}\left[\hat{\mathbf{x}}\mathrm{Re}\left\{\frac{k\cos\phi}{\mu_{ry}}\right\} + \hat{\mathbf{y}}\mathrm{Re}\left\{\frac{k\sin\phi}{\mu_{rx}}\right\}\right] \\ &\quad \times \exp\{-2\mathrm{Im}\{k\hat{\boldsymbol{\rho}}\}\cdot\mathbf{r}\},\end{aligned} \tag{5.9}$$

and

$$\mathbf{S}\cdot\hat{\boldsymbol{\rho}} = \frac{|E_0|^2}{2\omega\mu_0}\mathrm{Re}\{\frac{k}{\mu_{re}}\}\mathrm{Exp}\{-2\mathrm{Im}\{k\hat{\boldsymbol{\rho}}\}\cdot\mathbf{r}\}. \tag{5.10}$$

This indicates that some information on the alignment of $\mathbf{S}$ relative to $\hat{\boldsymbol{\rho}}$ can be determined by considering $\mathrm{Re}\{\frac{k}{\mu_{re}}\}$. Rewrite ε_{rz} and μ_{re} in polar forms as

$$\varepsilon_{rz} = |\varepsilon_{rz}|e^{i\phi_\varepsilon}, \quad 0 \le \phi_\varepsilon \le \pi, \tag{5.11}$$

$$\mu_{re} = |\mu_{re}|e^{i\phi_\mu}, \quad 0 \le \phi_\mu \le \pi. \tag{5.12}$$

Substituting Eqs. (5.11) and (5.12) into Eq. (5.6) and solving for k, then we get

$$k_\pm = \pm\frac{\omega}{c}\sqrt{|\varepsilon_{rz}||\mu_{re}|}e^{i(\phi_\varepsilon+\phi_\mu)/2}, \quad 0 \le (\phi_\varepsilon+\phi_\mu)/2 \le \pi, \tag{5.13}$$

$$\frac{k_\pm}{\mu_{re}} = \pm\frac{\omega}{c}\sqrt{\frac{|\varepsilon_{rz}|}{|\mu_{re}|}}e^{i(\phi_\varepsilon-\phi_\mu)/2}, \quad -\pi/2 \le (\phi_\varepsilon-\phi_\mu)/2 \le \pi/2, \tag{5.14}$$

where k_+ and k_- lie on the upper-half and lower-half of the complex plane, respectively. Using Eq. (5.14) in Eq. (5.10), it can be concluded that

$$\mathbf{S}\cdot\hat{\boldsymbol{\rho}} > 0, \quad \text{for} \quad k = k_+, \tag{5.15}$$

$$\mathbf{S}\cdot\hat{\boldsymbol{\rho}} < 0, \quad \text{for} \quad k = k_-. \tag{5.16}$$

These situations are illustrated in Fig. 5.2, in which the unit vectors $\hat{\boldsymbol{\rho}}$ and $\hat{\boldsymbol{\phi}}$ divide the plane into the four regions of Q_1, Q_2, Q_3 and Q_4.

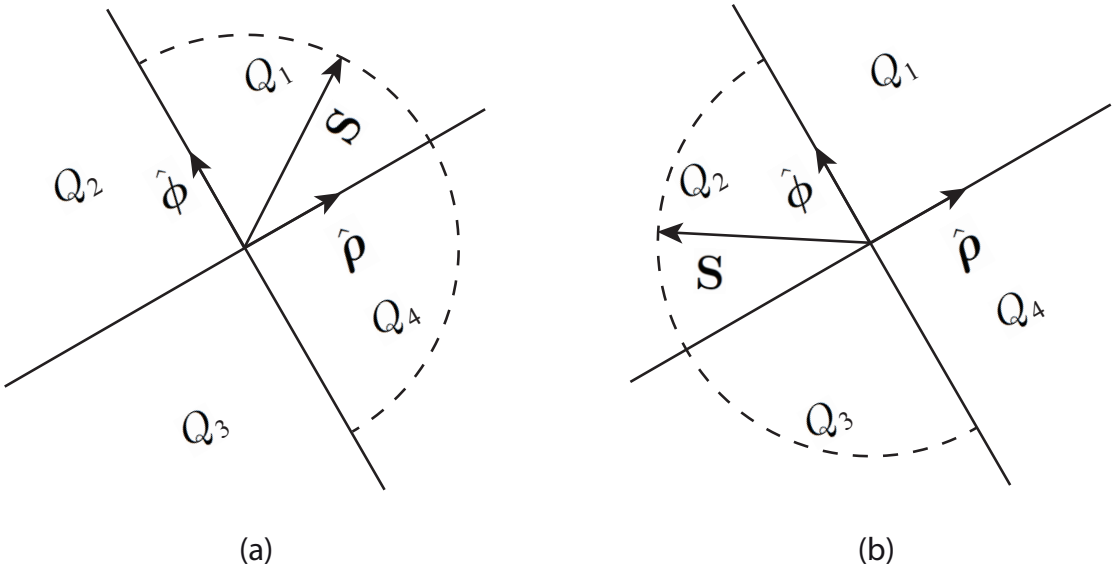

Figure 5.2: The relative direction of $\mathbf{S}$ with respect to $\hat{\boldsymbol{\rho}}$. (a) for $\mathbf{S} \cdot \hat{\boldsymbol{\rho}} > 0$ amd (b) for $\mathbf{S} \cdot \hat{\boldsymbol{\rho}} < 0$.

To satisfy the negative phase velocity condition, the phase velocity must have a negative projection along the average Poynting vector. The direction of the phase velocity is determined from $\mathrm{Re}\{k\}\hat{\boldsymbol{\rho}}$, as can be seen by rewriting the exponential terms:

$$e^{i(\mathbf{k}\cdot\mathbf{r}-\omega t)} = e^{-\mathrm{Im}\{k\}\hat{\boldsymbol{\rho}}\cdot\mathbf{r}} e^{i(\mathrm{Re}\{k\}\hat{\boldsymbol{\rho}}\cdot\mathbf{r}-\omega t)}. \tag{5.17}$$

Hence, if $\mathrm{Re}\{k\} > 0$, the phase velocity is in the same direction as $\hat{\boldsymbol{\rho}}$ and if $\mathrm{Re}\{k\} < 0$, it is opposite. Since for k_+, the average Poynting vector can lie on Q_1 or Q_4, and for k_-, it can lie on Q_2 or Q_3, then the negative phase velocity condition is satisfied if

$$\mathrm{Re}\{k_+\} < 0 \quad \text{and} \quad \mathrm{Re}\{k_-\} > 0. \tag{5.18}$$

This can be recast into the general condition involving the material parameters (Appendix A) as

$$\mathrm{Re}\{\varepsilon_{rz}\}|\mu_{re}| + \mathrm{Re}\{\mu_{re}\}|\varepsilon_{rz}| < 0. \tag{5.19}$$

This relationship is similar to and can be reduced to the Lakhtakia-Depline relation [10] for isotropic lossy media. Obviously, a simple condition that will satisfy Eq.

(5.20) is

$$\mathrm{Re}\{\varepsilon_{rz}\} < 0 \quad \text{and} \quad \mathrm{Re}\{\mu_{re}\} < 0. \tag{5.20}$$

Note that μ_{re} depends on the propagation angle (ϕ) as does the conditions (5.19) and (5.20). The angle-independent condition can be obtained by substituting Eq. (5.8) into Eq. (5.20). Then, with a little algebra, we get

$$\mathrm{Re}\{\varepsilon_{rz}\} < 0, \quad \mathrm{Re}\{\mu_{rx}\} < 0 \quad \text{and} \quad \mathrm{Re}\{\mu_{ry}\} < 0. \tag{5.21}$$

These results can also be reduced to the isotropic conditions [10] by substituting $\varepsilon_{rx} = \varepsilon_{ry} = \varepsilon_{rz} = \varepsilon_r$ and $\mu_{rx} = \mu_{ry} = \mu_{rz} = \mu_r$.

To support these results, we perform a numerical estimation of the angle between the average Poynting vector and the phase velocity for two sets of sample parameters (Figs. (5.3) and (5.4)). Starting from a propagation angle and the sample parameters, the vectors $\mathbf{S}$ and $\mathrm{Re}\{k\}\hat{\boldsymbol{\rho}}$ are calculated. Then the angle between these two vectors is computed. In Case 1 ($\varepsilon_{rz} = -0.137 + 0.019i$, $\mu_{rx} = -0.361 + 0.023i$ and $\mu_{ry} = -0.777 + 0.030i$), the sample parameters satisfy the angle-independent condition. So from our theoretical analysis, the phase velocity should be negative ($\theta > 90^0$) for all propagation angles (ϕ). The numerical result (Fig. 5.3a) demonstrates this exact agreement. The general condition (5.19) is satisfied for all propagation angles (Fig. 5.3b). In Case 2 ($\varepsilon_{rz} = 0.556 + 0.007i$, $\mu_{rx} = -0.361 + 0.023i$ and $\mu_{ry} = -0.777 + 0.030i$), the general condition (5.19) is not satisfied for any propagation angle (Fig. 5.3b), so we expect that the phase velocity should be positive for any ϕ (the magnitude of θ is less than 90^0), which agrees with the numerical result (Fig. 5.4a).

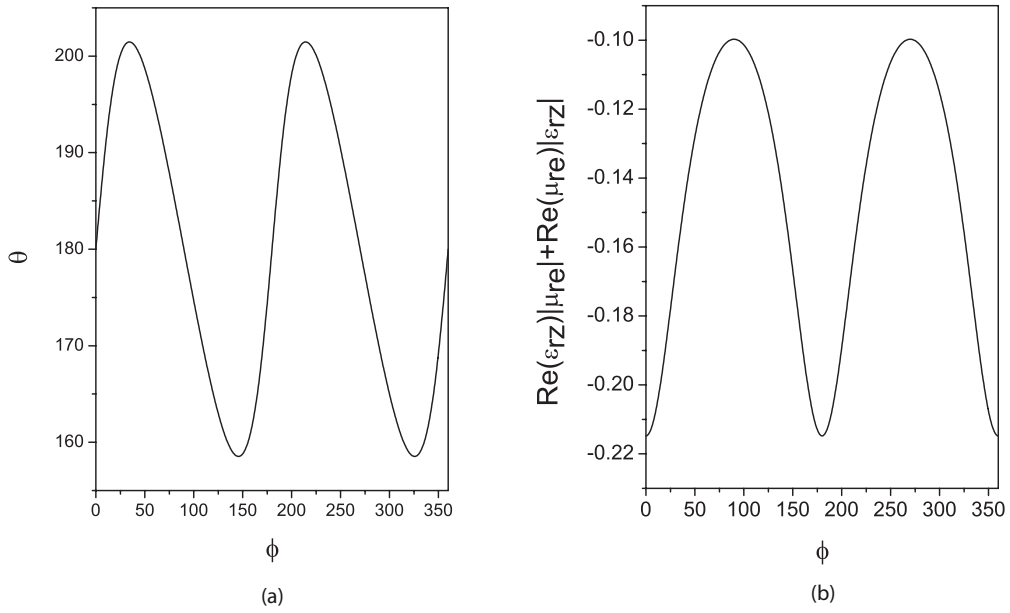

Figure 5.3: Case 1. $\varepsilon_{rz} = -0.137 + 0.019i$, $\mu_{rx} = -0.361 + 0.023i$ and $\mu_{ry} = -0.777 + 0.030i$. The plot of (a) the angle between **S** and the phase velocity with respect to the propagation angle, and (b) the general condition with respect to the propagation angle.

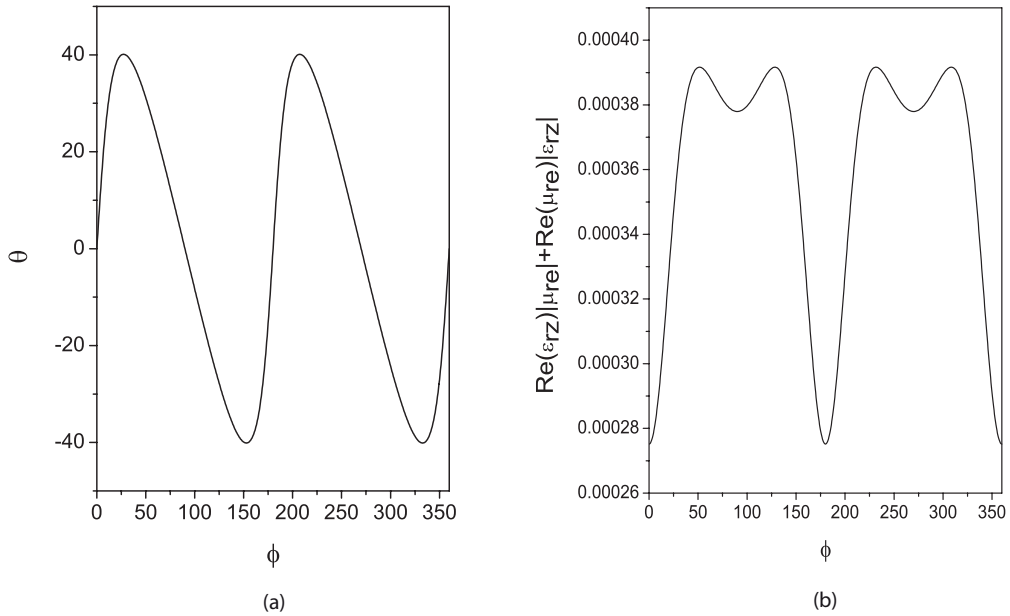

Figure 5.4: Case 2. $\varepsilon_{rz} = 0.556 + 0.007i$, $\mu_{rx} = -0.361 + 0.023i$ and $\mu_{ry} = -0.777 + 0.030i$. The plot of (a) the angle between **S** and the phase velocity with respect to the propagation angle, and (b) the general condition with respect to the propagation angle.

5.2 Negative Refraction in a Biaxial Anisotropic Lossy Media

Consider the problem of refraction and reflection when a z-polarized (TE) plane wave travels from a free space into a biaxial anisotropic medium, as shown in Fig. 5.5.

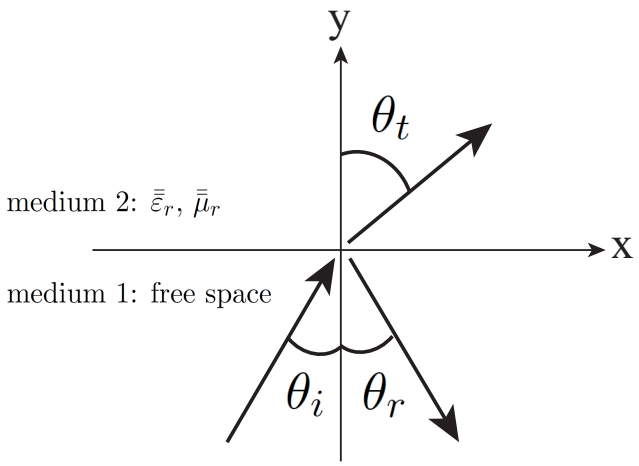

Figure 5.5: The TE wave incident on the interface between free space and a biaxial anisotropic medium.

The electric field of the incident wave can be written as

$$\mathbf{E}_i = \hat{\mathbf{z}} E_{0i} \exp\left(ik_1 \sin\theta_i \, x + ik_1 \cos\theta_i \, y - i\omega t\right), \tag{5.22}$$

and the magnetic intensity is

$$\begin{aligned} \mathbf{H}_i &= \frac{\mathbf{k}_1 \times \mathbf{E}_i}{\omega\mu_0} \\ &= \frac{1}{\mu_0\omega}(k_1 \sin\theta_i \hat{\mathbf{x}} + k_1 \cos\theta_i \hat{\mathbf{y}}) \times \mathbf{E}_i, \end{aligned} \tag{5.23}$$

where $k_1 = \omega/c$ and $\mathbf{k}_1$ is the incident wave vector. Consequently, the electric fields of the reflected and the transmitted waves are also z-polarized

$$\mathbf{E}_r = \hat{\mathbf{z}} E_{0r} \exp\left(ik_1 \sin\theta_r \, x - ik_1 \cos\theta_r \, y - i\omega t\right), \tag{5.24}$$

$$\mathbf{H}_r = \frac{1}{\mu_0\omega}(k_1 \sin\theta_r \hat{\mathbf{x}} - k_1 \cos\theta_r \hat{\mathbf{y}}) \times \mathbf{E}_r, \tag{5.25}$$

$$\mathbf{E}_t = \hat{\mathbf{z}} E_{0t} \exp\left(ik_x x + ik_y y - i\omega t\right), \tag{5.26}$$

$$\mathbf{H}_t = \frac{1}{\mu_0\omega} \bar{\bar{\mu}}_r^{-1} \left[(k_x \hat{\mathbf{x}} + k_y \hat{\mathbf{y}}) \times \mathbf{E}_t\right] \tag{5.27}$$

where k_x and k_y are the complex wave numbers along the x- and y-axes, respectively, which have to be evaluated later. The dispersion relation for the transmitted wave can be obtained by substituting Eq. (5.27) into $\nabla \times \mathbf{H}_t = -\omega\varepsilon_0\bar{\bar{\varepsilon}}_r \cdot \mathbf{E}_t$, then we get

$$\frac{k_x^2}{\mu_{ry}} + \frac{k_y^2}{\mu_{rx}} = \frac{\omega^2}{c^2}\varepsilon_{rz}. \tag{5.28}$$

Using the boundary conditions $\mathbf{E}_{1//} = \mathbf{E}_{2//}$ and $\mathbf{H}_{1//} = \mathbf{H}_{2//}$ at the interface (the plane $y = 0$), we obtain

$$\theta_i = \theta_r, \tag{5.29}$$

$$k_x = \frac{\omega}{c}\sin\theta_i, \tag{5.30}$$

$$E_{0r} = \left(\frac{\omega\mu_{rx}\cos\theta_i - k_y c}{\omega\mu_{rx}\cos\theta_i + k_y c}\right)E_{0i}, \tag{5.31}$$

$$E_{0t} = \left(\frac{2\omega\mu_{rx}\cos\theta_i}{\omega\mu_{rx}\cos\theta_i + k_y c}\right)E_{0i}. \tag{5.32}$$

Substituting Eq. (5.30) into Eq. (5.28) yields

$$k_y^2 = \frac{\omega^2}{c^2}\varepsilon_{re}\mu_{rx}, \tag{5.33}$$

where

$$\varepsilon_{re} = \varepsilon_{rz} - \frac{\sin^2\theta_i}{\mu_{ry}}. \tag{5.34}$$

Since Eq. (5.33) resembles the isotropic dispersion relation, we shall call ε_{re} the effective isotropic permittivity. It can easily be shown that ε_{re} also lies on the upper half of the complex plane. So we can solve for k_y by rewriting ε_{re} and μ_{rx} in the polar forms

$$\varepsilon_{re} = |\varepsilon_{re}|e^{i\phi_\epsilon}, \quad 0 \le \phi_\varepsilon \le \pi, \tag{5.35}$$

$$\mu_{rx} = |\mu_{rx}|e^{i\phi_\mu}, \quad 0 \le \phi_\mu \le \pi. \tag{5.36}$$

Then

$$k_y^{\pm} = \pm\frac{\omega}{c}\sqrt{|\varepsilon_{re}||\mu_{rx}|}e^{i(\phi_\varepsilon+\phi_\mu)/2}, \quad 0 \le (\phi_\varepsilon + \phi_\mu)/2 \le \pi. \tag{5.37}$$

The remaining question is the choice of k_y, such that it is physically meaningful. This can be answered by considering the average Poynting vector of the transmitted wave:

$$\mathbf{S}_t = \frac{1}{2}\mathrm{Re}\{\mathbf{E}_t \times \mathbf{H}_t^*\} = \frac{|E_{0t}|^2}{2\omega}(\mathrm{Re}\{\frac{k_x}{\mu_{ry}}\}\hat{\mathbf{x}} + \mathrm{Re}\{\frac{k_y}{\mu_{rx}}\}\hat{\mathbf{y}})e^{-2\mathrm{Im}\{k_y\}y}. \tag{5.38}$$

Since the wave propagates from medium 1 into medium 2, we expect that the y-component of $\mathbf{S}_t$ must be positive, that is,

$$\mathrm{Re}\{\frac{k_y}{\mu_{rx}}\} > 0. \tag{5.39}$$

As a consequence of Eq. (5.37), we always have

$$\mathrm{Re}\{\frac{k_y^+}{\mu_{rx}}\} > 0, \tag{5.40}$$

and

$$\mathrm{Re}\{\frac{k_y^-}{\mu_{rx}}\} < 0. \tag{5.41}$$

So the k_y^+ is chosen.

With the problem solved, the fields of the transmitted wave take the forms

$$\mathbf{E}_t = \hat{\mathbf{z}}E_{0t}\exp[-\mathrm{Im}\{k_y^+\}y]\exp(ik_x x + i\mathrm{Re}\{k_y^+\}y - i\omega t), \tag{5.42}$$

$$\mathbf{H}_t = \frac{E_{0t}}{\omega\mu_0}(\frac{k_y^+}{\mu_{rx}}\hat{x} - \frac{k_x}{\mu_{ry}}\hat{y})\exp[-\mathrm{Im}\{k_y^+\}y] \times \exp(ik_x x + i\mathrm{Re}\{k_y^+\}y - i\omega t). \tag{5.43}$$

Note that the wave is nonuniform and its amplitudes decreases in the +y direction. From the argument in the second exponentials shown in Eqs. (5.42) or (5.43), we can see that the refraction angle with respect to the y-axis is given by

$$\tan\theta_t = \frac{k_x}{\mathrm{Re}\{k_y^+\}}. \tag{5.44}$$

Since k_x is always positive, the range of θ_t is from 0 to 180^0. The negative refraction occurs when the phase velocity is towards the interface ($\theta_t > 90^0$), as shown in Fig. 5.6, which implies that

$$\mathrm{Re}\{k_y^+\} < 0. \tag{5.45}$$

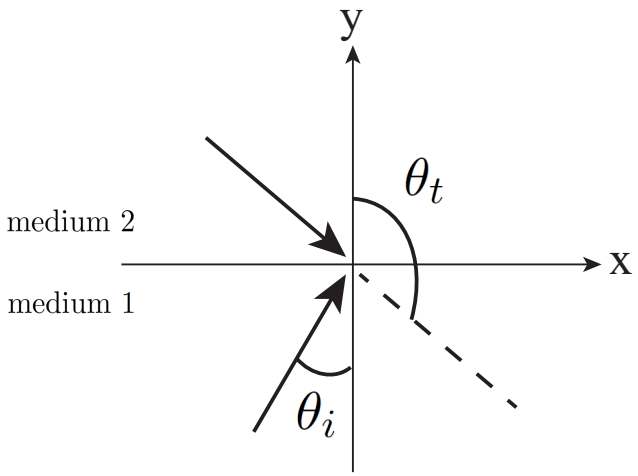

Figure 5.6: The negative refraction ($\theta_t > 90^0$) is depicted. The arrows in medium 1 and 2 indicate the phase velocity of the incident and the transmitted waves, respectively.

By using the method presented in Appendix A, we obtain the general condition for the negative refraction as

$$\mathrm{Re}\{\varepsilon_{re}\}|\mu_{rx}| + \mathrm{Re}\{\mu_{rx}\}|\varepsilon_{re}| < 0, \tag{5.46}$$

which include the special case:

$$\mathrm{Re}\{\varepsilon_{re}\} = \mathrm{Re}\{\varepsilon_{rz}\} - \mathrm{Re}\{\mu_{ry}\}\frac{\sin^2\theta_i}{|\mu_{ry}|^2} < 0 \quad \text{and} \quad \mathrm{Re}\{\mu_{rx}\} < 0. \tag{5.47}$$

This condition also suggests the angle-independent condition:

$$\mathrm{Re}\{\mu_{rx}\} < 0, \quad \mathrm{Re}\{\mu_{ry}\} > 0 \quad \text{and} \quad \mathrm{Re}\{\varepsilon_{rz}\} < 0, \tag{5.48}$$

which is applicable for anisotropic cases only. It can be shown that isotropic lossless media with $\varepsilon_r < 0$ and $\mu_r < 0$ satisfy Eq. (5.47).

To determine if the transmitted wave possess a positive or a negative phase velocity, we consider the relationship

$$\mathbf{S}_t \cdot \mathbf{k}_t = \frac{\omega|E_{0t}|^2}{2c^2} T \exp[-2\mathrm{Im}\{k_y^+\}y], \tag{5.49}$$

where

$$\mathbf{k}_t = k_x\hat{\mathbf{x}} + \mathrm{Re}\{k_y^+\}\hat{\mathbf{y}}, \tag{5.50}$$

and

$$T = \sin^2\theta_i \mathrm{Re}\{\frac{1}{\mu_{rx}}\} + \frac{c^2}{\omega^2}\mathrm{Re}\{\frac{k_y^+}{\mu_{rx}}\}\mathrm{Re}\{k_y^+\}. \tag{5.51}$$

If $T > 0$ ($\mathbf{S}_t \cdot \mathbf{k}_t > 0$), the phase velocity is positive, whilst if $T < 0$ ($\mathbf{S}_t \cdot \mathbf{k}_t < 0$), the phase velocity is negative. Fig. 5.7 shows the plots of the refraction angle and T with respect to the incident angle. The relevant parameters are $\varepsilon_{rz} = -0.137 + i0.019$, $\mu_{rx} = -0.361 + i0.023$ and $\mu_{ry} = 0.777 + i0.030$, which are chosen purposely to satisfy the angle-independent condition Eq. (5.48). The refraction is negative for all θ_i values because $\theta_t > 90^0$. Fig. 5.7b shows that this negative refraction can occur even when the phase velocity is positive ($T > 0$).

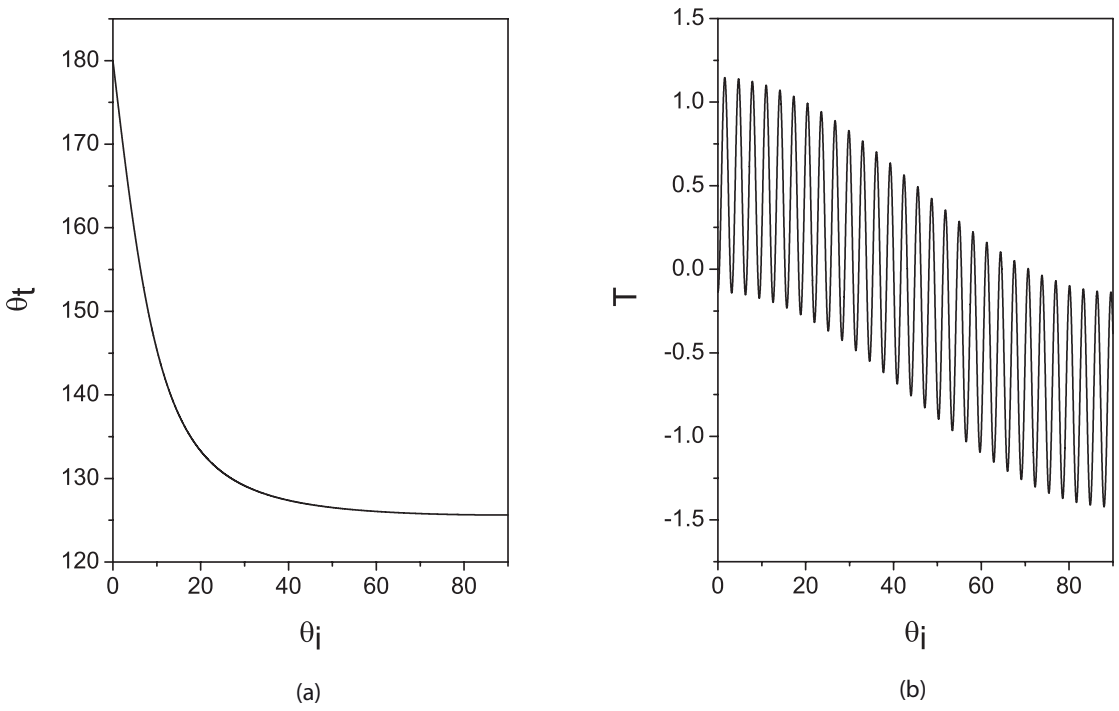

Figure 5.7: The plot of (a) the refraction angle (θ_t) with respect to the incident angle (θ_i), and (b) the parameter T that can be used to specify if the phase velocity is positive ($T > 0$) or negative ($T < 0$).

CHAPTER VI

Nonlinear Dielectric Composites with Elliptic Cylindrical Inclusions

In this chapter, the formulae for evaluating the effective nonlinear coefficients up to the ninth order of weakly nonlinear composites subject to a DC electric field are presented. Then we evaluate the effective DC coefficients of a composite consisting of weakly nonlinear dielectric inclusions with elliptic cylindrical shapes, randomly embedded and oriented in a linear dielectric medium. The results are used to study the shape effects on the enhancements of these nonlinear coefficients. Finally we consider weakly nonlinear composites under an applied AC electric field of the forms $\mathrm{E}_0 \sin(\omega t)$ and $\mathrm{E}_1 \sin \omega t + \mathrm{E}_3 \sin 3\omega t$. With a simple method, the general connections between the effective DC and AC coefficients are established.

6.1 DC Applied Electric Field

6.1.1 Problem Formulation

Consider a general structure of a composite consisting of weakly nonlinear dielectric inclusions in a linear dielectric medium (Fig. 6.1). The constitutive relation for the inclusions is assumed to take the form

$$\mathbf{D}^i = \varepsilon_i \mathbf{E}^i + \chi_i |\mathbf{E}^i|^2 \mathbf{E}^i + \eta_i |\mathbf{E}^i|^4 \mathbf{E}^i, \tag{6.1}$$

and for the medium, it is

$$\mathbf{D}^m = \varepsilon_m \mathbf{E}^m, \tag{6.2}$$

where ε_i and ε_m are the permittivities or the first-order dielectric coefficients of the two media, and χ_i and η_i are the third- and fifth-order nonlinear dielectric coefficients of the inclusions. The weakly nonlinearity means that the condition $1 >> \chi_i|\mathbf{E}^i|^2/\varepsilon_i >> \eta_i|\mathbf{E}^i|^4/\varepsilon_i$ is satisfied.

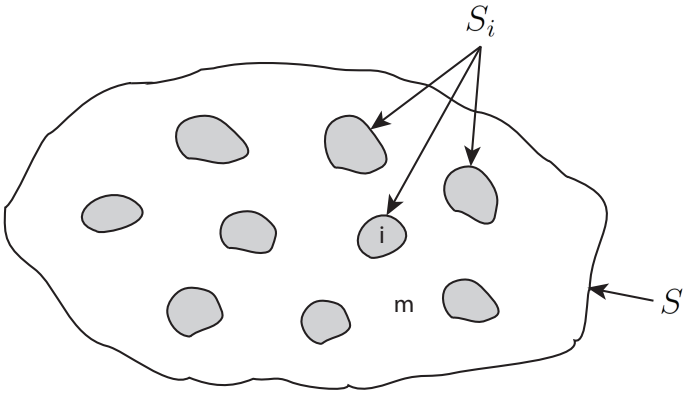

Figure 6.1: A typical structure of a composite, which consists of inclusions embedded in a medium. S_i denotes the inclusion surfaces and S denotes the composite surface.

Under an applied DC electric field ($\mathbf{E}_0$), the electric displacements and the electric fields in the inclusions and the medium satisfy the electrostatic equations:

$$\boldsymbol{\nabla} \cdot \mathbf{D} = 0, \tag{6.3}$$

$$\boldsymbol{\nabla} \times \mathbf{E} = 0 \quad \text{or} \quad \mathbf{E} = -\boldsymbol{\nabla}\Phi, \tag{6.4}$$

which lead to the boundary conditions at the inclusion surfaces S_i as follows:

$$\Phi^i = \Phi^m, \qquad \text{on} \quad S_i, \tag{6.5}$$

$$\mathbf{D}^i \cdot \hat{\mathbf{n}} = \mathbf{D}^m \cdot \hat{\mathbf{n}}\,, \qquad \text{on} \quad S_i, \tag{6.6}$$

where i and m denote the inclusions and the medium, respectively. In the theoretical analyses of nonlinear dielectric composites, it is customary to assume the boundary condition for the DC applied field ($\mathbf{E}_0$) as

$$\Phi^m = -\mathbf{E}_0 \cdot \mathbf{x}\,, \qquad \text{on} \quad S, \tag{6.7}$$

where S denotes the composite surface. Such boundary condition can be realized by the potential between a parallel plate capacitor.

For weakly nonlinear composites, the effective nonlinear dielectric coefficients relate the spatial average of $\mathbf{D}$ and $\mathbf{E}$ as follows

$$\langle \mathbf{D} \rangle = \varepsilon_e \langle \mathbf{E} \rangle + \chi_e |\langle \mathbf{E} \rangle|^2 \langle \mathbf{E} \rangle + \eta_e |\langle \mathbf{E} \rangle|^4 \langle \mathbf{E} \rangle + \delta_e |\langle \mathbf{E} \rangle|^6 \langle \mathbf{E} \rangle + \mu_e |\langle \mathbf{E} \rangle|^8 \langle \mathbf{E} \rangle + \dots , \quad (6.8)$$

where $\langle ... \rangle$ denote the spatial average over the composite region, and ε_e, χ_e, η_e, δ_e and μ_e are the effective first-, third-, fifth-, seventh- and the ninth-order dielectric coefficients, respectively. Using Eq. (6.7) it can easily be shown that $\langle \mathbf{E} \rangle = \mathbf{E}_0$. Thus

$$\langle \mathbf{D} \rangle = \varepsilon_e \mathbf{E}_0 + \chi_e |\mathbf{E}_0|^2 \mathbf{E}_0 + \eta_e |\mathbf{E}_0|^4 \mathbf{E}_0 + \delta_e |\mathbf{E}_0|^6 \mathbf{E}_0 + \mu_e |\mathbf{E}_0|^8 \mathbf{E}_0 + \dots . \quad (6.9)$$

6.1.2 Perturbation Expansion Method

Since the inclusions are assumed to be weakly nonlinear, the order of magnitude of the first-order term ($\varepsilon_i \mathbf{E}^i$) is much larger than the third-order term ($\chi_i |\mathbf{E}^i|^2 \mathbf{E}^i$) which in turn is much larger than the fifth-order term ($\eta_i |\mathbf{E}^i|^4 \mathbf{E}^i$). Therefore we can employ the perturbation method to analyze this problem. With this method, we rewrite the ($\mathbf{D} - \mathbf{E}$) relation of the inclusions as

$$\mathbf{D}^i = \varepsilon_i \mathbf{E}^i + \lambda \chi_i |\mathbf{E}^i|^2 \mathbf{E}^i + \lambda^2 \eta_i |\mathbf{E}^i|^4 \mathbf{E}^i, \quad (6.10)$$

where λ is a dimensionless parameter, which indicates the order of magnitude. For the medium, the ($\mathbf{D} - \mathbf{E}$) relation is still the same as that given in Eq. (6.2) because it does not contain any nonlinear terms. The perturbation expansion of the electric potentials are given as

$$\Phi^i = \Phi^{0i} + \lambda \Phi^{1i} + \lambda^2 \Phi^{2i} + \dots , \quad (6.11)$$

$$\Phi^m = \Phi^{0m} + \lambda \Phi^{1m} + \lambda^2 \Phi^{2m} + \dots , \quad (6.12)$$

where Φ^{ki} and Φ^{km} are the kth order perturbative potentials in the inclusions and medium, respectively. Using $\mathbf{E} = -\boldsymbol{\nabla} \Phi$, we get the perturbation expansion of the electric fields as

$$\mathbf{E}^i = \mathbf{E}^{0i} + \lambda \mathbf{E}^{1i} + \lambda^2 \mathbf{E}^{2i} + \dots , \quad (6.13)$$

$$\mathbf{E}^m = \mathbf{E}^{0m} + \lambda \mathbf{E}^{1m} + \lambda^2 \mathbf{E}^{2m} + \dots , \quad (6.14)$$

where $\mathbf{E}^{ki} = -\boldsymbol{\nabla}\Phi^{ki}$ and $\mathbf{E}^{km} = -\boldsymbol{\nabla}\Phi^{km}$. Substituting Eqs. (6.15) and (6.16) into Eqs. (6.10) and (6.2), we can arrive at the perturbations of the electric displacements:

$$\mathbf{D}^{i} = \mathbf{D}^{0i} + \lambda\mathbf{D}^{1i} + \lambda^2\mathbf{D}^{2i} + \dots, \tag{6.15}$$

$$\mathbf{D}^{m} = \mathbf{D}^{0m} + \lambda\mathbf{D}^{1m} + \lambda^2\mathbf{D}^{2m} + \dots. \tag{6.16}$$

Using these perturbation expansions in Eqs. (6.3), (6.5), (6.6) and (6.7), we obtain a linear boundary value problem for each perturbative order:

$$\boldsymbol{\nabla}\cdot\mathbf{D}^{k\alpha} = 0, \qquad \alpha = i,\ m \tag{6.17}$$

with the boundary condition on the inclusion surfaces

$$\mathbf{D}^{ki}\cdot\hat{\mathbf{n}} = \mathbf{D}^{km}\cdot\hat{\mathbf{n}}, \qquad \text{on } S_i, \tag{6.18}$$

$$\Phi^{ki} = \Phi^{km}, \qquad \text{on } S_i, \tag{6.19}$$

and on the composite surface

$$\Phi^{km} = \begin{cases} -\mathbf{E}_0\cdot\hat{\mathbf{x}}, & \text{if } k = 0 \\ 0, & \text{otherwise} \end{cases} \qquad \text{on } S. \tag{6.20}$$

Hence the nonlinear problem is decomposed into a consecutive set of linear problems. In order to solve for these perturbative potentials, we must solve them from the lowest order potential up to any required order, consecutively, which may be laborious. Fortunately, it turns out in subsequent sections that to compute the effective dielectric coefficients of our composites, only the potentials in the inclusions are required and there exists a technique to solve these potentials quickly and easily.

6.1.3 Effective DC Coefficients

Following the perturbation method, we specify the order of the terms in Eq. (6.21) with the parameter λ as

$$\langle\mathbf{D}\rangle = \varepsilon_e\mathbf{E}_0 + \lambda\chi_e|\mathbf{E}_0|^2\mathbf{E}_0 + \lambda^2\eta_e|\mathbf{E}_0|^4\mathbf{E}_0 + \lambda^3\delta_e|\mathbf{E}_0|^6\mathbf{E}_0 + \lambda^4\mu_e|\mathbf{E}_0|^8\mathbf{E}_0 + \dots. \tag{6.21}$$

The effective coefficients can be estimated by considering the integral (first employed to analyze a linear composite by Landau [49])

$$\frac{1}{V}\int_V (\mathbf{D}-\varepsilon_m\mathbf{E})dV = \langle\mathbf{D}\rangle - \varepsilon_m\mathbf{E}_0, \tag{6.22}$$

where V are the volume of the composite. Note that the integrand vanishes in medium so it is left with the integral in the inclusion volume (V_i) as

$$\frac{1}{V}\int_{V_i} (\mathbf{D}^i-\varepsilon_m\mathbf{E}^i)dV = \langle\mathbf{D}\rangle - \varepsilon_m\mathbf{E}_0, \tag{6.23}$$

By substituting Eq. (6.10) and (6.21) into (6.23), we get

$$\begin{aligned}\frac{1}{V}\int_{V_i}[(\varepsilon_i-\varepsilon_m)\mathbf{E}^i+\lambda\chi_i|\mathbf{E}^i|^2\mathbf{E}^i+\lambda^2\eta_i|\mathbf{E}^i|^4\mathbf{E}^i]dV &= (\varepsilon_e-\varepsilon_m)\mathbf{E}_0+\lambda\chi_e|\mathbf{E}_0|^2\mathbf{E}_0\\ &+\lambda^2\eta_e|\mathbf{E}_0|^4\mathbf{E}_0+\lambda^3\delta_e|\mathbf{E}_0|^6\mathbf{E}_0\\ &+\lambda^4\mu_e|\mathbf{E}_0|^8\mathbf{E}_0+\dots\ . \end{aligned}\tag{6.24}$$

Using the perturbation expansion of the electric field in the inclusions $\mathbf{E}^i = \sum_{k=0}^{\infty}\lambda^k\mathbf{E}^{ki}$ in Eq. (6.24) and dotting both sides by $\mathbf{E}_0$, we get

$$\begin{aligned}&\frac{1}{V}\int_{V_i}\Big[\sum_k\lambda^k(\varepsilon_i-\varepsilon_m)\mathbf{E}^{ki}+\chi_i\sum_{k,l,m}\lambda^{k+l+m+1}(\mathbf{E}^{ki}\cdot\mathbf{E}^{li})\mathbf{E}^{mi}\\ &+\eta_i\sum_{k,l,m,n,p}\lambda^{k+l+m+n+p+2}(\mathbf{E}^{ki}\cdot\mathbf{E}^{li})(\mathbf{E}^{mi}\cdot\mathbf{E}^{ni})\mathbf{E}^{pi}\Big]\cdot\mathbf{E}_0\,dV = (\varepsilon_e-\varepsilon_m)\mathrm{E}_0^2+\lambda\chi_e\mathrm{E}_0^4\\ &+\lambda^2\eta_e\mathrm{E}_0^6+\lambda^3\delta_e\mathrm{E}_0^8+\lambda^4\mu_e\mathrm{E}_0^{10},\end{aligned}\tag{6.25}$$

where k, l, m, n, p are integers that range from 0 to ∞. By equating the terms with the same power of λ, i.e. λ^0, λ^1, λ^2, λ^3 and λ^4 we obtain the equations for determining ε_e, χ_e, η_e, δ_e and μ_e, respectively. These are shown in Appendix C where the derivation for the effective coefficients up to the ninth order is presented. We report the results as follows:

$$\varepsilon_e = \varepsilon_m + \frac{\mathbf{E}_0}{VE_0^2}\cdot\int_{V_i}(\varepsilon_i-\varepsilon_m)\mathbf{E}^{0i}\,dV \tag{6.26}$$

$$\chi_e = \frac{\mathbf{E}_0}{VE_0^4}\cdot\int_{V_i}[(\varepsilon_i-\varepsilon_m)\mathbf{E}^{1i}+\chi_i|\mathbf{E}^{0i}|^2\mathbf{E}^{0i}]dV \tag{6.27}$$

$$\begin{aligned}\eta_e = \frac{\mathbf{E}_0}{VE_0^6}\cdot\int_{V_i}&\big[(\varepsilon_i-\varepsilon_m)\mathbf{E}^{2i}+2\chi_i(\mathbf{E}^{0i}\cdot\mathbf{E}^{1i})\mathbf{E}^{0i}\\ &+\chi_i|\mathbf{E}^{0i}|^2\mathbf{E}^{1i}+\eta_i|\mathbf{E}^{0i}|^4\mathbf{E}^{0i}\big]\,dV\end{aligned}\tag{6.28}$$

$$\begin{aligned}\delta_e &= \frac{\mathbf{E}_0}{VE_0^8}\cdot\int_{V_i}\big[(\varepsilon_i-\varepsilon_m)\mathbf{E}^{3i}+\chi_i|\mathbf{E}^{1i}|^2\mathbf{E}^{0i}+2\chi_i(\mathbf{E}^{0i}\cdot\mathbf{E}^{1i})\mathbf{E}^{1i}\\ &\quad +2\chi_i(\mathbf{E}^{0i}\cdot\mathbf{E}^{2i})\mathbf{E}^{0i}+\chi_i|\mathbf{E}^{0i}|^2\mathbf{E}^{2i}+4\eta_i(\mathbf{E}^{0i}\cdot\mathbf{E}^{1i})|\mathbf{E}^{0i}|^2\mathbf{E}^{0i}\\ &\quad +\eta_i|\mathbf{E}^{0i}|^4\mathbf{E}^{1i}\big]\,dV \qquad (6.29)\end{aligned}$$

$$\begin{aligned}\mu_e &= \frac{\mathbf{E}_0}{VE_0^{10}}\cdot\int_{V_i}\big[(\varepsilon_i-\varepsilon_m)\mathbf{E}^{4i}+\chi_i|\mathbf{E}^{1i}|^2\mathbf{E}^{1i}+2\chi_i(\mathbf{E}^{0i}\cdot\mathbf{E}^{1i})\mathbf{E}^{2i}\\ &\quad +2\chi_i(\mathbf{E}^{0i}\cdot\mathbf{E}^{2i})\mathbf{E}^{1i}+2\chi_i(\mathbf{E}^{1i}\cdot\mathbf{E}^{2i})\mathbf{E}^{0i}+2\chi_i(\mathbf{E}^{0i}\cdot\mathbf{E}^{3i})\mathbf{E}^{0i}\\ &\quad +\chi_i|\mathbf{E}^{0i}|^2\mathbf{E}^{3i}+2\eta_i|\mathbf{E}^{0i}|^2|\mathbf{E}^{1i}|^2\mathbf{E}^{0i}+4\eta_i(\mathbf{E}^{0i}\cdot\mathbf{E}^{1i})^2\mathbf{E}^{0i}\\ &\quad +4\eta_i|\mathbf{E}^{0i}|^2(\mathbf{E}^{0i}\cdot\mathbf{E}^{1i})\mathbf{E}^{1i}+4\eta_i(\mathbf{E}^{0i}\cdot\mathbf{E}^{2i})|\mathbf{E}^{0i}|^2\mathbf{E}^{0i}+\eta_i|\mathbf{E}^{0i}|^4\mathbf{E}^{2i}\big]\,dV. \qquad (6.30)\end{aligned}$$

Note that the calculation of the effective coefficients requires only the potentials inside the inclusions.

6.1.4 Composites with Elliptic Cylindrical Inclusions

In this section, the general formulae of the effective coefficients, Eqs. (6.27)-(6.30), are applied to evaluate the effective DC response of a weakly nonlinear composite with elliptic cylindrical inclusions. The shapes of the inclusions are assumed to be identical and the volume packing fraction is dilute ($p < 0.1$). Therefore, the electric potential inside each inclusion can be determined by neglecting the effect of the other inclusions. So the problem is reduced to a single inclusion in an infinite medium with an applied uniform field $\mathbf{E_0}$, as shown in Fig. 6.2. The lengths of the semi-major and semi-minor axes are denoted by M and N, respectively, and α is the angle between the applied electric field and the semi-major axis. Since the inclusion shape is an elliptic cylindrical, we employ the elliptic cylindrical coordinates (u, v) to solve this problem. These coordinates are related to the Cartesian coordinates (x, y) by:

$$x = a\,\cosh u\cos v, \qquad (6.31)$$

$$y = a\,\sinh u\sin v, \qquad (6.32)$$

where the focal length (a) of elliptic cylindrical coordinates is chosen to coincide with that of the inclusion. Since the medium is linear, the potential Φ^m obey

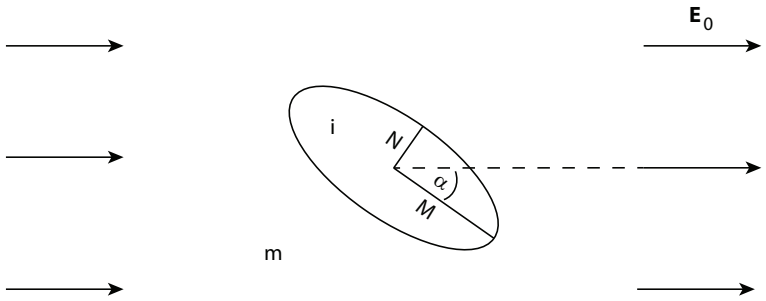

Figure 6.2: A single elliptic cylindrical inclusion in a linear dielectric medium with an applied electric field $\mathbf{E}_0$ making the angle α with the semi-major axis.

the Laplace equation, the general solution in elliptic cylindrical coordinates (Eq. (2.33)) can be employed. Thus the electric potential in the medium can be written to provide the uniform electric field ($\mathbf{E}_0$) at far distances as

$$\begin{aligned}\Phi^m &= -\mathrm{E}_0\, a\cos\alpha\cosh u\cos v - \mathrm{E}_0\, a\sin\alpha\sinh u\sin v \\ &\quad + C\, a\exp(-u)\cos v + D\, a\exp(-u)\sin v. \end{aligned} \tag{6.33}$$

Because of the nonlinearity, the potential inside the inclusion does not necessarily satisfy Laplace equation. However we will assume that the electric field in the inclusion is uniform. This assumption may be justified by the uniqueness theorem after the potentials are solved to satisfy all of the required boundary conditions. Thus

$$\Phi^i = -A\, a\cosh u\cos v - B\, a\sinh u\sin v. \tag{6.34}$$

Using the boundary conditions, Eqs. (6.5) and (6.6), we obtain

$$\Phi^i(u_0, v) = \Phi^m(u_0, v), \tag{6.35}$$

$$\varepsilon_i \frac{\partial\Phi^i}{\partial u}\bigg|_{(u_0,v)} + \chi_i|\boldsymbol{\nabla}\Phi^i|^2\frac{\partial\Phi^i}{\partial u}\bigg|_{(u_0,v)} + \eta_i|\boldsymbol{\nabla}\Phi^i|^4\frac{\partial\Phi^i}{\partial u}\bigg|_{(u_0,v)} = \varepsilon_m\frac{\partial\Phi^m}{\partial u}\bigg|_{(u_0,v)}, \tag{6.36}$$

where the points with coordinates (u_0, v) where $0 \le v \le 2\pi$, are on the inclusion surface. From Eqs. (6.35) and (6.36), we have

$$(M + K\,N)A + \frac{\chi_i}{\varepsilon_m}N(A^2+B^2)A + \frac{\eta_i}{\varepsilon_m}N(A^2+B^2)^2A = \mathrm{E}_0\cos\alpha(M+N), \tag{6.37}$$

$$(K\,M + N)B + \frac{\chi_i}{\varepsilon_m}M(A^2+B^2)B + \frac{\eta_i}{\varepsilon_m}M(A^2+B^2)^2B = \mathrm{E}_0\sin\alpha(M+N), \tag{6.38}$$

$$C = \frac{(E_0 \cos\alpha - A)M}{M - N}, \tag{6.39}$$

$$D = \frac{(E_0 \sin\alpha - B)N}{M - N}. \tag{6.40}$$

To solve for the constants A, B, C and D, we expand them as a power series of E_0 as follows:

$$A = \sum_{k=0}^{\infty} A_k {\mathrm{E}_0}^k,\ B = \sum_{k=0}^{\infty} B_k {\mathrm{E}_0}^k,\ C = \sum_{k=0}^{\infty} C_k {\mathrm{E}_0}^k,\ D = \sum_{k=0}^{\infty} D_k {\mathrm{E}_0}^k. \tag{6.41}$$

The details of the derivation of A_k, B_k, C_k and D_k are shown in Appendix D, including the results of the potentials up to the fourth order. Substituting the electric fields from Eq. (D.19) into Eqs. (6.27) - (6.30) and then performing the angular average $\frac{1}{\pi}\int_{-\pi/2}^{\pi/2} ... \, d\alpha$, we obtain the effective coefficients up to the ninth order. The closed form result of the ninth-order coefficient is not reported here due to the length of the expression but will be depicted. Therefore we show the results of the effective coefficients up to the seventh order as follows:

$$\varepsilon_e = \varepsilon_m + p\frac{\varepsilon_m}{2}(K-1)\Big\{F(s) + F(s^{-1})\Big\}, \tag{6.42}$$

$$\chi_e = p\chi_i\Big\{\frac{3}{8}F^4(s) + \frac{1}{4}F^2(s)F^2(s^{-1}) + \frac{3}{8}F^4(s^{-1})\Big\}, \tag{6.43}$$

$$\begin{aligned}\eta_e = p\Bigg[&\frac{5\eta_i}{16}\Big\{F^6(s) + F^6(s^{-1})\Big\} - \frac{15{\chi_i}^2}{16\varepsilon_m}\Big\{\frac{F^6(s)}{K+s} + \frac{F^6(s^{-1})}{K+s^{-1}})\Big\} \\ &+\frac{3\eta_i}{16}\Big\{F^4(s)F^2(s^{-1}) + F^2(s)F^4(s^{-1})\Big\} \\ &-\frac{3{\chi_i}^2}{16\varepsilon_m}\Big\{\big(1+3Ks+2s^2\big)F_1(s) + \big(2s^{-2}+3Ks^{-1}+1\big)F_1(s^{-1})\Big\}\Bigg],\end{aligned} \tag{6.44}$$

$$\begin{aligned}\delta_e = p\Bigg[&-\frac{35\eta_i\chi_i}{16\varepsilon_m}\Big\{\frac{F^8(s)}{K+s} + \frac{F^8(s^{-1})}{K+s^{-1}}\Big\} - \frac{5\eta_i\chi_i}{16\varepsilon_m}\Big\{\big(1+4Ks+3s^2\big)F_1(s)F^2(s^{-1}) \\ &+\big(3s^{-2}+4Ks^{-1}+1\big)F_1(s^{-1})F^2(s)\Big\} - \frac{9\eta_i\chi_i}{16\varepsilon_m}F_2(s) \\ &+\frac{105{\chi_i}^3}{32{\varepsilon_m}^2}\Big\{\frac{F^8(s)}{(K+s)^2} + \frac{s^2F^8(s^{-1})}{(1+Ks)^2}\Big\} \\ &+\frac{5{\chi_i}^3}{32{\varepsilon_m}^2}\Big\{F_3(s) + F_3(s^{-1})\Big\} + \frac{3{\chi_i}^3}{32{\varepsilon_m}^2}F_4(s)\Bigg],\end{aligned} \tag{6.45}$$

where

$$F(s) = \frac{1+s}{K+s}, \quad F_1(s) = \frac{(1+s)^6}{(K+s)^3(1+Ks)^5},$$
$$F_2(s) = \frac{(1+s)^8(1+2Ks+s^2)}{(K+s)^5(1+Ks)^5},$$
$$F_3(s) = \frac{(1+s)^8(1+6Ks+4(1+3K^2)s^2+18Ks^3+7s^4)}{(K+s)^4(1+Ks)^8},$$
$$F_4(s) = \frac{(1+s)^8(5+18Ks+2(4+9K^2)s^2+18Ks^3+5s^4)}{(K+s)^6(1+Ks)^6}, \quad (6.46)$$

$K = \varepsilon_i/\varepsilon_m$ is the relative permittivity, p is the volume fraction of inclusions and s is the aspect ratio, the ratio between semi-minor and semi-major axes or vice versa.

Note that the effective coefficients Eqs. (6.42)-(6.45) are invariant under the transformation from s to s^{-1} which is trivial because interchanging between the semi-major and semi-minor axes does not affects the inclusion shape. For $s = 1$, the shapes of inclusions reduce to circular cylinders and the effective coefficients reported here correspond to those obtained by Natenapit et al. [35].

6.1.5 Results and Discussion

The shape effects of inclusions on the effective DC coefficients are shown in Figs. 6.3 - 6.6. In order to satisfy the weakly nonlinear condition, we set $\chi_i {E_0}^2/\varepsilon_i = 10^{-3}$ and $\eta_i {E_0}^4/\varepsilon_i = 10^{-6}$, which are much lower than one. The volume packing fraction of inclusions is dilute and is chosen to be 0.05. The symmetrical plots of the relative third- and fifth-order coefficients (χ_e/χ_i and η_e/η_i) versus $\log s$ ($s = N/M$) with $K = \varepsilon_i/\varepsilon_m$ are shown in Figs. 6.3 and 6.4, respectively. For $K << 1$, the third- and fifth-order nonlinear effects are greatly enhanced with the increasing eccentricity of inclusions. From Figs. 6.3a and 6.4a, at $\log s = 1$ and $K = 0.1$, the magnitude of the third- and fifth-order effective coefficients are about 17 and 216 times larger than the third- and fifth-order coefficients of inclusions, respectively. The large enhancement is due to the increase of the electric field in the inclusions when the relative permittivity K becomes much lower than 1. In the contrast, the effective nonlinear response is very small for $K >> 1$. A

large reduction in the nonlinear responses are observed in Figs. 6.3b and 6.4b, which can be explained by realizing that if $K >> 1$ ($\varepsilon_i >> \varepsilon_m$), the electric fields in all inclusions are reduced and will approach zero. Therefore, physically, the inclusions behave as ideal conductors. Thus, the composite can be considered to be equivalent to that of ideal-conductor inclusions dispersed in a linear dielectric medium, which is a linear composite system. So the nonlinear response disappears under such condition.

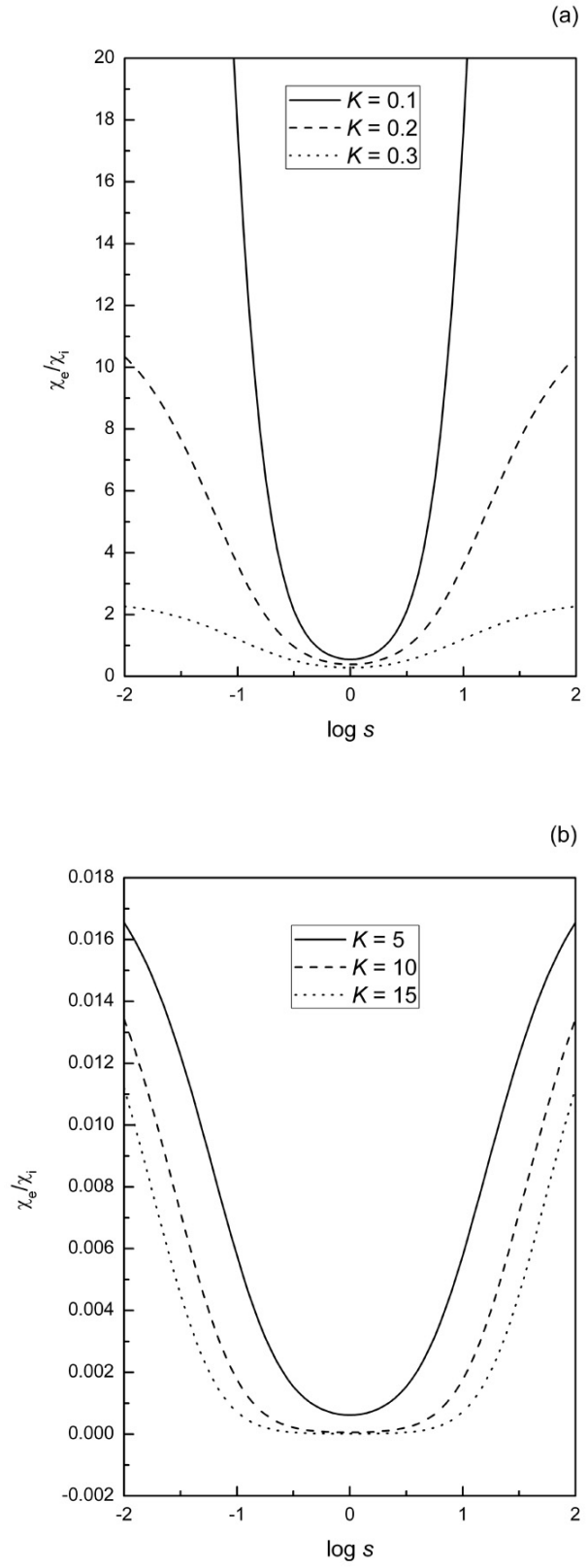

Figure 6.3: The variation of the relative third-order nonlinear coefficients upon the inclusion aspect ratios (s) at the packing fraction of 0.05 for (a) the relative permittivity $K = \varepsilon_i/\varepsilon_m$ less than 1 and (b) K larger than 1.

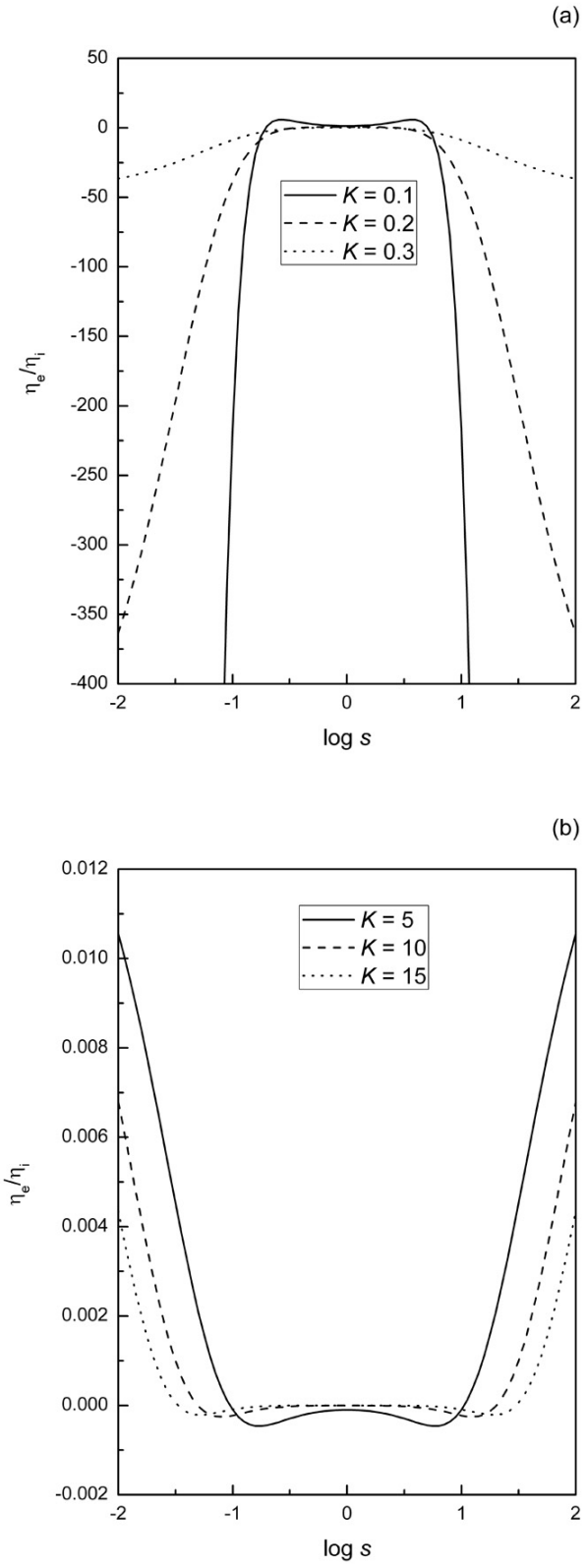

Figure 6.4: The variation of the relative fifth-order nonlinear coefficients upon the inclusion aspect ratios (s) at the packing fraction of 0.05 for (a) the relative permittivity $K = \varepsilon_i/\varepsilon_m$ less than 1 and (b) K larger than 1.

The effect of varying the relative permittivity on the seventh- and ninth-order effective coefficients for aspect ratios (s) of 0.4, 0.5 and 0.6 are shown in Figs. 6.5 and 6.6. In order to show the entire behaviors of the effective responses, a logarithmic scale for relative permittivity (K) is used. Although $K = 10^{-4}$ is rather an ideal situation, it is considered for complete predictions. The results revealed that at $\chi_i {E_0}^2/\varepsilon_i = 10^{-3}$ for both $\eta_i = 0$ and $\eta_i E_0^4/\varepsilon_i = 10^{-6}$, there exists some peaks which represent the extreme conditions under each aspect ratio. Furthermore, the peaks become higher when the eccentricity of inclusions is increased (in this case the reduction of the aspect ratio). As explained earlier, increasing the relative permittivity will transform the nonlinear system to a linear one, and the composite can then be considered as composed of ideal-conductor inclusions in a linear host medium. Therefore, the seventh- and ninth-order effective coefficients approach zero for large values of K, as expected. In order to verify our results on the effective DC coefficients, we also calculate the effective coefficients from the average energy method [35] which takes into account the total energy of the composite and that of the homogeneous effective medium. It turns out that the results from the average energy method are in exact agreement with our results presented here. It should be noted that there are realistic application materials having high-order nonlinearity, such as for dyn doped glasses as reported by Ormachea [50]. The measurements of Rhodamine 6G dyn solution in Ref. [51] have shown not only the third- but also the fifth- and seventh-order nonlinear susceptibilities. Although we have considered elliptic cylindrical inclusions, the method developed here can be applied to similar composites with ellipsoidal inclusions. By using the general solutions of a linear dielectric ellipsoid in a linear medium subjected to an applied uniform electric field [15] and imposing the boundary conditions at the surface of the ellipsoid, we can determine the potentials as a power series of the applied field similar to the results shown in Appendix D. Thus the high-order effective nonlinear coefficients can be evaluated.

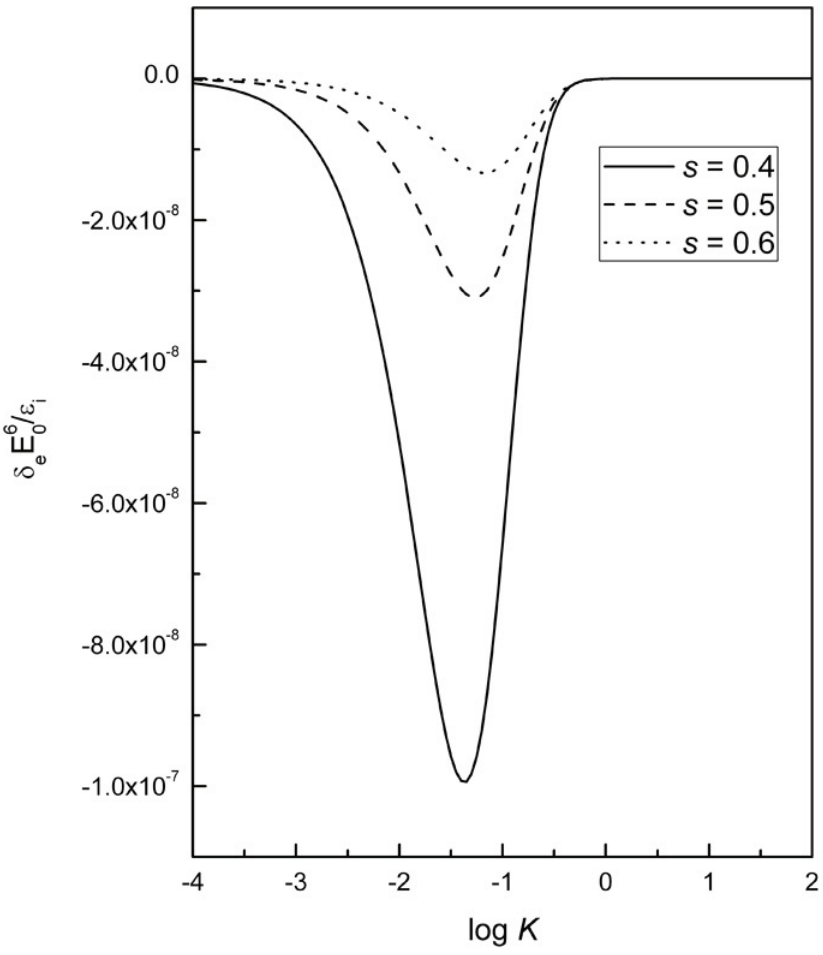

Figure 6.5: The plot of the dimensionless seventh-order effective coefficients versus log K, $K = \varepsilon_i/\varepsilon_m$ for different aspect ratios (s) at a volume fraction of 0.05.

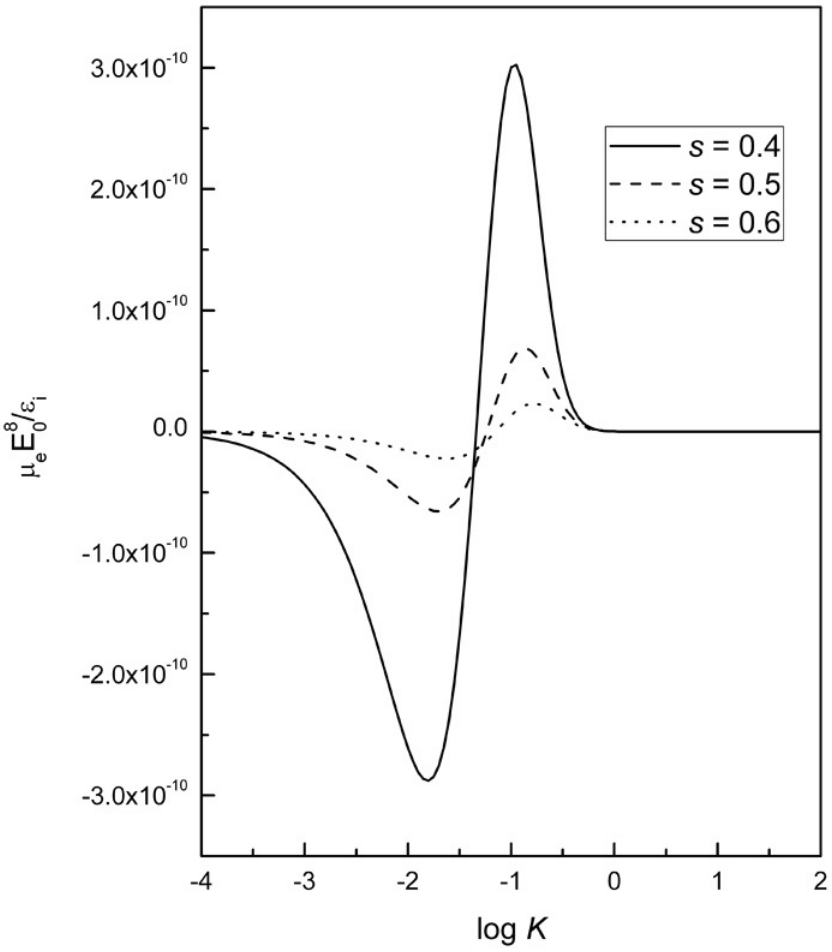

Figure 6.6: The plot of the dimensionless ninth-order effective coefficients versus log K, $K = \varepsilon_i/\varepsilon_m$ for different aspect ratios (s) at a volume fraction of 0.05.

6.2 AC Applied Electric Field

6.2.1 Transformation from DC to AC response

For sinusoidal applied field $\mathbf{E}_0 \sin \omega t$, the boundary condition on the composite surface becomes $-\mathbf{E}_0 \sin \omega t \cdot \hat{\mathbf{x}}$ (Fig. 6.7).

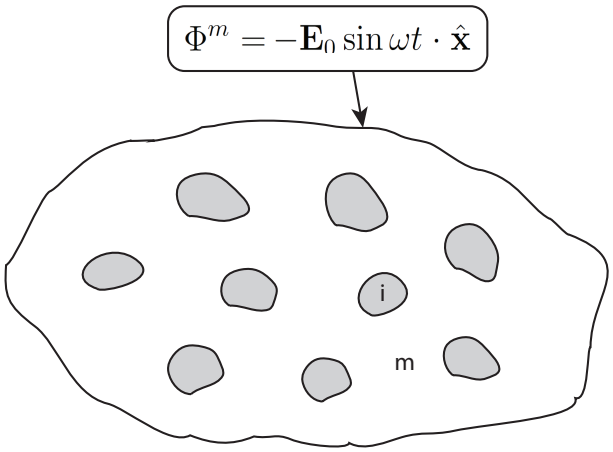

Figure 6.7: A weakly nonlinear composite subject to an AC applied electric field. The boundary condition $\Phi^m = -\mathbf{E}_0 \sin \omega t \cdot \hat{\mathbf{x}}$ is imposed on the surface of the composite, which try to establish the electric field ($\mathbf{E}_0 \sin \omega t$) inside the composite.

Assuming that the frequency is low, the electric displacement and the electric field still satisfy the electrostatic equations (Eqs. (6.3) and (6.4)). Hence the boundary conditions on the inclusion surface are the same as those of the DC case. Since the electrostatic equations are time independent, the spatial average of the electric displacement $\langle \mathbf{D} \rangle$ must relates to the applied field $\mathbf{E}_0 \sin \omega t$ at a particular time t via the effective DC coefficients as in Eq. (6.21). Therefore

$$\begin{aligned} \langle \mathbf{D} \rangle &= \varepsilon_e \mathbf{E}_0 \sin(\omega t) + \chi_e |\mathbf{E}_0 \sin(\omega t)|^2 \mathbf{E}_0 \sin(\omega t) + \eta_e |\mathbf{E}_0 \sin(\omega t)|^4 \mathbf{E}_0 \sin(\omega t) \\ &\quad + \delta_e |\mathbf{E}_0 \sin(\omega t)|^6 \mathbf{E}_0 \sin(\omega t) + \mu_e |\mathbf{E}_0 \sin(\omega t)|^8 \mathbf{E}_0 \sin(\omega t) + \dots . \end{aligned} \tag{6.47}$$

Using trigonometric identities, this can be written as

$$\begin{aligned}\langle \mathbf{D} \rangle &= \big[\varepsilon_e \mathbf{E}_0 + \frac{3}{4}\chi_e |\mathbf{E}_0|^2 \mathbf{E}_0 + \frac{5}{8}\eta_e |\mathbf{E}_0|^4 \mathbf{E}_0 + \frac{35}{64}\delta_e |\mathbf{E}_0|^6 \mathbf{E}_0 + \frac{63}{128}\mu_e |\mathbf{E}_0|^8 \mathbf{E}_0 \\ &\quad +...\big] \sin(\omega t) + \big[-\frac{1}{4}\chi_e |\mathbf{E}_0|^2 \mathbf{E}_0 - \frac{5}{16}\eta_e |\mathbf{E}_0|^4 \mathbf{E}_0 - \frac{21}{64}\delta_e |\mathbf{E}_0|^6 \mathbf{E}_0 \\ &\quad -\frac{21}{64}\mu_e |\mathbf{E}_0|^8 \mathbf{E}_0 + ...\big] \sin(3\omega t) + \big[\frac{1}{16}\eta_e |\mathbf{E}_0|^4 \mathbf{E}_0 + \frac{7}{64}\delta_e |\mathbf{E}_0|^6 \mathbf{E}_0 \\ &\quad +\frac{9}{64}\mu_e |\mathbf{E}_0|^8 \mathbf{E}_0 + ...\big] \sin(5\omega t) + \big[-\frac{1}{64}\delta_e |\mathbf{E}_0|^6 \mathbf{E}_0 \\ &\quad -\frac{9}{256}\delta_e |\mathbf{E}_0|^8 \mathbf{E}_0 + ...\big] \sin(7\omega t) + \big[\frac{1}{256}\mu_e |\mathbf{E}_0|^8 \mathbf{E}_0 + ...\big] \sin(9\omega t). \quad (6.48)\end{aligned}$$

The general expression for the effective AC response is firstly proposed by [31] as

$$\begin{aligned}\langle \mathbf{D} \rangle &= \big[\varepsilon^*_\omega \mathbf{E}_0 + \chi^*_\omega |\mathbf{E}_0|^2 \mathbf{E}_0 + \eta^*_\omega |\mathbf{E}_0|^4 \mathbf{E}_0 + \delta^*_\omega |\mathbf{E}_0|^6 \mathbf{E}_0 + \mu^*_\omega |\mathbf{E}_0|^8 \mathbf{E}_0\big] \sin(\omega t) \\ &\quad +\big[\varepsilon^*_{3\omega} \mathbf{E}_0 + \chi^*_{3\omega} |\mathbf{E}_0|^2 \mathbf{E}_0 + \eta^*_{3\omega} |\mathbf{E}_0|^4 \mathbf{E}_0 + \delta^*_{3\omega} |\mathbf{E}_0|^6 \mathbf{E}_0 \\ &\quad +\mu^*_{3\omega} |\mathbf{E}_0|^8 \mathbf{E}_0\big] \sin(3\omega t) + \big[\varepsilon^*_{5\omega} \mathbf{E}_0 + \chi^*_{5\omega} |\mathbf{E}_0|^2 \mathbf{E}_0 + \eta^*_{5\omega} |\mathbf{E}_0|^4 \mathbf{E}_0 \\ &\quad +\delta^*_{5\omega} |\mathbf{E}_0|^6 \mathbf{E}_0 + \mu^*_{5\omega} |\mathbf{E}_0|^8 \mathbf{E}_0\big] \sin(5\omega t) + \dots, \quad (6.49)\end{aligned}$$

where $\varepsilon^*_{n\omega}$, $\chi^*_{n\omega}$, $\eta^*_{n\omega}$, $\delta^*_{n\omega}$ and $\mu^*_{n\omega}$ are the effective AC coefficients at the n^{th} harmonics. Comparing Eq. (6.48) with (6.49), we get the relationships between the effective DC and AC coefficients as

$\varepsilon^*_\omega = \varepsilon_e \qquad \chi^*_\omega = \frac{3}{4}\chi_e \qquad \eta^*_\omega = \frac{10}{16}\eta_e$

$\delta^*_\omega = \frac{35}{64}\delta_e \qquad \mu^*_\omega = \frac{126}{256}\mu_e \qquad \varepsilon^*_{3\omega} = 0$

$\chi^*_{3\omega} = -\frac{1}{4}\chi_e \qquad \eta^*_{3\omega} = -\frac{5}{16}\eta_e \qquad \delta^*_{3\omega} = -\frac{21}{64}\delta_e$

$\mu^*_{3\omega} = -\frac{84}{256}\mu_e \qquad \varepsilon^*_{5\omega} = 0 \qquad \chi^*_{5\omega} = 0$

$\eta^*_{5\omega} = \frac{1}{16}\eta_e \qquad \delta^*_{5\omega} = \frac{7}{64}\delta_e \qquad \mu^*_{5\omega} = \frac{36}{256}\mu_e$

$\varepsilon^*_{7\omega} = 0 \qquad \chi^*_{7\omega} = 0 \qquad \eta^*_{7\omega} = 0$

$\delta^*_{7\omega} = -\frac{1}{64}\delta_e \qquad \mu^*_{7\omega} = -\frac{9}{256}\mu_e \qquad \varepsilon^*_{9\omega} = 0$

$\chi^*_{9\omega} = 0 \qquad \eta^*_{9\omega} = 0 \qquad \delta^*_{9\omega} = 0$

$\mu^*_{9\omega} = \frac{1}{256}\mu_e$

Using the effective DC coefficients obtained in the previous section, we can easily obtain the effective quasi-static AC coefficients for composites with elliptic cylindrical inclusions. In fact, these relationships are quite general because it can be

applied to all weakly isotropic nonlinear composites. The effective DC coefficients calculated from any methods developed for isotropic weakly nonlinear composites can be directly transformed to the effective AC coefficients.

6.2.2 Transformation from DC to fundamental plus third harmonic AC response

Now we consider the external field of the form $(E_1 \sin \omega t + E_3 \sin 3\omega t)\hat{\mathbf{u}}$, where $\hat{\mathbf{u}}$ is a unit vector indicating the direction of the applied field. The boundary condition on the surface of the composite is indicated in Fig. 6.8. For cylindrical composites, the direction of $\hat{\mathbf{u}}$ is arbitrary but perpendicular to the cylindrical axes.

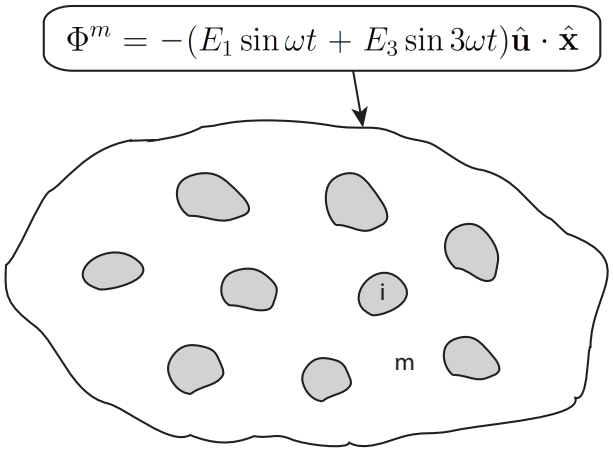

Figure 6.8: A weakly nonlinear composite subject to fundamental and third harmonic applied electric fields. The boundary condition $\Phi^m = -(E_1 \sin \omega t + E_3 \sin 3\omega t)\hat{\mathbf{u}} \cdot \hat{\mathbf{x}}$ is imposed on the surface of the composite, which try to establish the electric field $(E_1 \sin \omega t + E_3 \sin 3\omega t)\hat{\mathbf{u}}$ inside the composite.

Using the similar argument in the previous section, we replace $\mathbf{E}_0$ in Eq. (6.21) by $(E_1 \sin \omega t + E_3 \sin 3\omega t)\hat{\mathbf{u}}$:

$$\begin{aligned} \langle \mathbf{D} \rangle &= [\varepsilon_e (E_1 \sin \omega t + E_3 \sin 3\omega t) + \chi_e (E_1 \sin \omega t + E_3 \sin 3\omega t)^3 \\ &\quad + \eta_e (E_1 \sin \omega t + E_3 \sin 3\omega t)^5 + \delta_e (E_1 \sin \omega t + E_3 \sin 3\omega t)^7 + \ldots]\hat{\mathbf{u}}. \end{aligned} \tag{6.50}$$

By using some identities of sine function, we can re-express Eq. (6.50) as:

$$\begin{aligned}\langle \mathbf{D} \rangle &= [(\varepsilon_e E_1 + \frac{3}{4}\chi_e E_1^3 - \frac{3}{4}\chi_e E_1^2 E_3 + \frac{3}{2}\chi_e E_1 E_3^2 + \frac{5}{8}\eta_e E_1^5 - \frac{25}{16}\eta_e E_1^4 E_3 + \frac{15}{4}\eta_e E_1^3 E_3^2 \\ &\quad -\frac{15}{8}\eta_e E_1^2 E_3^3 + \frac{15}{8}\eta_e E_1 E_3^4 + \frac{35}{64}\delta_e E_1^7 - \frac{147}{64}\delta_e E_1^6 E_3 + \frac{441}{64}\delta_e E_1^5 E_3^2 \\ &\quad -\frac{525}{64}\delta_e E_1^4 E_3^3 + \frac{315}{32}\delta_e E_1^3 E_3^4 - \frac{105}{32}\delta_e E_1^2 E_3^5 + \frac{35}{16}\delta_e E_1 E_3^6) \sin\omega t + (\varepsilon_e E_3 - \frac{1}{4}\chi_e E_1^3 \\ &\quad +\frac{3}{2}\chi_e E_1^2 E_3 + \frac{3}{4}\chi_e E_3^3 - \frac{5}{16}\eta_e E_1^5 + \frac{15}{8}\eta_e E_1^4 E_3 - \frac{15}{8}\eta_e E_1^3 E_3^2 + \frac{15}{4}\eta_e E_1^2 E_3^3 \\ &\quad +\frac{5}{8}\eta_e E_3^5 - \frac{21}{64}\delta_e E_1^7 + \frac{147}{64}\delta_e E_1^6 E_3 - \frac{315}{64}\delta_e E_1^5 E_3^2 + \frac{315}{32}\delta_e E_1^4 E_3^3 - \frac{175}{32}\delta_e E_1^3 E_3^4 \\ &\quad +\frac{105}{16}\delta_e E_1^2 E_3^5 + \frac{35}{64}\delta_e E_3^7) \sin 3\omega t + \dots]\hat{\mathbf{u}}. \end{aligned} \tag{6.51}$$

The effective response of nonlinear composites under an external AC electric field of the form $(E_1 \sin\omega t + E_3 \sin 3\omega t)\hat{\mathbf{u}}$ has been investigated by Wei et al. [34]. They report the general form of the effective response up to the third-order. In this work, we further generalize the form up to the seventh-order as

$$\begin{aligned}\langle \mathbf{D} \rangle &= [(\varepsilon^*_{\omega;\,\omega} E_1 + \varepsilon^*_{3\omega;\,\omega} E_3 + \chi^*_{\omega^3;\,\omega} E_1^3 + \chi^*_{\omega^2 3\omega;\,\omega} E_1^2 E_3 + \chi^*_{\omega(3\omega)^2;\,\omega} E_1 E_3^2 + \chi^*_{(3\omega)^3;\,\omega} E_3^3 \\ &\quad +\eta^*_{\omega^5;\,\omega} E_1^5 + \eta^*_{\omega^4 3\omega;\,\omega} E_1^4 E_3 + \eta^*_{\omega^3(3\omega)^2;\,\omega} E_1^3 E_3^2 + \eta^*_{\omega^2(3\omega)^3;\,\omega} E_1^2 E_3^3 + \eta^*_{\omega(3\omega)^4;\,\omega} E_1 E_3^4 \\ &\quad +\eta^*_{(3\omega)^5;\,\omega} E_3^5 + \delta^*_{\omega^7;\,\omega} E_1^7 + \delta^*_{\omega^6 3\omega;\,\omega} E_1^6 E_3 + \delta^*_{\omega^5(3\omega)^2;\,\omega} E_1^5 E_3^2 + \delta^*_{\omega^4(3\omega)^3;\,\omega} E_1^4 E_3^3 \\ &\quad +\delta^*_{\omega^3(3\omega)^4;\,\omega} E_1^3 E_3^4 + \delta^*_{\omega^2(3\omega)^5;\,\omega} E_1^2 E_3^5 + \delta^*_{\omega(3\omega)^6;\,\omega} E_1 E_3^6 + \delta^*_{(3\omega)^7;\,\omega} E_3^7) \sin\omega t \\ &\quad +(\varepsilon^*_{\omega;\,3\omega} E_1 + \varepsilon^*_{3\omega;\,3\omega} E_3 + \chi^*_{\omega^3;\,3\omega} E_1^3 + \chi^*_{\omega^2 3\omega;\,3\omega} E_1^2 E_3 + \chi^*_{\omega(3\omega)^2;\,3\omega} E_1 E_3^2 \\ &\quad +\chi^*_{(3\omega)^3;\,3\omega} E_3^3 + \eta^*_{\omega^5;\,3\omega} E_1^5 + \eta^*_{\omega^4 3\omega;\,3\omega} E_1^4 E_3 + \eta^*_{\omega^3(3\omega)^2;\,3\omega} E_1^3 E_3^2 \\ &\quad +\eta^*_{\omega^2(3\omega)^3;\,3\omega} E_1^2 E_3^3 + \eta^*_{\omega(3\omega)^4;\,3\omega} E_1 E_3^4 + \eta^*_{(3\omega)^5;\,3\omega} E_3^5 + \delta^*_{\omega^7;\,3\omega} E_1^7 + \delta^*_{\omega^6 3\omega;\,3\omega} E_1^6 E_3 \\ &\quad +\delta^*_{\omega^5(3\omega)^2;\,3\omega} E_1^5 E_3^2 + \delta^*_{\omega^4(3\omega)^3;\,3\omega} E_1^4 E_3^3 + \delta^*_{\omega^3(3\omega)^4;\,3\omega} E_1^3 E_3^4 + \delta^*_{\omega^2(3\omega)^5;\,3\omega} E_1^2 E_3^5 \\ &\quad +\delta^*_{\omega(3\omega)^6;\,3\omega} E_1 E_3^6 + \delta^*_{(3\omega)^7;\,3\omega} E_3^7) \sin 3\omega t + \dots]\hat{\mathbf{u}}, \end{aligned} \tag{6.52}$$

where $\varepsilon^*_{\omega^m(3\omega)^n;k\omega}$, $\chi^*_{\omega^m(3\omega)^n;k\omega}$, $\eta^*_{\omega^m(3\omega)^n;k\omega}$, $\delta^*_{\omega^m(3\omega)^n;k\omega}$ and $\mu^*_{\omega^m(3\omega)^n;k\omega}$ are coupled effective AC coefficients at the k^{th} harmonics. Comparing Eq. (6.51) with (6.52), we obtain the relationships between the effective DC and AC coefficients as:

$$\varepsilon^*_{\omega;\,\omega} = \varepsilon_e \qquad \varepsilon^*_{3\omega;\,\omega} = 0 \qquad \chi^*_{\omega^3;\,\omega} = \tfrac{3}{4}\chi_e$$

$$\chi^*_{\omega^2 3\omega;\,\omega} = -\tfrac{3}{4}\chi_e \qquad \chi^*_{\omega(3\omega)^2;\,\omega} = \tfrac{3}{2}\chi_e \qquad \chi^*_{(3\omega)^3;\,\omega} = 0$$

$$\eta^*_{\omega^5;\,\omega} = \tfrac{5}{8}\eta_e \qquad \eta^*_{\omega^4 3\omega;\,\omega} = -\tfrac{25}{16}\eta_e \qquad \eta^*_{\omega^3(3\omega)^2;\,\omega} = \tfrac{15}{4}\eta_e$$

$\eta^*_{\omega^2(3\omega)^3;\,\omega} = -\frac{15}{8}\eta_e \qquad \eta^*_{\omega(3\omega)^4;\,\omega} = \frac{15}{8}\eta_e \qquad \eta^*_{(3\omega)^5;\,\omega} = 0$

$\delta^*_{\omega^7;\,\omega} = \frac{35}{64}\delta_e \qquad \delta^*_{\omega^6 3\omega;\,\omega} = -\frac{147}{64}\delta_e \qquad \delta^*_{\omega^5(3\omega)^2;\,\omega} = \frac{441}{64}\delta_e$

$\delta^*_{\omega^4(3\omega)^3;\,\omega} = -\frac{525}{64}\delta_e \qquad \delta^*_{\omega^3(3\omega)^4;\,\omega} = \frac{315}{32}\delta_e \qquad \delta^*_{\omega^2(3\omega)^5;\,\omega} = -\frac{105}{32}\delta_e$

$\delta^*_{\omega(3\omega)^6;\,\omega} = \frac{35}{16}\delta_e \qquad \delta^*_{(3\omega)^7;\,\omega} = 0$

$\varepsilon^*_{\omega;\,3\omega} = 0 \qquad \varepsilon^*_{3\omega;\,3\omega} = \varepsilon_e \qquad \chi^*_{\omega^3;\,3\omega} = -\frac{1}{4}\chi_e$

$\chi^*_{\omega^2 3\omega;\,3\omega} = \frac{3}{2}\chi_e \qquad \chi^*_{\omega(3\omega)^2;\,3\omega} = 0 \qquad \chi^*_{(3\omega)^3;\,3\omega} = \frac{3}{4}\chi_e$

$\eta^*_{\omega^5;\,3\omega} = -\frac{5}{16}\eta_e \qquad \eta^*_{\omega^4 3\omega;\,3\omega} = \frac{15}{8}\eta_e \qquad \eta^*_{\omega^3(3\omega)^2;\,3\omega} = -\frac{15}{8}\eta_e$

$\eta^*_{\omega^2(3\omega)^3;\,3\omega} = \frac{15}{4}\eta_e \qquad \eta^*_{\omega(3\omega)^4;\,3\omega} = 0 \qquad \eta^*_{(3\omega)^5;\,3\omega} = \frac{5}{8}\eta_e$

$\delta^*_{\omega^7;\,3\omega} = -\frac{21}{64}\delta_e \qquad \delta^*_{\omega^6 3\omega;\,3\omega} = \frac{147}{64}\delta_e \qquad \delta^*_{\omega^5(3\omega)^2;3\,\omega} = -\frac{315}{64}\delta_e$

$\delta^*_{\omega^4(3\omega)^3;\,3\omega} = \frac{315}{32}\delta_e \qquad \delta^*_{\omega^3(3\omega)^4;\,3\omega} = -\frac{175}{32}\delta_e \qquad \delta^*_{\omega^2(3\omega)^5;\,3\omega} = \frac{105}{16}\delta_e$

$\delta^*_{\omega(3\omega)^6;\,3\omega} = 0 \qquad \delta^*_{(3\omega)^7;\,3\omega} = \frac{35}{64}\delta_e$

Again these relationships are valid for all weakly nonlinear isotropic composites. By substituting the results of the effective DC coefficients from Eqs. (6.42) - (6.45), the effective AC coefficients of the elliptic cylindrical composite up to the seventh-order and third-harmonics are obtained.

CHAPTER VII

Conclusions

The Lakhtakia-Depine condition [12] for the negative refractive index in lossy isotropic media has been investigated. This condition is based on the phenomena of the negative phase velocity of a uniform plane wave which imply that the direction of the phase velocity is antiparallel to the direction of the power flow or the Poynting vector. The special case of the Lakhtakia-Depine condition, namely, $\mathrm{Re}\{\varepsilon_r\} < 0$ and $\mathrm{Re}\{\mu_r\} < 0$, is used in designing a negative index composite at infrared frequencies. The structure of this composite consists of two different group of nonmagnetic spheres. The negative real part of the effective permeability of the composite is accomplished by the resonance of the magnetic scattering coefficient of the first group of spheres. This resonance condition requires high values of the relative permittivity of the first group of spheres ($\varepsilon_{r1} > 100$) around the infrared frequencies, when the size of spheres are a few micron. Such high values of the relative permittivity can be achieved by using $LiTaO_3$ as the material for the first group of spheres.

For the real part of the effective relative permittivity to be negative, we employ the resonance of the effective relative permittivity itself. This resonance requires that the relative permittivity of the second group of spheres must be negative, which can be achieved by using a semiconductor that satisfies the Drude model relation because it can provide negative values under its plasma frequency. Based on the resonance condition, the plasma frequency of the semiconductor spheres is derived.

When combining these two group of spheres into a composite, the numerical result of the effective relative permittivity, the effective relative permeability

and the effective refractive index show that this composite satisfies the Lakhtakia-Depine condition for the negative refractive index around 3.48 - 3.68 THz. Since the Lakhtakia-Depine condition is based on the negative phase velocity, this condition can not generally ensure a negative angle of refraction when an electromagnetic wave propagates into the material. However this condition can be a good approximation of the negative refraction if the electric and magnetic losses are low.

Next we investigate the characteristics of uniform and nonuniform plane wave propagations in a biaxial anisotropic lossy medium. Under the principal axes of the medium, we assume that the relative permittivity and the relative permeability tensors can be diagonalized simultaneously. the elements of the relative permittivity and the relative permeability tensors are assumed to satisfy the passivity condition, which imply that the elements must lie on the upper half of the complex plane.

A uniform plane wave propagation with the electric field polarization along one of the medium principal axes is studied and the general condition of the negative phase velocity is derived. This condition depends on the elements of the relative permittivity and the relative permeability tensors together with the propagation direction. If we let the elements of each tensors to be equal, the medium is lossy isotropic and the negative phase velocity condition is reduced exactly to the Lakhtakia-Depine condition. To ensure our theoretical result, we show the plots of the angle between the average Poynting vector and the phase velocity angle for two sets of sample parameters.

Then we consider a problem of refraction when a TE plane wave propagates from free space into the biaxial anisotropic media. In this case, it turns out that the transmitted wave is nonuniform, implying that the planes of constant amplitude and the planes of constant phase do not coincide. Based on the solutions of this problem, the general condition of the negative angle of refraction is derived, which depends on the elements of the relative permittivity and the relative permeability tensors of the biaxial medium and the incident angle. Although the general condition is for TE wave, it can be transformed into TM case by the elec-

tromagnetic dualities. In order to confirm our theoretical result, we show a plot of the angle of refraction with respect to the incident angle for a set of sample parameters which satisfy our negative refraction condition. Moreover a plot of a term relating to the phase velocity of the transmitted wave indicates that the angle of refraction can be negative even if the phase velocity is positive.

We also investigated the effective responses of a weakly nonlinear dielectric composite subject to an externally applied uniform electric field. The structure of this composite consists of dilute fifth-order nonlinear elliptic cylindrical inclusions randomly distributed in a linear host medium. All inclusions are assumed to be parallel and identical in shape to each other but the orientations are random. The electric potential and field of a single inclusion are then determined using elliptic cylindrical coordinates and a power series method. The general formulae for higher-order effective coefficients up to the ninth order are derived using the Landau formula [49]. The obtained results of the effective nonlinear coefficients are symmetric under the exchange between the semi-major and semi-minor axes and the third-order effective coefficient agrees with that of Yu et al. [26]. Moreover, the general features of the magnitude of η_e/η_i (Fig. 6.4a) are similar to that of χ_e/χ_i (Fig. 6.3a) and the negative result of the fifth-order coefficient has also been observed previously by Filho et al. [51]. Furthermore, the shape effect reveals large enhancement of the effective responses for aspect ratios of significantly less than one, especially at a high contrast between the linear coefficients of the inclusion and host medium with the relative permittivity (K) being much lower than one.

The scope of our nonlinearity enhancement is mainly on dielectric composites with an electrostatic applied field. However, this could also be applied, in the cases of time-varying fields at low frequencies. A general problem involving weakly nonlinear composites subject to an AC applied fields of the form $\mathrm{E}_0 \sin(\omega t)$ and $\mathrm{E}_1 \sin(\omega t) + \mathrm{E}_3 \sin(3\omega t)$ in the quasi-static limit was considered and general relationships or transformations between the effective DC and AC coefficients were established. The transformations were extended from the work of Wei et al. [34] to include the effective coefficients up to the seventh order. Furthermore, the transformations for non-decoupling coefficients at fundamental harmonics ($\varepsilon_{\omega;\omega}$, $\chi_{\omega;\omega}$,

$\eta_{\omega;\omega}$ and $\delta_{\omega;\omega}$) are the same as the transformation of our published results [35]. Following the same procedures as presented here, we note that the transformation can be generalized to predict responses up to any order and harmonics.

References

[1] Milton, G. W. *The theory of composites,* (USA: Cambridge University Press, 2002).

[2] Lakes, R. Cellular solid structures with unbounded thermal expansion. *J. Mater. Sci. Lett.* 15 (1996) 475-477.

[3] Vesselago, V. G. The electodynamics of substances with simultaneously negative value of ε and μ. *Soviet Physics USPEKHI* 10 (1968) 509-514.

[4] Pendry, J. B. Nagative refraction makes a perfect lens. *Phys. Rev. Lett.* 85 (2000) 3966-3969.

[5] Pendry, J. B., Holden A. J., Robbins D. J. and Stewart W. J. Low frequency plasmons in thin-wire structures. *J. Phys. Condens. Matter.* 10 (1998) 4785-4809.

[6] Pendry, J. B., Holden, A. J., Robbins, D. J. and Stewart, W. J. Magnetism from conductors and enhanced nonlinear phenomena. *IEEE Trans. Microwave Theory Tech.* 47 (1999) 2075-2084.

[7] Smith, D. R., Padilla, W. J., Vier D. C., Nemat-Nasser, S. C. and Schultz, S. Composite medium with simultaneously negative permeability and permittivity. *Phys. Rev. Lett.* 84 (2000) 4184-4187.

[8] Wheeler, M. S., Aitchison, J. S., Mojahedi M. Coated nonmagnetic spheres with a negative index of refraction at infrared frequencies. *Phys. Rev. B* 73 (2006) 045105:1-7.

[9] Yannopapas, V. Negative refraction in random photonic alloys of polaritonic and plasmonic microspheres. *Phys. Rev. B* 75 (2007) 035112:1-7.

[10] Shalaev, V. M., Cai, W., Chettiar, U. K., Yuan, H., Sarychev, A. K., Drachev, V. P. and Kildishev, V. A. Negative index of refraction in optical metamaterials. *Opt. Lett.* 30 (2005) 3356-3358.

[11] McCall, M. W., Lakhtakia, A, Weiglhofer, W. S. The negative index of refraction demystified. *Eur. J. Phys.* 23 (2002) 353-359.

[12] Depine, R. A., Lakhtakia, A. A new condition to identify isotropic dielectric-magnetic materials displaying negative phase velocity. *Microwave. Opt. Technol. Lett.* 41 (2004) 315-316.

[13] Kinsler, P., McCall, M. W. Criteria for negative refraction in active and passive media. *Microwave. Opt. Technol. Lett.* 50 (2008) 1804–1807.

[14] Lakhtakia, A., Mackay, T. G., Geddes, J. B. On the inapplicability of a negative-phase-velocity condition as a negative-refraction condition for active materials. *Microwave. Opt. Technol. Lett.* 51 (2009) 1230.

[15] Stratton, J. A. *Electromagnetic Theory*, (London: McGraw-Hill, 1941).

[16] Mackay, T. G., Lakhtakia, A. Negative refraction, negative phase velocity, and counterposition in bianisotropic materials and metamaterials. *Phys. Rev. B* 79 (2009) 235121:1-5.

[17] Woodley, J., Mojahedi, M. Backward wave propagation in left-handed media with isotropic and anisotropic permittivity tensors. *J. Opt. Soc. Am. B* 23 (2006) 2377-2382.

[18] Ding, W., Chen, L. and Liang, C. H. Characteristics of electromagnetic wave propagation in biaxially anisotropic left-handed materials. *Progress In Electromagnetics Research* 70 (2007) 37-52.

[19] Liu, S. H., Guo, L. X. Negative refraction in an anisotropic metamaterial with a rotation angle between the principal axis and the planar interface. *Progress In Electromagnetics Research* 115 (2011) 243-257.

[20] Manna, S. S. and Chakrabarti, B. K. Dielectric breakdown in the presence of random conductors. *Phys. Rev. B* 36 (1987) 4078-4081.

[21] Levy, O. and Bergman, D. J. Clausius-Mossotti approximation for a family of nonlinear composites. *Phys. Rev. B* 46 (1992) 7189-7192.

[22] Stroud, D. and Hui, P. M. Nonlinear susceptibilities of granular matter. *Phys. Rev. B* 37 (1988) 8719-8724.

[23] Shalaev, V. M., Stockman, M. I. and Botet, R. Resonant excitations and nonlinear optics of fractals. *Physica A* 185 (1992) 181-186.

[24] Hui, P. M. and Stroud, D. Theory of second harmonic generation in composites of nonlinear dielectrics. *J. Appl. Phys.* 82 (1997) 4740-4743.

[25] Hui, P. M., Cheung, P. and Stroud, D. Theory of third harmonic generation in random composites of nonlinear dielectrics. *J. Appl. Phys.* 84 (1998) 3451-3458.

[26] Yu, K. W., Hui, P. M. and Stroud, D. Effective dielectric response of nonlinear composites. *Phys. Rev. B* 47 (1992) 14150-14156.

[27] Natenapit, M., Thongboonrithi, C. Effective higher-order nonlinear coefficients of composites with weakly nonlinear media. *Physica B* 405 (2010) 2367-2375.

[28] Gu, G. Q. and Yu, K. W. Effective conductivity of nonlinear composites. *Phys. Rev. B* 46 (1992) 4502-4507.

[29] Castaneda, P. P., deBotton, G. and Li, G. Effective properties of nonlinear inhomogeneous dielectrics *Phys. Rev. B* 46 (1992) 4387-4394.

[30] Stroud, D. and Wood, V. E. Decoupling approximation for the nonlinear-optical response of composite media *J. Opt. Soc. Am. B* 6 (1989) 778-786.

[31] Gu, G. Q., Hui, P. M. and Yu, K. W. A theory of nonlinear AC response in nonlinear composites. *Physica B* 279 (2000) 62-65.

[32] Wei, E. B., Song, J. B. and Gu, G. Q. Effective dielectric response of nonlinear composites with external ac and dc electric field. *J. Appl. Phys.* 95 (2004) 1377-1381.

[33] Wei, E. B., Song, J. B., Tian, J. W. and Gu, G. Q. Higher order response of nonlinear composite in external AC electric field. *Phys. Lett. A* 309 (2003) 160-164.

[34] Wei, E. B., Yang, Z. D. and Gu, G. Q. Effective ac response in weakly nonlinear composites. *J. Phys. D: Appl. Phys.* 37 (2004) 107-111.

[35] Natenapit, M., Thongboonrithi, C. and Potisook, C. Ninth-order effective responses of nonlinear composites in external DC and AC electric fields. *Physica B* 403 (2008) 4314-4318.

[36] Goncharenko, A. V., Popelnukh, V. V. and Venger, E. F. Effect of weak nonsphericity on linear and nonlinear optical properties of small particle composites. *J. Phys. D: Appl. Phys.* 35 (2002) 1833-1838.

[37] Natenapit, M. and Thongsri, J. Shape effect on strongly nonlinear response of elliptical composites. *Eur. Phys. Appl. Phys.* 46 (2009) 20701-20705.

[38] Giordano, S. Order and disorder in the microstructure of dielectrically nonlinear heterogeneous materials. *J. Electrostat.* 68 (2010) 227-236.

[39] Lakhtakia, A. and Weiglhofer, W. S. Maxwell Garnett formalism for weakly nonlinear, bianisotropic, dilute, particulate composite media. *Int. J. Electron.* 87 (2000) 1401-1408.

[40] Lakhtakia, M. N. and Lakhtakia, A. Anisotropic Composite Materials with Intensity-Dependent Permittivity Tensor: The Bruggeman Approach. *Electromagnetics* 21 (2001) 129-137.

[41] Mackay, T. G. Geometrically derived anisotropy in cubically nonlinear dielectric composites. *J. Phys. D: Appl. Phys.* 36 (2003) 583-591.

[42] Gao, L., Huang, Y. and Li, Z. Effective medium approximation for strongly nonlinear composite media with shape distribution. *Phys. Lett. A* 306 (2003) 337-343.

[43] Yang, B., Zhang, C. and Tian, D. Optical nonlinearity enhancement of a periodic array of semiconductor elliptical cylinders. *J. Opt. Soc. Am. B* 19 (2002) 2632-2636.

[44] Thongsri, J. and Natenapit, M. Shape effect on weakly nonlinear elliptical composites. *Composites: Part B* 43 (2012) 1252-1257.

[45] Potisook, C. and Natenapit, M. Effective responses of nonlinear elliptic cylindrical composites. *Physica B* 407 (2012) 598-605.

[46] Bottcher, C. J. F. *Theory of Electric Polarization*, 2^{nd} ed. vol. 1. (Amsterdam: Elsevier Scientific Publishing Company, 1973).

[47] Bohren, C. F. and Huffman, D. R. *Absorbtion and Scattering of Light by Small Particles,* (New York: Wiley-Interscience, 1983).

[48] Jackson, J. D. *Classical electrodynamics*, 3^{rd} ed. (New York: Wiley, 1999).

[49] Landau, L. D. and Lifshitz, E. M. *Electrodynamics of Continuous Media,* (Oxford: Pergamon, 1984).

[50] Ormachea, O. Comparative analysis of multi-wave mixing and measurements of the higher-order nonlinearities in resonant media. *Opt. Commun.* 268 (2006) 317-322.

[51] Filho, E. L., Araujo, C.B. and Rodrigues, J. J. High-order nonlinearities of aqueous colloids containing silver nanoparticles. *J. Opt. Soc. Am. B* 24 (2007) 2948-2956.

APPENDICES

Appendix A

Derivation of the Material Condition from $\mathbf{Re}\{k_+\} < 0$ and $\mathbf{Re}\{k_-\} > 0$

In Chapter 3, we conclude that $\mathrm{Re}\{k_+\} < 0$ or $\mathrm{Re}\{k_-\} > 0$ will be satisfied if ε_r and μ_r are related by the inequality:

$$\varepsilon_r' \sqrt{\mu_r'^2 + \mu_r''^2} + \mu_r' \sqrt{\varepsilon_r'^2 + \varepsilon_r''^2} < 0, \tag{A.1}$$

where $\varepsilon_r' = \mathrm{Re}\{\varepsilon_r\}$, $\varepsilon_r'' = \mathrm{Im}\{\varepsilon_r\}$, $\mu_r' = \mathrm{Re}\{\mu_r\}$ and $\mu_r'' = \mathrm{Im}\{\mu_r\}$. Here, we show the detailed derivation of this inequality as follows. Taking the real part of Eq. (3.11) yields

$$\mathrm{Re}\{k_\pm\} = \pm \frac{\omega}{c} \sqrt{|\varepsilon_r||\mu_r|} \cos\left(\frac{\phi_\varepsilon + \phi_\mu}{2}\right). \tag{A.2}$$

Then the conditions $\mathrm{Re}\{k_+\} < 0$ or $\mathrm{Re}\{k_-\} > 0$ lead to

$$\begin{aligned}
\frac{\omega}{c} \sqrt{|\varepsilon_r||\mu_r|} \cos\left(\frac{\phi_\varepsilon + \phi_\mu}{2}\right) &< 0, \\
\cos\left(\frac{\phi_\varepsilon + \phi_\mu}{2}\right) &< 0, \\
\cos\left(\frac{\phi_\varepsilon}{2}\right)\cos\left(\frac{\phi_\mu}{2}\right) - \sin\left(\frac{\phi_\varepsilon}{2}\right)\sin\left(\frac{\phi_\mu}{2}\right) &< 0, \\
\sqrt{\frac{\cos\phi_\varepsilon + 1}{2}}\sqrt{\frac{\cos\phi_\mu + 1}{2}} - \sqrt{\frac{1 - \cos\phi_\varepsilon}{2}}\sqrt{\frac{1 - \cos\phi_\mu}{2}} &< 0, \\
\big(\cos\phi_\varepsilon + 1\big)\big(\cos\phi_\mu + 1\big) < \big(1 - \cos\phi_\varepsilon\big)&\big(1 - \cos\phi_\mu\big).
\end{aligned} \tag{A.3}$$

Rewrite ε_r and μ_r as

$$\varepsilon_r' + i\varepsilon_r'' = \sqrt{\varepsilon_r'^2 + \varepsilon_r''^2}\big(\cos\phi_\varepsilon + i\sin\phi_\varepsilon\big), \tag{A.4}$$

$$\mu_r' + i\mu_r'' = \sqrt{\mu_r'^2 + \mu_r''^2}\big(\cos\phi_\mu + i\sin\phi_\mu\big). \tag{A.5}$$

Therefore

$$\cos\phi_\varepsilon = \frac{\varepsilon'_r}{\sqrt{\varepsilon'^2_r + \varepsilon''^2_r}}, \qquad \cos\phi_\mu = \frac{\mu'_r}{\sqrt{\mu'^2_r + \mu''^2_r}}. \tag{A.6}$$

Substituting Eqs. (A.6) into Eq. (A.3), we get

$$\begin{aligned}
\left(\frac{\varepsilon'_r}{\sqrt{\varepsilon'^2_r + \varepsilon''^2_r}} + 1\right)\left(\frac{\mu'_r}{\sqrt{\mu'^2_r + \mu''^2_r}} + 1\right) &< \left(1 - \frac{\varepsilon'_r}{\sqrt{\varepsilon'^2_r + \varepsilon''^2_r}}\right)\left(1 - \frac{\mu'_r}{\sqrt{\mu'^2_r + \mu''^2_r}}\right), \\
\frac{\left(\varepsilon'_r + \sqrt{\varepsilon'^2_r + \varepsilon''^2_r}\right)\left(\mu_r + \sqrt{\mu'^2_r + \mu''^{2'}_r}\right)}{\sqrt{\varepsilon'^2_r + \varepsilon''^2_r}\sqrt{\mu'^2_r + \mu''^2_r}} &< \frac{\left(\sqrt{\varepsilon'^2_r + \varepsilon''^2_r} - \varepsilon'_r\right)\left(\sqrt{\mu'^2_r + \mu''^2_r} - \mu'_r\right)}{\sqrt{\varepsilon'^2_r + \varepsilon''^2_r}\sqrt{\mu'^2_r + \mu''^2_r}}, \\
\left(\varepsilon'_r + \sqrt{\varepsilon'^2_r + \varepsilon''^2_r}\right)\left(\mu_r + \sqrt{\mu'^2_r + \mu''^{2'}_r}\right) &< \left(\sqrt{\varepsilon'^2_r + \varepsilon''^2_r} - \varepsilon'_r\right)\left(\sqrt{\mu'^2_r + \mu''^2_r} - \mu'_r\right), \\
\varepsilon'_r\sqrt{\mu'^2_r + \mu''^2_r} + \mu'_r\sqrt{\varepsilon'^2_r + \varepsilon''^2_r} &< -\varepsilon'_r\sqrt{\mu'^2_r + \mu''^2_r} - \mu'_r\sqrt{\varepsilon'^2_r + \varepsilon''^2_r}, \\
2\varepsilon'_r\sqrt{\mu'^2_r + \mu''^2_r} + 2\mu'_r\sqrt{\varepsilon'^2_r + \varepsilon''^2_r} &< 0, \\
\varepsilon'_r\sqrt{\mu'^2_r + \mu''^2_r} + \mu'_r\sqrt{\varepsilon'^2_r + \varepsilon''^2_r} &< 0.
\end{aligned} \tag{A.7}$$

Appendix B

Polarizabilities of Nonmagnetic Spheres

The electric and magnetic polarizabilities of a nonmagnetic sphere can be obtained by solving the scattering problem of a plane electromagnetic wave by that sphere. Consider a plane wave incident on a nonmagnetic sphere of radius r_0, having the relative permittivity ε_r and the relative permeability $\mu_r = 1$. The electric and magnetic fields of the wave are polarized in x and y direction. This situation is shown in Figure B.1.

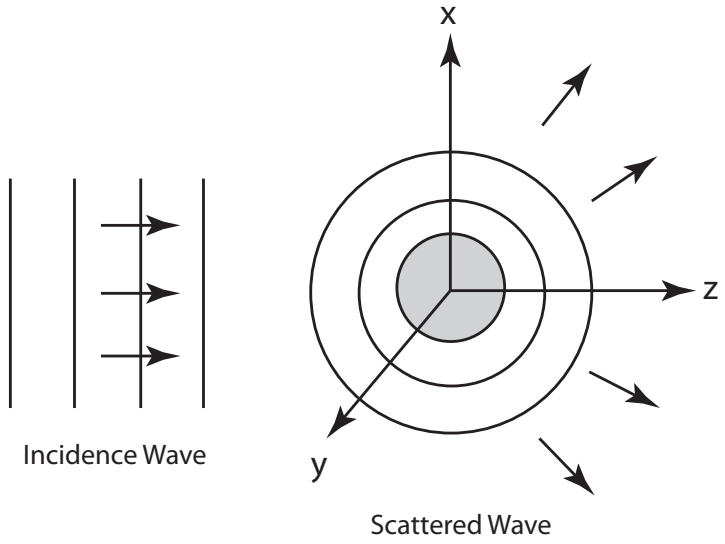

Figure B.1: Scattering of a plane wave by a sphere.

The incident plane wave of angular frequency ω can be written (omitting $e^{-i\omega t}$) as

$$\mathbf{E}_{inc} = \hat{x}\mathrm{E}_0 e^{ikz} \tag{B.1}$$

$$\mathbf{H}_{inc} = \hat{y}\mathrm{H}_0 e^{ikz} \tag{B.2}$$

where $k_0 = \omega/c$ is the free space wave number and $\mathrm{H}_0 = k_0\mathrm{E}_0/(\omega\mu_0)$.

The total fields outside the sphere are the incident fields plus the scattered fields:

$$\mathbf{E}_{out} = \mathbf{E}_{inc} + \mathbf{E}_{sc} \tag{B.3}$$

$$\mathbf{H}_{out} = \mathbf{H}_{inc} + \mathbf{H}_{sc} \tag{B.4}$$

Since the process for solving this problem involves a very lengthy mathematics [47], we simply give the result of the scattered fields

$$\mathbf{E}_{sc} = \sum_{n=1}^{\infty} \mathrm{E}_0 i^n \frac{2n+1}{n(n+1)} (i a_n \mathbf{N}_{e1n}^{(3)} - i b_n \mathbf{M}_{o1n}^{(3)}), \tag{B.5}$$

$$\mathbf{H}_{sc} = \frac{k}{\omega\mu} \sum_{n=1}^{\infty} \mathrm{E}_0 i^n \frac{2n+1}{n(n+1)} (i b_n \mathbf{N}_{o1n}^{(3)} + a_n \mathbf{M}_{e1n}^{(3)}). \tag{B.6}$$

where $\mathbf{M}_{emn}$, $\mathbf{M}_{omn}$, $\mathbf{N}_{emn}$ and $\mathbf{N}_{omn}$ are the vector spherical harmonics:

$$\begin{aligned} \mathbf{M}_{emn} = & -\frac{m}{\sin\theta} \sin m\phi P_n^m(\cos\theta) z_n(\rho) \hat{\boldsymbol{\theta}} \\ & - \cos m\phi \frac{dP_n^m(cos\theta)}{d\theta} z_n(\rho) \hat{\boldsymbol{\phi}}, \end{aligned} \tag{B.7}$$

$$\begin{aligned} \mathbf{M}_{omn} = & \frac{m}{\cos\theta} \sin m\phi P_n^m(\sin\theta) z_n(\rho) \hat{\boldsymbol{\theta}} \\ & - \cos m\phi \frac{dP_n^m(cos\theta)}{d\theta} z_n(\rho) \hat{\boldsymbol{\phi}}, \end{aligned} \tag{B.8}$$

$$\begin{aligned} \mathbf{N}_{emn} = & \frac{z_n(\rho)}{\rho} \cos m\phi \, n(n+1) P_n^m(\cos\theta) \hat{\mathbf{r}} \\ & + \cos m\phi \frac{dP_n^m(\cos\theta)}{\theta} \frac{1}{\rho} \frac{d}{d\rho} [\rho z_n(\rho)] \hat{\boldsymbol{\theta}} \\ & - m \sin m\phi \frac{dP_n^m(\cos\theta)}{\theta} \frac{1}{\rho} \frac{d}{d\rho} [\rho z_n(\rho)] \hat{\boldsymbol{\phi}}, \end{aligned} \tag{B.9}$$

$$\begin{aligned} \mathbf{N}_{emn} = & \frac{z_n(\rho)}{\rho} \sin m\phi \, n(n+1) P_n^m(\cos\theta) \hat{\mathbf{r}} \\ & + \sin m\phi \frac{dP_n^m(\cos\theta)}{\theta} \frac{1}{\rho} \frac{d}{d\rho} [\rho z_n(\rho)] \hat{\boldsymbol{\theta}} \\ & - m \cos m\phi \frac{dP_n^m(\cos\theta)}{\theta} \frac{1}{\rho} \frac{d}{d\rho} [\rho z_n(\rho)] \hat{\boldsymbol{\phi}}, \end{aligned} \tag{B.10}$$

where $\rho = k_0 r$, P_n^m is the associated Lergendre function and z_n is a spherical Bessel function. The superscript (3) in Eqs. (B.5) and (B.6) indicate that we

must represent $z_n(\rho)$ by the spherical Bessel function of the third kind $h_n^{(1)}(\rho)$. the scattering coefficients a_n and b_n are

$$a_n = \frac{m\psi_n(mx)\psi_n'(x) - \psi_n(x)\psi_n'(mx)}{m\psi_n(mx)\xi_n'(x) - \xi_n(x)\psi_n'(mx)}, \tag{B.11}$$

$$b_n = \frac{\psi_n(mx)\psi_n'(x) - m\psi_n(x)\psi_n'(mx)}{\psi_n(mx)\xi_n'(x) - m\xi_n(x)\psi_n'(mx)}, \tag{B.12}$$

where $m = \varepsilon_r^2$, $x = k_0 r_0$, and $\psi_1(z) = z j_1(z)$ and $\xi_1(z) = z h_1^{(1)}(z)$ are the Riccati-Bessel functions which relate to the spherical Bessel functions of the first and the third kinds, respectively. The prime denotes differentiation with respect to the argument.

In the Eqs. (B.5) and (B.6), the terms n = 1 correspond to the dipole fields, n = 2 correspond to the quadrupole fields and so on. To calculate the electric and magnetic polarizabilities, we keep only the dipole terms (n=1) and rewrite Eqs. (B.5) and (B.6) as

$$\begin{aligned}
\mathbf{E} &= \frac{1}{4\pi\varepsilon_0}\Bigg\{k_0^2\big(\hat{\mathbf{r}}\times(6\pi\varepsilon_0 i a_1/k_0^3)\mathrm{E}_0\hat{\mathbf{x}}\big)\times\hat{\mathbf{r}}\frac{e^{ik_0 r}}{r} + \big[3\hat{\mathbf{r}}\big(\hat{\mathbf{r}}\cdot(6\pi\varepsilon_0 i a_1/k_0^3)\mathrm{E}_0\hat{\mathbf{x}}\big) \\
&\quad -(6\pi\varepsilon_0 i a_1/k_0^3)\mathrm{E}_0\hat{\mathbf{x}}\big]\left(\frac{1}{r^3} - \frac{ik_0}{r^2}\right)e^{ik_0 r}\Bigg\} \\
&\quad -\frac{Z_0}{4\pi}k_0^2\big(\hat{r}\times(6\pi i b_1/k_0^3)\mathrm{H}_0\hat{\mathbf{y}}\big)\frac{e^{ik_0 r}}{r}\left(1 - \frac{1}{ik_0 r}\right),
\end{aligned} \tag{B.13}$$

$$\begin{aligned}
\mathbf{H} &= \frac{ck_0^2}{4\pi}\big(\hat{r}\times(6\pi\varepsilon_0 i a_1/k_0^3)\mathrm{E}_0\hat{\mathbf{x}}\big)\frac{e^{ik_0 r}}{r}\left(1 - \frac{1}{ik_0 r}\right) \\
&\quad +\frac{1}{4\pi}\Bigg\{k_0^2\big(\hat{\mathbf{r}}\times(6\pi i b_1/k_0^3)\mathrm{H}_0\hat{\mathbf{y}}\big)\times\hat{\mathbf{r}}\frac{e^{ik_0 r}}{r} + \big[3\hat{\mathbf{r}}\big(\hat{\mathbf{r}}\cdot(6\pi i b_1/k_0^3)\mathrm{H}_0\hat{\mathbf{y}}\big) \\
&\quad -(6\pi i b_1/k_0^3)\mathrm{H}_0\hat{\mathbf{y}}\big]\left(\frac{1}{r^3} - \frac{ik_0}{r^2}\right)e^{ik_0 r}\Bigg\},
\end{aligned} \tag{B.14}$$

Comparing Eqs. (B.13) and (B.14) with the standard forms of the electric + magnetic dipole fields [48]

$$\begin{aligned}
\mathbf{E} &= \frac{1}{4\pi\varepsilon_0}\Bigg\{k^2(\hat{\mathbf{r}}\times\mathbf{p})\times\hat{\mathbf{r}}\frac{e^{ikr}}{r} + [3\hat{\mathbf{r}}(\hat{\mathbf{r}}\cdot\mathbf{p}) - \mathbf{p}]\left(\frac{1}{r^3} - \frac{ik}{r^2}\right)e^{ikr}\Bigg\} \\
&\quad -\frac{Z_0}{4\pi}k^2(\hat{r}\times\mathbf{m})\frac{e^{ikr}}{r}\left(1 - \frac{1}{ikr}\right),
\end{aligned} \tag{B.15}$$

$$\begin{aligned}
\mathbf{H} &= \frac{ck^2}{4\pi}(\hat{r}\times\mathbf{p})\frac{e^{ikr}}{r}\left(1 - \frac{1}{ikr}\right) \\
&\quad +\frac{1}{4\pi}\Bigg\{k^2(\hat{\mathbf{r}}\times\mathbf{m})\times\hat{\mathbf{r}}\frac{e^{ikr}}{r} + [3\hat{\mathbf{r}}(\hat{\mathbf{r}}\cdot\mathbf{m}) - \mathbf{m}]\left(\frac{1}{r^3} - \frac{ik}{r^2}\right)e^{ikr}\Bigg\},
\end{aligned} \tag{B.16}$$

we can see that the electric and magnetic dipole moments of the spheres are

$$\mathbf{p} = (6\pi\varepsilon_0 i a_1/k_0^3)\mathrm{E}_0\hat{\mathbf{x}} \tag{B.17}$$

$$\mathbf{m} = (6\pi i b_1/k_0^3)\mathrm{H}_0\hat{\mathbf{y}} \tag{B.18}$$

$$\tag{B.19}$$

Since $\mathrm{E}_0\hat{\mathbf{x}}$ and $\mathrm{H}_0\hat{\mathbf{y}}$ are the valuee of the external fields at the center of the sphere, we can conclude that the electric and magnetic polarizabilities of this sphere are

$$\alpha_e = 6\pi\varepsilon_0 i a_1/k_0^3 \tag{B.20}$$

$$\alpha_m = 6\pi i b_1/k_0^3 \tag{B.21}$$

Appendix C

Derivation of the Effective Coefficients

From Eq. (6.25), equating the terms with the same power of λ yields for λ^0 to λ^4 as

$$(\varepsilon_e - \varepsilon_m)\mathrm{E}_0^2 = \frac{\mathbf{E}_0}{V} \cdot \int_{V_i} (\varepsilon_i - \varepsilon_m)\mathbf{E}^{0i}\, dV, \tag{C.1}$$

$$\chi_e \mathrm{E}_0^4 = \frac{\mathbf{E}_0}{V} \cdot \int_{V_i} [(\varepsilon_i - \varepsilon_m)\mathbf{E}^{1i} + \chi_i' |\mathbf{E}^{0i}|^2 \mathbf{E}^{0i}\,] dV, \tag{C.2}$$

$$\begin{aligned} \eta_e \mathrm{E}_0^6 = \frac{\mathbf{E}_0}{V} \cdot \int_{V_i} \big[& (\varepsilon_i - \varepsilon_m)\mathbf{E}^{2i} + 2\chi_i(\mathbf{E}^{0i} \cdot \mathbf{E}^{1i})\mathbf{E}^{0i} \\ & + \chi_i |\mathbf{E}^{0i}|^2 \mathbf{E}^{1i} + \eta_i |\mathbf{E}^{0i}|^4 \mathbf{E}^{0i} \big]\, dV, \end{aligned} \tag{C.3}$$

$$\begin{aligned} \delta_e \mathrm{E}_0^8 = \frac{\mathbf{E}_0}{V} \cdot \int_{V_i} \big[& (\varepsilon_i - \varepsilon_m)\mathbf{E}^{3i} + \chi_i |\mathbf{E}^{1i}|^2 \mathbf{E}^{0i} + 2\chi_i(\mathbf{E}^{0i} \cdot \mathbf{E}^{1i})\mathbf{E}^{1i} \\ & + 2\chi_i(\mathbf{E}^{0i} \cdot \mathbf{E}^{2i})\mathbf{E}^{0i} + \chi_i |\mathbf{E}^{0i}|^2 \mathbf{E}^{2i} + 4\eta_i(\mathbf{E}^{0i} \cdot \mathbf{E}^{1i})^2 |\mathbf{E}^{0i}|^2 \mathbf{E}^{0i} \\ & + \eta_i |\mathbf{E}^{0i}|^4 \mathbf{E}^{1i} \big]\, dV, \end{aligned} \tag{C.4}$$

$$\begin{aligned} \mu_e \mathrm{E}_0^{10} = \frac{\mathbf{E}_0}{V} \cdot \int_{V_i} \big[& (\varepsilon_i - \varepsilon_m)\mathbf{E}^{4i} + \chi_i |\mathbf{E}^{1i}|^2 \mathbf{E}^{1i} + 2\chi_i(\mathbf{E}^{0i} \cdot \mathbf{E}^{1i})\mathbf{E}^{2i} \\ & + 2\chi_i(\mathbf{E}^{0i} \cdot \mathbf{E}^{2i})\mathbf{E}^{1i} + 2\chi_i(\mathbf{E}^{1i} \cdot \mathbf{E}^{2i})\mathbf{E}^{0i} + 2\chi_i(\mathbf{E}^{0i} \cdot \mathbf{E}^{3i})\mathbf{E}^{0i} \\ & + \chi_i |\mathbf{E}^{0i}|^2 \mathbf{E}^{3i} + 2\eta_i |\mathbf{E}^{0i}|^2 |\mathbf{E}^{1i}|^2 \mathbf{E}^{0i} + 4\eta_i(\mathbf{E}^{0i} \cdot \mathbf{E}^{1i})^2 \mathbf{E}^{0i} \\ & + 4\eta_i |\mathbf{E}^{0i}|^2 (\mathbf{E}^{0i} \cdot \mathbf{E}^{1i})\mathbf{E}^{1i} + 4\eta_i(\mathbf{E}^{0i} \cdot \mathbf{E}^{2i}) |\mathbf{E}^{0i}|^2 \mathbf{E}^{0i} + \eta_i |\mathbf{E}^{0i}|^4 \mathbf{E}^{2i} \big]\, dV. \end{aligned} \tag{C.5}$$

So $\varepsilon_e, \chi_e, \eta_e, \delta_e$ and μ_e can be obtained from Eqs.(C.1)-(C.5), respectively.

Appendix D

Determination of the Potentials in Composite Constituents

Using the power series Eq.(6.41) in Eqs. (6.37) - (6.40), we obtain:

$$\begin{aligned} \mathrm{E}_0 \cos\alpha(M+N) &= \sum_k (M+K\,N) A_k {\mathrm{E}_0}^k + \sum_{k,l,m} \frac{\chi_i\, N}{\varepsilon_m} (A_k A_l + B_k B_l) A_m {\mathrm{E}_0}^{k+l+m} \\ &\quad + \sum_{k,l,m,n,p} \frac{\eta_i\, N}{\varepsilon_m} (A_k A_l + B_k B_l)(A_m A_n + B_m B_n) A_p {\mathrm{E}_0}^{k+l+m+n+p}, \end{aligned} \tag{D.1}$$

$$\begin{aligned} \mathrm{E}_0 \sin\alpha(M+N) &= \sum_k (K\,M+N) B_k {\mathrm{E}_0}^k + \sum_{k,l,m} \frac{\chi_i\, M}{\varepsilon_m} (A_k A_l + B_k B_l) B_m {\mathrm{E}_0}^{k+l+m} \\ &\quad + \sum_{k,l,m,n,p} \frac{\eta_i\, M}{\varepsilon_m} (A_k A_l + B_k B_l)(A_m A_n + B_m B_n) B_p {\mathrm{E}_0}^{k+l+m+n+p}, \end{aligned} \tag{D.2}$$

$$\sum_k C_k \mathrm{E}_0^k = \frac{(E_0 \cos\alpha - \sum_k A_k \mathrm{E}_0^k) M}{M-N}, \tag{D.3}$$

$$\sum_k D_k \mathrm{E}_0^k = \frac{(E_0 \cos\alpha - \sum_k B_k \mathrm{E}_0^k) M}{M-N}, \tag{D.4}$$

where k, l, m, n and p are the integers that range from 0 to ∞. By equating the term proportional to the same power of E_0, we obtain $A_k = B_k = C_k = D_k = 0$ for k is even and:

$$A_1 = \cos\alpha \frac{M+N}{M+K\,N}, \tag{D.5}$$

$$B_1 = \sin\alpha \frac{M+N}{K\,M+N}, \tag{D.6}$$

$$A_3 = -\frac{\chi_i N({A_1}^2 + {B_1}^2)A_1}{\varepsilon_m(M + K\,N)}, \tag{D.7}$$

$$B_3 = -\frac{\chi_i M({A_1}^2 + {B_1}^2)B_1}{\varepsilon_m(K\,M + N)}, \tag{D.8}$$

$$\begin{aligned} A_5 \;=\; & -\frac{1}{M + K\,N}\Big[\frac{\chi_i N}{\varepsilon_m}\Big\{2(A_1A_3 + B_1B_3)A_1 + ({A_1}^2 + {B_1}^2)A_3\Big\} \\ & +\frac{\eta_i N}{\varepsilon_m}\Big\{({A_1}^2 + {B_1}^2)^2A_1\Big\}\Big], \end{aligned} \tag{D.9}$$

$$\begin{aligned} B_5 \;=\; & -\frac{1}{K\,M + N}\Big[\frac{\chi_i M}{\varepsilon_m}\Big\{2(A_1A_3 + B_1B_3)B_1 + ({A_1}^2 + {B_1}^2)B_3\Big\} \\ & +\frac{\eta_i M}{\varepsilon_m}\Big\{({A_1}^2 + {B_1}^2)^2B_1\Big\}\Big], \end{aligned} \tag{D.10}$$

$$\begin{aligned} A_7 \;=\; & -\frac{1}{M + K\,N}\Big[\frac{\chi_i N}{\varepsilon_m}\Big\{2(A_1A_3 + B_1B_3)A_3 + ({A_3}^2 + {B_3}^2)A_1 \\ & +2(A_1A_5 + B_1B_5)A_1 + ({A_1}^2 + {B_1}^2)A_5\Big\} \\ & +\frac{\eta_i N}{\varepsilon_m}\Big\{4(A_1A_3 + B_1B_3)({A_1}^2 + {B_1}^2)A_1 \\ & +({A_1}^2 + {B_1}^2)^2A_3\Big\}\Big], \end{aligned} \tag{D.11}$$

$$\begin{aligned} B_7 \;=\; & -\frac{1}{K\,M + N}\Big[\frac{\chi_i M}{\varepsilon_m}\Big\{2(A_1A_3 + B_1B_3)B_3 + ({A_3}^2 + {B_3}^2)B_1 \\ & +2(A_1A_5 + B_1B_5)B_1 + ({A_1}^2 + {B_1}^2)B_5\Big\} \\ & +\frac{\eta_i M}{\varepsilon_m}\Big\{4(A_1A_3 + B_1B_3)({A_1}^2 + {B_1}^2)B_1 \\ & +({A_1}^2 + {B_1}^2)^2B_3\Big\}\Big], \end{aligned} \tag{D.12}$$

$$C_1 = \frac{(\cos\alpha - A_1)M}{M - N}, \tag{D.13}$$

$$D_1 = \frac{(\sin\alpha - B_1)N}{M - N}, \tag{D.14}$$

$$C_k = \frac{-A_kM}{M - N}, \qquad k = 3,\ 5,\ 7, ... \tag{D.15}$$

$$D_k = \frac{-B_kN}{M - N}, \qquad k = 3,\ 5,\ 7, ... \tag{D.16}$$

Thus, from Eqs. (6.34) and (6.33), the potentials in the inclusions and the host medium are obtained as follows:

$$\begin{aligned}\Phi^i &= -(A_1x + B_1y)\mathrm{E}_0 - (A_3x + B_3y){\mathrm{E}_0}^3 \\ &\quad -(A_5x + B_5y){\mathrm{E}_0}^5 - (A_7x + B_7y){\mathrm{E}_0}^7 + \dots\ , \end{aligned} \tag{D.17}$$

$$\begin{aligned}\Phi^m &= (C_1\, a\exp(-u)\cos v - a\cos\alpha\cosh u\cos v \\ &\quad + D_1\, a\exp(-u)\sin v - a\sin\alpha\sinh u\sin v)E_0 \\ &\quad + (C_3 a\exp(-u)\cos v + D_3 a\exp(-u)\sin v)E_0^3 \\ &\quad + C_5 a\exp(-u)\cos v + D_5 a\exp(-u)\sin v)E_0^5 \\ &\quad + C_7 a\exp(-u)\cos v + D_7 a\exp(-u)\sin v)E_0^7 + \dots\ . \end{aligned} \tag{D.18}$$

It turns out that, the terms on the right hand side of Eqs. (D.17) and (D.18) with E_0^{2k+1} correspond to the perturbative potentials Φ^{ki} and Φ^{km} of order k. Thus the perturbative electric fields in the inclusion ($\mathbf{E}^{ki} = -\boldsymbol{\nabla}\Phi^{ki}$) are

$$\mathbf{E}^{ki} = \mathrm{E}_0^{2k+1}(A_{2k+1}\hat{\mathbf{x}} + B_{2k+1}\hat{\mathbf{y}}). \tag{D.19}$$

Vitae

Name: Mr. Chanin Potisook

Birthdate and Birthplace: October 18, 1981 at Saraburi, Thailand

Educations:

2004 B.Sc. (Physics) Faculty of Science, Chulalongkorn University, Bangkok, Thailand.

Publications:

2007 M. Natenapit, C. Thongboonrithi and C. Potisook, Ninth-order effective responses of nonlinear composites in external DC and AC electric fields. *Physica B* **403** (2008) 4314-4318.

2012 C. Potisook and M. Natenapit, High-order Effective Responses in Weakly Nonlinear Elliptic Cylindrical Composites. *Physica B* **407** (2012) 598-605.

2013 C. Potisook and M. Natenapit, Negative Phase Velocity and Negative Refraction in Biaxial Anisotropic Lossy Media. Article has been submitted for publishing in Progress In Electromagnetics Research (PIER) and is under reviewed.

International Presentations:

2008 C. Potisook and M. Natenapit. Effective DC and AC Responses of Weakly Nonlinear Composites 4^{th} *Mathematics and Physical Sciences Graduate Congress, National University of Singapore*, Singapore (17-19 December 2008)

2012 C. Potisook and M. Natenapit. General Condition on the Negative Phase Velocity in Biaxial Anisotropic Lossy Media 8^{th} *Mathematics and Physical Sciences Graduate Congress, Chulalongkorn University*, Bangkok, Thailand (8-10 December 2012)